POLITECNICO DI TORINO

Master's Degree in Biomedical Engineering

Master's Degree Thesis

Neurofeedback in Virtual Reality Naturalistic Scenarios for Enhancing Relaxation: Visual and Auditory Stimulation to Promote Brain Entrainment

Supervisors

Prof. Luca MESIN

Ing. Giovanni CHIARION

Candidates

Diletta CALCERANO

Gianluigi CIURLIA

ACADEMIC YEAR 2022-2023

Abstract

Biofeedback is a procedure aimed at increasing a subject's proprioception based on the principle of "physiological mirroring". The subject has the opportunity to receive visual and/or auditory feedback in real time correlated to one or more physiological parameters acquired. The goal is to find a strategy to modify these parameters and learn from the feedback received to have a greater awareness of his/her own body. The various biofeedback trainings aim to normalize the functional state of the various body systems such as the central nervous system (CNS), the cardiovascular system, and others. In Neurofeedback, in particular, the subject is provided with real-time information on his/her brain rhythms (EEG) and brain functioning; the brain, thanks to its neuroplasticity, takes note of this information and gradually modulates its activity in response to it. The main weakness of neurofeedback treatment is that simple and uninteresting designs can demotivate or exhaust the patient during training sessions. The creation of scenarios in virtual reality turns out to gain more interest in the patient, making the treatment more immersive and therefore more engaging. The purpose of this study is to promote subject's relaxation in the shortest possible time after a stressful situation, and to support a gradual learning of how to manage his/her own brain rhythms over the course of the various training sessions. To achieve this, a virtual reality neurofeedback system, set in a naturalistic and semi-realistic scenario, was designed. To support the treatment, visual and auditory stimulation was added promoting Brain Entrainment, which is the dragging of brain waves towards a specific frequency, i.e., that of the subject's intrinsic oscillator. A Single Case Study was conducted over three weeks (three sessions per week), and robust results were obtained for the individual trainings: throughout the acquisition, a Relaxation Score, correlated to the beta-to-alpha ratio (BAR), showed an increasing trend during the stress test (BAR=1.29 ± 0.41 during the last session) and a decreasing trend during the relaxation phase (BAR=0.49 ± 0.15 during the last session), in accordance with the expected results. Furthermore, the effect of the training is shown to be long-lasting, supported by a statistically significant difference between the initial and final baselines. It is also demonstrated that, during the various trainings, the subject achieves a tendentially better Maximal Relaxation Score, also increasing the time for which she can keep the BAR below a fixed predetermined threshold. ECG signal was also evaluated in post-processing, comparing Heart Rate and Heart Rate Variability between the various phases of the training. On these parameters, results consistent with the study are obtained, but not as robust as those obtained on EEG. Further analysis is needed to determine whether the results are related to the combination of Neurofeedback and Brain Entrainment or only to one of these. The work was mainly based on the design and testing of the system, so it would be appropriate to carry out in the future a study on a larger number of subjects in order to make the results more solid. Moreover, the project paves the way for a study on subjects with generalized anxiety disorder, post-traumatic stress disorder, and other types of mental diseases.

Table of Contents

Chapter 1

Background and notations

The work of this thesis is organised as follows: Chapter 1 focuses both on a physiological description of the nervous and cardiovascular system , and on the specifics of the EEG and ECG signal. Chapter 2 presents the topic of biofeedback, describes the different types of biofeedback including neurofeedback and finally introduces brain entrainment. The third chapter explains Virtual Reality, its history and applications. The methods of the study are extensively reported in Chapter 4, the processing of the acquired data in Chapter 5, the results are presented in Chapter 6 and finally the conclusions and future studies in Chapter 7.

1.1 Human brain anatomy

In the following sections, we will briefly describe the anatomical structure of the brain, its main functions and how the action potential between neurons is generated, in turn causing an electric current to flow.

1.1.1 Nervous system

The nervous system can be divided into two major anatomical parts: the central nervous system and the peripheral nervous system. The central nervous system (CNS) consists of the encephalon and spinal cord, receives information from the sensory organs to determine the state of external and internal environment, processes this information and makes decisions based on it. It then sends instructions to the various organs in order to perform appropriate tasks. The central nervous system is also the seat of learning, memory, emotions, language and other complex functions.
On the other hand, the peripheral nervous system ensures communication between the central nervous system and the organs. It can be divided into two lines: afferent line and efferent line. Nerve cells in the first line transmit information from the organs to the CNS. Nerve cells of the efferent line, on the other hand, follow the reverse pathway, transmitting information from the CNS to the peripheral organs, which perform functions in response to commands from neurons.
The efferent division can be further divided into two branches: the somatic nervous system and the autonomic nervous system. The first consists of nerve cells, the motor neurons, that regulate skeletal muscle contraction. The autonomic nervous system, on the other hand, regulates the function of internal organs and structures that are not under voluntary control. This in turn is divided into the parasympathetic nervous system and the sympathetic nervous system; the two tend to have opposite effects on organs.
The CNS contains around 10^{11} neurons connected by 10^{14} synapses in the brain and spinal cord. [1]

1.1.2 Brain structures

The CNS has a very orderly arrangement of neurons to form grey clusters (grey matter) and white structures (white matter). The grey matter makes up about 40 % of the CNS and it is where neuronal transmission and integration take place. The remaining 60% of the CNS is made up of white matter, which is mostly made up of myelin axons, which have a high lipid content and are therefore white. Myelin axons are specialised in the rapid transmission of information, which propagates over long distances in the form of action potentials.
The outer surface of the encephalon appears all grey because most of the globe-shaped structure (brain) that makes up the encephalon mass is internally covered by a thin layer of grey matter, called the cerebral cortex.

The cerebral cortex represents the outermost portion of the brain. It consists of a thin layer filled with circumvolutions that originate from *sulci* (invaginations) and *gyri* (crests) that allow the large volume of grey matter to be contained within the cranial box. The cerebral cortex performs the most evolved functions, it allows us to have perceptions of our surroundings, formulate thoughts, and have emotional experiences. To do all this, it acts as an integrating centre where it receives sensory signals of different origins, processes them and uses them to formulate thoughts and actions.

The brain is divided into two symmetrical areas called *hemispheres*. Each hemisphere is responsible for the opposite side of the body; not all the functions of the two hemispheres are shared, in fact while the left one is considered the 'rational' hemisphere, since it regulates abilities such as language, writing, logical reasoning, the right one is the 'artistic' one, which controls creativity, intuition or perception of space.

Each cerebral hemisphere is divided into four regions, known as lobes (Figure 1.1):

- the frontal lobe represents the front part of the brain. It contains the primary motor cortex, involved in the generation of commands that produce voluntary movements. It is also responsible for actions related to language, personality determination and movement planning.

- the parietal lobe is located posterior to the frontal lobe and is divided from it by the central sulcus that runs through each hemisphere of the brain. It contains the primary somatosensory cortex involved in processing sensory signals. It is also involved in language learning.

- the occipital lobe is located posterior and inferior to the parietal lobe. It contains the visual cortex involved in processing visual signals.

- the temporal lobe is located inferior to the frontal and parietal lobes of the brain and is separated from the frontal lobe by the lateral sulcus. It contains the auditory cortex, and performs mainly memory-related activities.
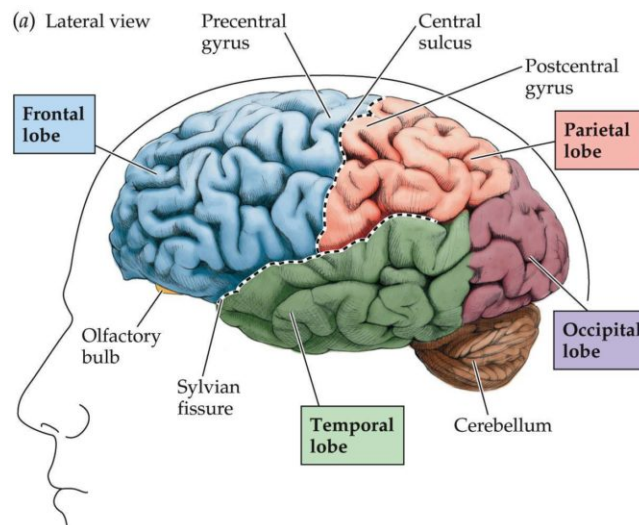
Figure 1.1: Representation of the brain lobes [2].

1.1.3 Cells of the nervous system and how they communicate

The nervous system consists of two main classes of cells: neurons and glial cells. The neuron (Figure 1.2) represents the functional unit, the smallest tissue unit capable of performing all the functions of brain tissue. Neurons are excitable cells that communicate by producing and transmitting large, rapid electrical signals called action potentials.

Anatomically, a neuron consists of three components: a cell body, called soma, a varying number of dendrites and an axon. The soma contains the nucleus and most of the intracellular organelles. It performs most of the functions accomplished by cells such as protein synthesis and cell metabolism (in many areas of the nervous system, however, mature neurons lose the ability to divide themselves). Dendrites branch off the cell body and receive afferents (in form of chemical neurotransmitters) from other neurons at specialised junctions called synapses. The axon is also a branch that starts from the cell body of the

neuron, but this, unlike the dendrites, has the role of sending information. This information is propagated over long distances in the form of electrical signals called action potentials, rapid and large changes in the membrane potential during which the inside of the cell becomes positive compared to the outside.
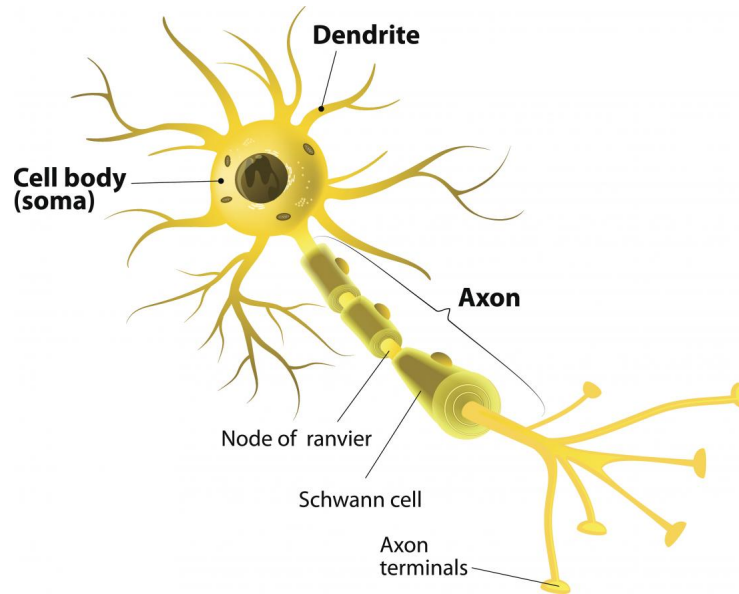
Figure 1.2: Structure of a neuron [3].

Neurons can be classified according to their structure, their morphology and their function. Structurally, depending on the number of axons and dendrites, bipolar and multipolar neurons are distinguished in humans. Bipolar neurons are generally sensory neurons with two projections, an axon and a dendrite branching off from the cell body. On the other hand, multipolar neurons, the most common, have multiple projections branching off from the cell body, the longest being the axon, all others are dendrites.
Regarding morphology, neurons are distinguished in pyramidal neurons, stellate cells and fusiform cells. Functionally, there are three categories of neurons: efferent neurons, afferent neurons and interneurons. Efferent neurons transmit information from the central nervous system to the effector organs (motor neurons and neurons of the autonomic nervous system). The cell bodies and dendrites of the efferent neurons are located in the central nervous system, however, the axons become part of the peripheral nervous system.
The afferent neurons transmit information from sensory receptors (from the external environment) and visceral receptors (from the internal organs) to the central nervous system for further processing. Most afferent neurons have their cell bodies located outside the CNS in a ganglion (a grouping of cell bodies located outside the CNS) and peripheral axon endings located in the peripheral organs; the central axon terminates in the CNS, where it releases a neurotransmitter to communicate with other neurons.
The third functional class of neurons is represented by interneurons which make up 99% of all neurons in the body. These are located in the CNS and perform all functions relevant to it there.

The second main class is represented by glial cells (Figure 1.3). Glial cells, make up 90% of the cells in the nervous system, they are not directly involved in signal transmission, but provide structural integrity and metabolic support enabling neurons to perform their functions.
There are five different types of glial cells, each type with a different function. For example, the main function of oligodendrocytes and Schwann cells is to form a myelin wrap around the axons of neurons, isolating them so that they can transmit action potentials more quickly and effectively. Astrocytes are the most highly differentiated glial cells and perform very important functions such as controlling the development of the blood-brain barrier, guiding neurons developing to their correct destination, regulating the creation and maintenance of synapses, maintaining the myelin envelope around the axons of neurons, maintaining the normal extracellular environment that surrounds the brain protecting it from toxic substances. [1].
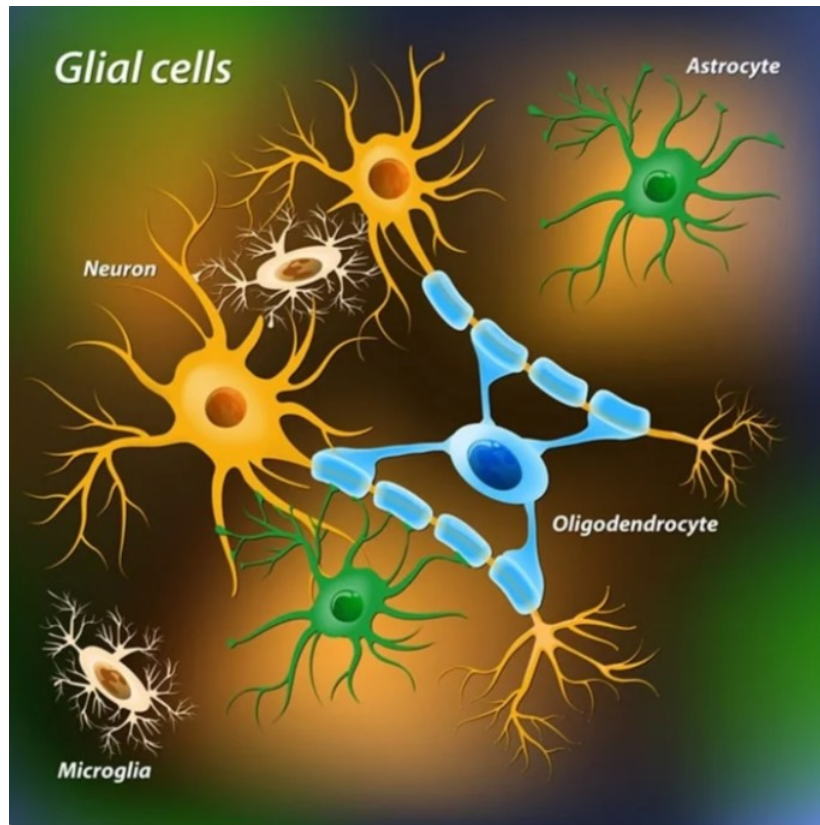
Figure 1.3: Glial cells [4].

1.1.4   Action Potential

The cells membrane is made up of ion channels that can open or close to specific electrical or chemical stimuli, and thus alter the transmembrane potential, which can generate hyperpolarization (the inside of the cell becomes more negative than the outside) or depolarization (the inside of the cell becomes less negative than the outside). The genesis of the action potential is essentially based on the selective permeability of the membrane to sodium ions (Na^+) and potassium ions (K^+) and on the electrochemical gradients of these two ions across the membrane.

The resting membrane potential is around -70 mV, so the inside of the cell membrane (the cytoplasm) is at a potential of 70 mV below the extracellular environment. In the resting situation, K^+ ions are much more concentrated inside the cell, while Na^+ ions outside.

A chemical, thermal, electrical or mechanical stimulus can disturb the stability of the membrane potential by increasing the conductivity of the sodium channels, which will tend to open. The case we are interested in is that of an electrical stimulus, thus a current flowing through the neuron's membrane.

For the action potential to be triggered, a certain voltage, called threshold voltage, must be exceeded (-55 mV). When an electrical stimulus alters the excitability of the cell, sodium channels open, Na^+ ions enter the cell increasing the positivity of the internal potential with respect to the outside (depolarization phenomenon).

For the threshold voltage to be exceeded and thus the action potential to be triggered, the stimulus must continue until the inside of the cell becomes weakly positive relative to the outside. The stimulus must last until the moment when the threshold voltage is reached. Once reached, even if the stimulus ceased, the action potential would already be triggered. Otherwise, if the stimulus were to cease, the active sodium pump phenomena would come into action, which would transport the Na^+ ions countergradient towards the outside of the cell and the cell would tend to repolarise, not allowing the action potential to arise.

The potential across the membrane must progressively increase, meaning that the inside of the cell must become less negative relative to the outside and then weakly positive relative to the outside.

Shortly before the sodium channels open completely, potassium channels also begin to open and K^+ ions, being more concentrated inside, tend to leave the cell. The transmembrane potential tends to become negative again (repolarization phase) until it first reaches a lower voltage value than the resting membrane potential (hyperpolarization phenomenon) and then returns to the basal level. In addition to the action
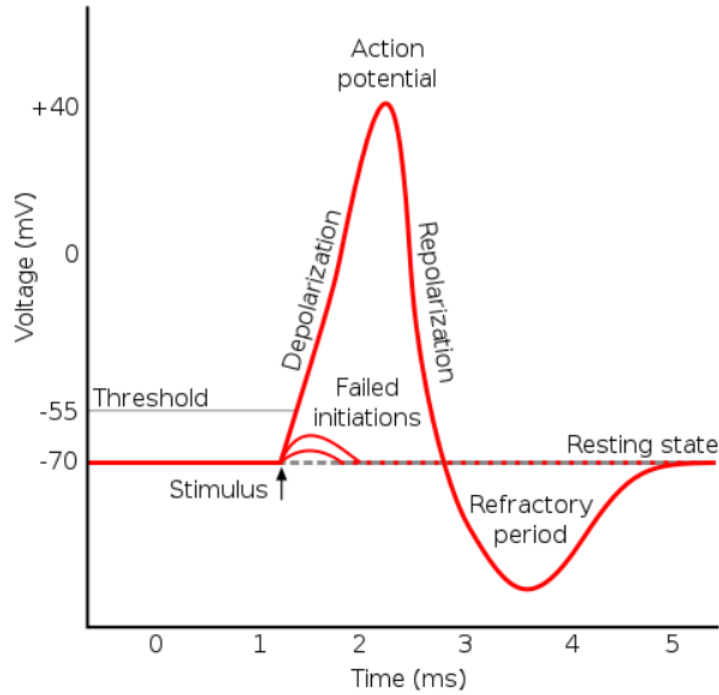
Figure 1.4: Diagram showing the phases of an action potential in relation to the membrane voltage over time [5].

potential, we also distinguish the synaptic potential which consists of two main phenomena: the excitatory post-synaptic potential (EPSP), that is a depolarization of the post-synaptic membrane potential, and the inhibitory post-synaptic potential (IPSP), which is a hyperpolarization of the post-synaptic membrane potential.

In the following paragraphs, we will give an overview of the EEG signal, describe its characteristics and how to acquire it.

1.2 EEG signal

EEG stands for "electroencephalography", which is the electrophysiological process of measuring and recording the electrical activity of the brain. Voltage changes come from ionic currents flowing between neurons [6].

Morphologically all brains are different. It has been demonstrated that only some characteristics are similar from one brain to another, for example the so-called *gyrus* and the *median sulcus* are common to all subjects while all the other convolutions are different from subject to subject because each brain, during the various evolutionary stages, develops in a different way in its own reduced volume. Inside it all these involutions are born, increasing the amount of total surface and giving a corrugated appearance. From a functional point of view, however, the functions of the brain, in the various evolutionary stages, are all located more or less in the same places and all work more or less in the same way.

The billions of cells in our brain produce very small electrical signals that form non-linear patterns called *brain waves*.

Research on the electrical activity of the brain dates back to the nineteenth century when the physicist Richard Caton, in 1875, published the discoveries derived from his experiments on rabbits and monkeys in the British Medical Journal. In 1890 Adolf Beck placed electrodes directly in contact with the brain of a dog and a rabbit to test sensory stimulation. His observations of fluctuating electrical brain activity led him to the discovery of brain waves and led to EEG becoming a scientific field. But the turning point with regard to electroencephalography was in 1924 thanks to the studies of the German physiologist and psychiatrist Hans Berger who recorded the first EEG human brain waves.

Berger was a revolutionary in this field because not only he was the one who discovered *alpha waves*, also called *Berger waves*, but he also worked a lot with the instrumentation. Being German, he had a collaboration with Siemens, a company little-known at the time, but today a giant in the world of medical
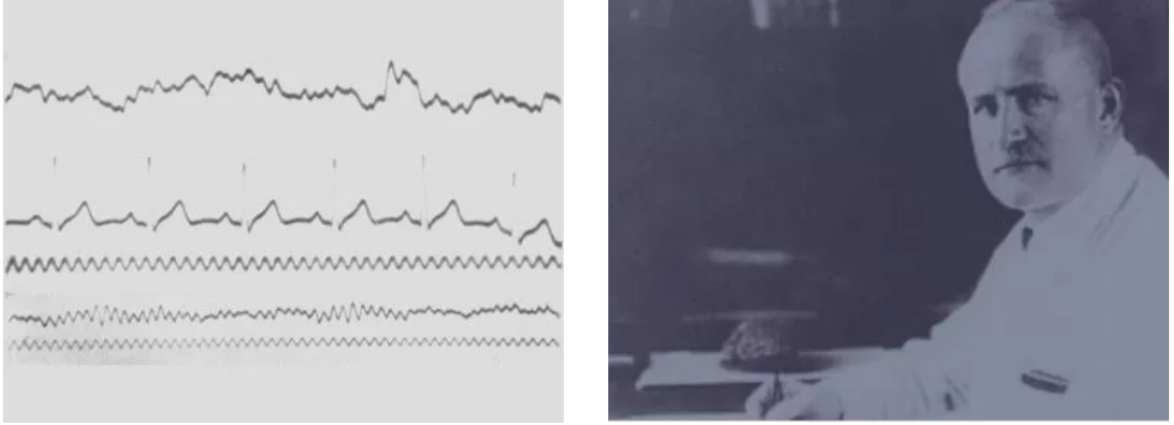
Figure 1.5: On the right Hans Berger, the first person to record EEG brainwaves in humans. On the left the first human EEG recording obtained by Hans Berger himself in 1924. The upper signal is EEG and the lower is a 10 Hz timing signal [6].

devices, with which he improved the instrumentation and tried to develop an EEG signal acquisition system that had the highest possible quality.

At the time invasive methods were used, steel micro-needles were placed, kept in a zinc bath to reduce the impedance between the electrode and the skin, and inserted under the scalp. A few years later, around 1934, electrodes were created that were placed externally on the scalp, which are still used today, allowing a totally non-invasive EEG sampling.

In fact, the neurons we are interested in are the neurons that perform functions, those that allow us to be attentive or to relax, to speak, to see, to react to external stimuli, to communicate, to move, etc., thus what we call the *functional neurons* that are those located in the cerebral cortex. They are called *pyramidal neurons* because they have a body that looks like a kind of three-dimensional pyramid, and they are characterised by having very long axons and a very high number of dendrites in their soma. This structure allows them to create very dense networks of synapses, having the possibility of storing the functions distributed on the cortical surface. So only the neurons that are on the cortical surface (outer layer of the brain, a few millimetres thick) give us the possibility of performing all the functions that interest us and that we want to study by acquiring biopotentials by placing the electrodes non-invasively. Neurons are excitable cells, which means that a membrane depolarization is triggered; this usually starts at the apical dendrites and propagates along the axon, creating a travelling current. The axon has a special type of conduction, it is covered by an insulator, myelin, so the speed of propagation of potentials on the axon is increased by about a factor of 10 compared to the conduction speed of the naked nerve fibre, i.e. without myelin (Figure 1.6). During the depolarization of this cell, an electromagnetic field is created; the EEG signal is precisely the measurement of this electric field, while the magnetic part is measured by a technique called magnetoencephalography, which instead produces an image rather than a signal, i.e. a map of current measurements over the entire cortical surface.

1.2.1 The International 10-20 Electrode Positioning System

The international 10-20 system is the most widely used method today to take the EEG signal non-invasively. In this system 21 electrodes are located on the surface of the scalp, as shown in Figure 1.7. It is so called since the distance between one electrode and the following is a percentage (10%-20%) of the two basic dimensions of the skull, the first being the length of the skull from the delve at the top of the nose, level with the eyes (*nasion*) to the bony lump at the base of the skull on the midline at the back of the head (*inion*) and the second dimension being the ear-to-ear distance.

From the two referece points (*nasion* and *inion*), the skull perimeters are measured in the transverse and median planes. Electrode locations are determined by dividing these perimeters into 10% and 20% intervals. Three other electrodes are placed on each side equidistant from the neighboring points. In addition to the 21 electrodes of the international 10-20 system, intermediate 10% electrode positions are also used [8]. Obviously the distance is not fixed but is variable because it goes by percentage of the size of the subject's skull.

Each electrode is associated with an alpha-numeric code that takes into account the positioning zone
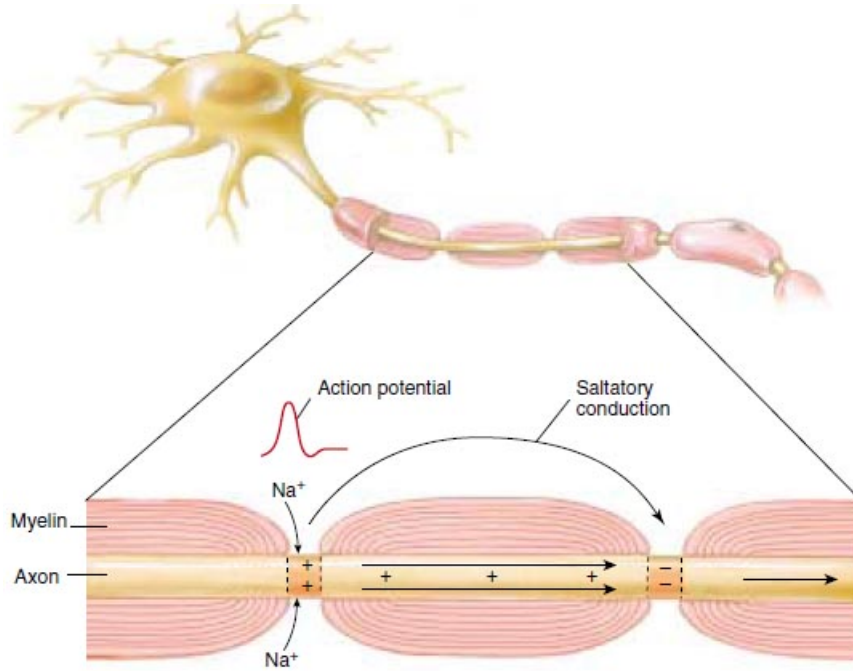
Figure 1.6: Representation of saltatory conduction [7].

(specified in Figure 1.7) and the hemisphere (right hemisphere even numbers, left hemisphere odd numbers); the letter z is used to indicate that scalp location falls along the central line running between the nasion and the inion. The locations and nomenclature of these electrodes are standardized by the American Electroencephalographic Society.

Note that in this recommendation, four electrodes have different names compared to the 10-20 system; these are T_7, T_8, P_7, and P_8. These electrodes are drawn black with white text in the figure [8]. To position these electrodes special adjustable helmets with specific sensors housings are used (Figure 1.8).

Bipolar or unipolar electrodes can be used in the EEG measurement. In the first method the potential difference between a pair of electrodes is measured. In the latter method the potential of each electrode is compared either to a reference potential. There are several possibilities for the reference potential: it can be the potential of an electrode taken in an area in which there is no cortical surface, for example the potential of the skin of the neck. In this case an electrode is placed on the ear or under the ear lobe and this is used as a reference, assuming that it remains constant. Also the average of the potentials acquired by all the electrodes is used as the reference potential.

Moreover a single-differential sampling is done in which the difference is made between neighbouring electrodes that belong to the same hemisphere and the same cortical area. From a clinical point of view the common practice is to use a fixed reference anyway, in an area where there is no particular cortical activity, this especially in EEG for diagnosis.

Each electrode, placed anywhere on the scalp, senses the electrical activity of a very large number of neurons, hence of sources, each emitting action potentials at a different rate and frequency. This means that, speaking in temporal terms, these sources are not synchronous. The EEG signal is, in fact, a random signal because the acquisition system measures the electrical contributions of many different sources with activities that are potentially independent from each other and not correlated with each other.

When we think of the EEG signal as a sum of many action potentials, we are not actually measuring action potentials coming from the axon but rather those created at the synapse (Figure 1.9), generated in the target cell, i.e. what are called **post-synaptic potentials**. This is because the action potential that arrives along the axon has been generated far away. Pyramidal neurons have very long axons and as action potentials propagate along them, they lose their amplitude. In order to be able to measure a signal with a good signal to noise ratio (SNR) from the outside, we would need all these sources to be synchronous, but this is not normally the case.

On the other hand, the action potential that is generated on the target cell (post-synaptic potential) has just been generated, it is precisely the origin of cell depolarization and therefore has the greatest possible amplitude. Therefore, in measuring it, we have a greater amplitude and a greater SNR ratio.

10
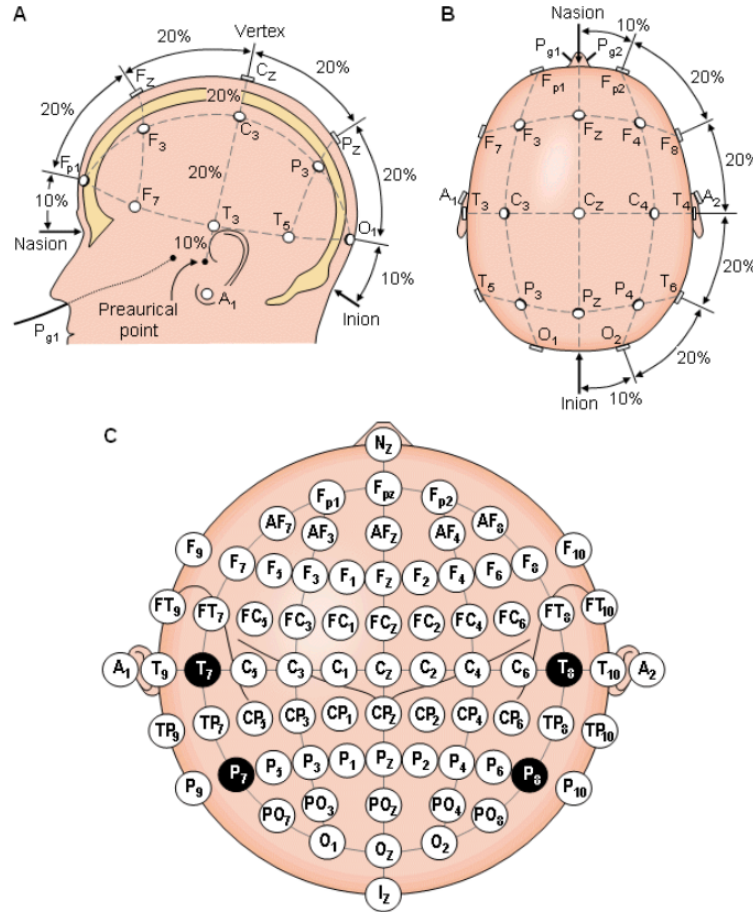
Figure 1.7: The international 10-20 system seen from (A) left and (B) above the head. A = Ear lobe, C = central, Pg = nasopharyngeal, P = parietal, F = frontal, Fp = frontal polar, O = occipital. (C) Location and nomenclature of the intermediate 10% electrodes, as standardized by the American Electroencephalographic Society (redrawn from Sharbrough, 1991) [8].


Figure 1.8: Example of an EEG helmet [9].

There is also another point, related to velocity. In the synapse there is a slowing down of these potentials because the electrochemical mediation is not as fast as the jumping propagation along the axon, it is much slower, and so again the probability that these action potentials temporally sum up to each other is greater.

11

Hence, as a matter of amplitude and of propagation speed, the EEG is predominantly the measurement of post-synaptic potentials.
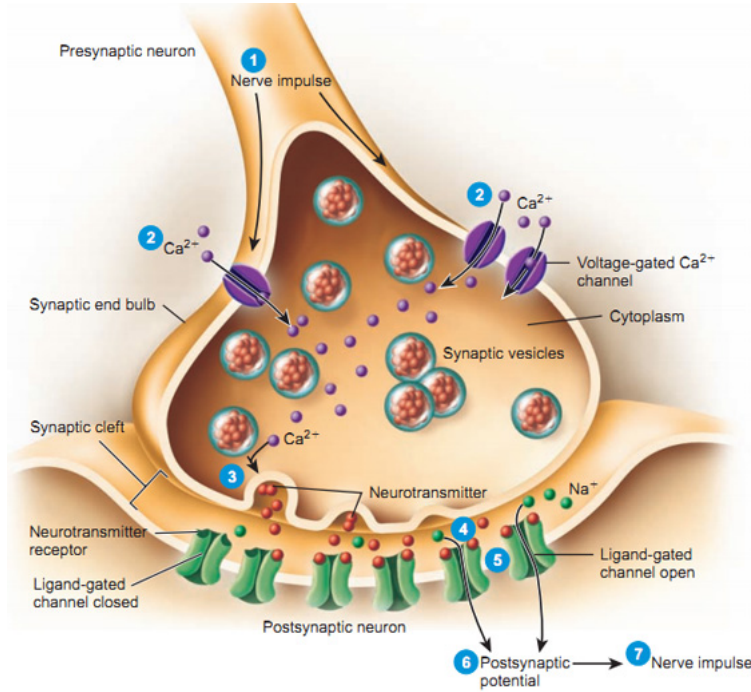
Figure 1.9: Generation of the post-synaptic potential [10].

1.2.2 Amplitude of EEG signal and the frequency bands

The amplitude of the EEG signal has a range between 10 and 500 μV, typically at a clinical level it is divided into three bands:

- Low amplitude: $< 30\ \mu$V

- Medium amplitude: 30-70 μV

- High amplitude: $> 70\ \mu$V

   Amplitude is not a fundamental parameter, it can be useful from a clinical point of view because it is a measure of how much the neurons heard by that specific electrode are working more intensely, less intensely, more synchronously, less synchronously, so it can have a functional meaning.

The bulk of the information content of the EEG signal is in the Fourier domain. The power spectrum of the EEG signal is subdivided into different frequency bands (Figure 1.10), each of which is assigned a precise name marked with Greek letters and each reflecting different attentional and cognitive states.

- ***delta*** δ: 0.5-3 Hz frequency, 20-200 μV amplitude, associated to pathological conditions and very deep sleep.

- ***theta*** θ: 4-7 Hz frequency, 5-100 μV amplitude, associated to deep sleep.

- ***alpha*** α: 8-13 Hz frequency, 10-200 μV amplitude, associated to mental relaxationn.

- ***beta*** β: 14-30 Hz frequency, 1-20 μV amplitude associated to attention, concentration, activated cortical areas.

- ***gamma*** γ: > 30 Hz frequency, 1-20 μV amplitude, associated to attention, concentration, activated cortical areas.

   Delta activity is predominantly found in infants and it is also associated with deep stages of sleep in older subjects. Delta waves have been documented interictally (between seizures) in patients with absence seizures, which involve brief, sudden lapses in attention. This waves are characterized by low-frequency

EEG Frequency Bands
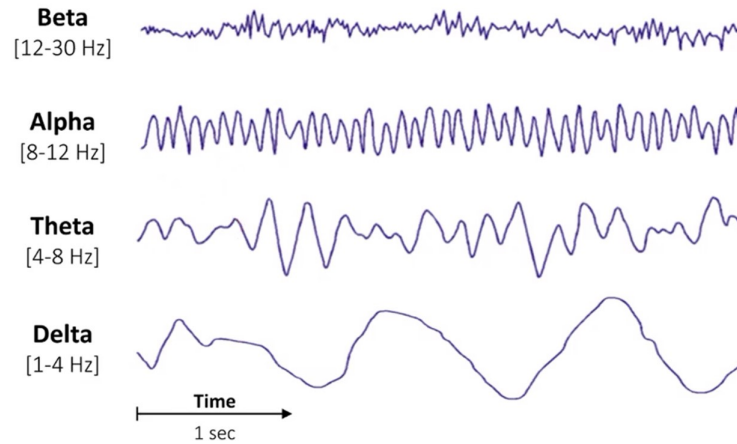
Figure 1.10: EEG frequency bands [11].

(about 3 Hz) and high amplitude. Delta rhythms can be present during wakefulness (they are responsive to eye-opening) and may be enhanced by hyperventilation as well.

Brain activity within a frequency range comprised between 4 and 7 Hz is referred to as **Theta activity**. Theta rhythm detected in EEG measurement is often found in young adults, particularly over the temporal regions and during hyperventilation. In older individuals, theta activity with an amplitude greater than about 30 μV is seen less commonly, except during drowsiness.

Alpha waves are often associated with a relaxed, calm and lucid state of mind and they can be found in the occipital and posterior regions of the brain. Alpha waves can be induced by closing one's eyes and relaxing, and they are rarely present during intense cognitive processes like thinking, mental calculus and problem-solving. In most adults, alpha waves range in frequency from 9 to 11 Hz [6].

The alpha band, which is perhaps most important of all for brain neurophysiology studies, is the band that measures mental relaxation. This band appears in many transition stages that are very important to us, for example the transition between sleep and wakefulness for all those cases where it is significant to analyze both sleep and falling asleep, that are two different things. Mental relaxation is also that part of the transition that separates the phase of high concentration or high attention from a phase in which concentration or attention is less.

Beta waves are most closely associated with being conscious or in an awake, attentive and alert state. Low-amplitude beta waves are associated with active concentration, or with a busy or anxious state of mind. Beta waves are also associated with motor decisions (suppression of movement and sensory feedback of motion).

Gamma-band activity comprises an EEG frequency range from 30 to 200 Hz, and is distributed widely throughout cerebral structures; it participates in various cerebral functions, such as perception, attention, memory, consciousness, synaptic plasticity, and motor control [12].

1.2.3   Main EEG artefacts

Although the EEG is designed to record brain activity, it also records electrical activity originating from sites outside the brain. Recorded activity that is not of brain origin is called "artefact" and can be divided into physiological and extra-physiological artefacts. The first are generated by the patient himself and originate from sources in the body other than the brain, while the latter originate from outside the body i.e. from the equipment and the environment.

The approach of recognising, identifying sources and eliminating artefacts is an important process in order to reduce the probability of EEG misinterpretation and to reduce all the consequences that this may entail.

The five main artefacts that can interfere in the interpretation of an EEG are [13]:
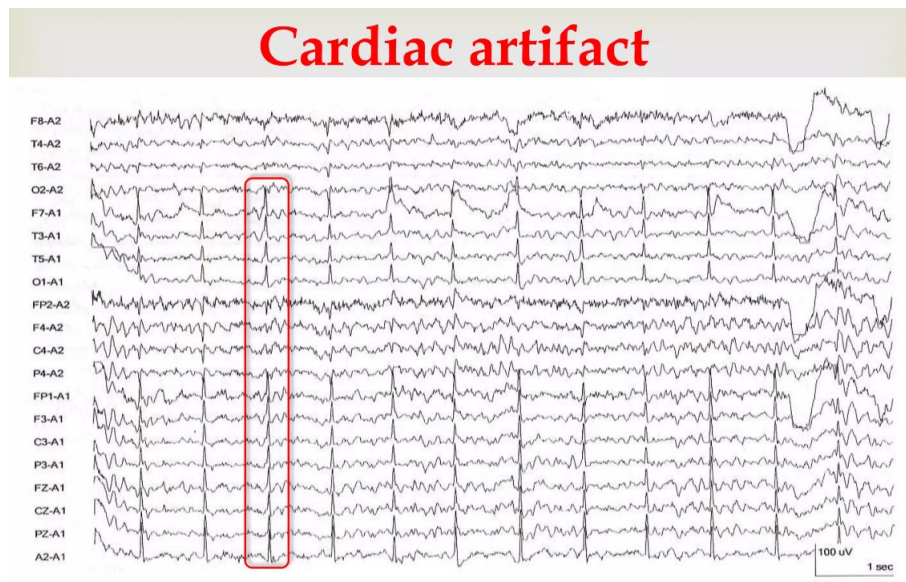
- Cardiac artefacts

- Electrode artefacts

- External device artefacts

- Muscle artefacts

- Ocular artefacts

Cardiac artefact

Heart produces two types of artefacts: electrical and mechanical. Both types are time-bound by heart contractions and are easily identified by their synchronization with complexes in the ECG channel.
The electrical artefact (Figure 1.11) is actually an ECG recorded by the head electrodes. It is essentially a poorly formed QRS complex [13]. This type of artefact occurs as a series of spikes, and being rhythmic, they might be misinterpreted and thought to be seizures or interactive spikes that happen between seizures because they look very sharp. Having an ECG channel at the bottom of the recording channels, it's easy to line it up with these spikes and that will give the clue for assuming that activity coming from the heart and not being epileptic activity [14].
Due to the equipotential field, mounts with an average reference present minimal ECG artefact. With bipolar montages, on the other hand, the artefact occurs with the greatest amplitude and the clearest QRS morphology in the temporal regions is often more pronounced on the left side. The mechanical artefact

Figure 1.11: Cardiac artefact from an ipsilateral ear referential montage [13].

from the heart is generated by the circulatory pulse and can be regarded as a type of electrode artefact. It occurs when an electrode rests on a vessel that exhibits the pulse and appears as a slow periodic wave with a regular interval following the peak of ECG artefact of approximately 200 ms. It occurs most commonly in the frontal and temporal regions and less commonly in the occipital ones; however it can be present anywhere. Pulse artefact (Figure 1.12) is easily identified by touching the electrode that produces it. [13]

Electrode artefact

Six types of electrode artefact can be distinguished:

- Electrode pop

- Electrode contact

- Electrode/lead movement

- Perspiration

- Salt bridge

14
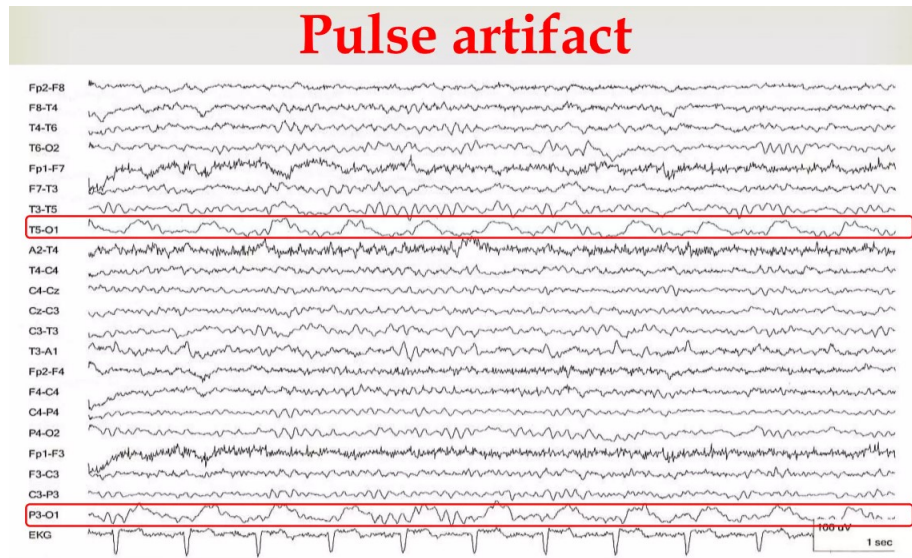
Figure 1.12: Pulse artefact. Focal slow waves at the left occipital channel follow each heart beat, as indicated in the ECG channel. These artefacts are due to electrode movement and, in this specific case, can be eliminated by repositioning the O1 electrode [13].

- Movement artefact

Electrode artefacts usually manifest themselves either as short transients limited to one electrode or as low-frequency rhythms in a region of the scalp. Short transients are due to spontaneous discharges of the electrical potential (called *electrode pops*) present between the electrode or its lead (Figure 1.13). These discharges reflect the ability of the electrode-skin interface to function as a capacitor and store electrical charge through the conductive gel that holds the electrode in place. The electrode snap has a characteristic morphology of a very steep ascent and a shallower descent.
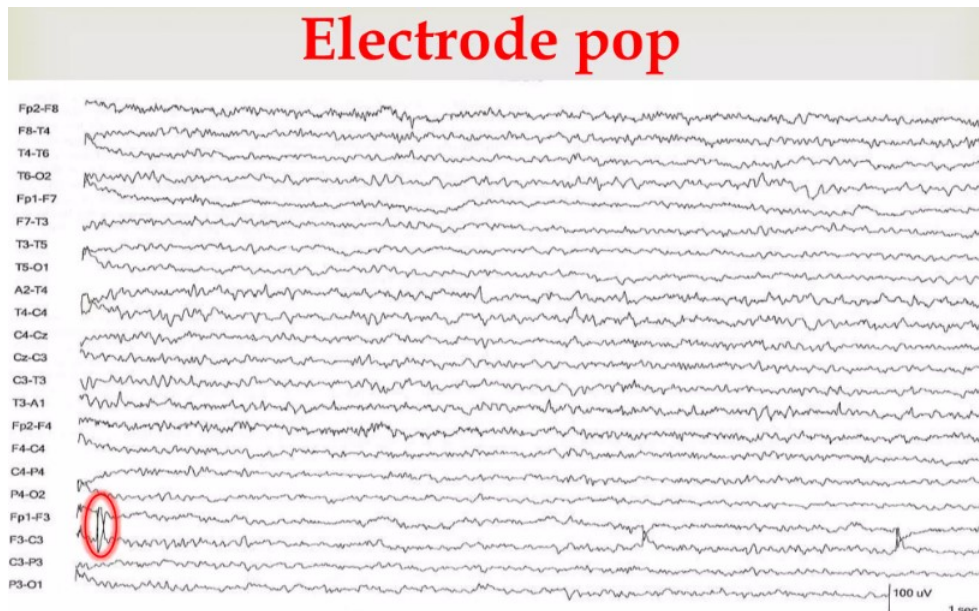
Figure 1.13: The nearly vertical rise followed by the slower fall is typical of electrode pop artifact. Other typical characteristics are an amplitude that is much greater than the surrounding activity, a field which is limited to one electrode and also repeated recurrence within a short time [13].

Poor electrode contact or lead movement produces artefact with a less conserved morphology than electrode pop (Figure 1.14): waves of varying morphology and amplitude that can be rhythmic if the bad

contact occurs in the context of a rhythmic movement, as in the case of tremor. On the other hand, lead
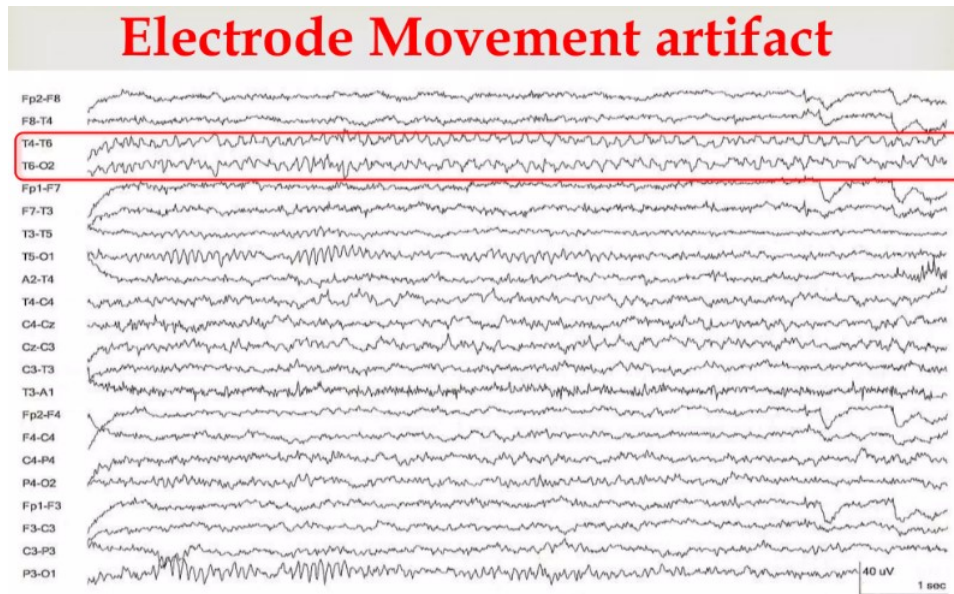
Figure 1.14: The focal slowing in the two red-framed channels has no field below the T6 electrode and has the oscillations typical of rhythmic electrode movement [13].

movement (Figure 1.15) has a more disorganised morphology that in no way resembles EEG activity and often includes a double phase inversion.

The spreading of electrode paste between the electrodes to form a salt bridge (Figure 1.17) on the one
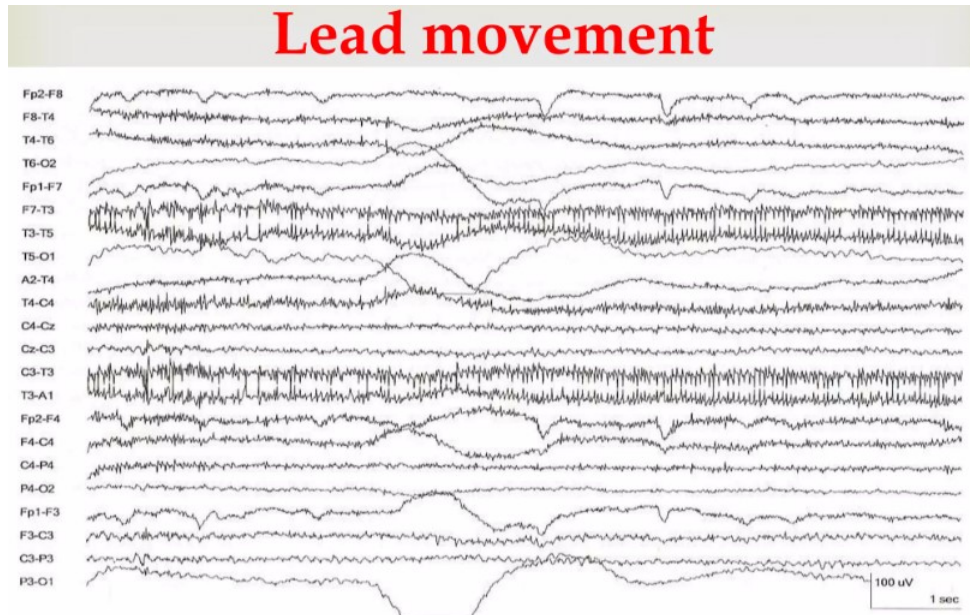
Figure 1.15: Several channels show the artefact through activity that has both unusual large amplitude and low frequency but also a disorganised appearance which is far from a plausible eeg field [13].

hand and the presence of sweat on the scalp (Figure 1.16) on the other hand both produce artefacts due to an unwanted electrical connection between the electrodes forming a channel. Perspiration artefact manifests itself as low-amplitude waves, which generally last longer than 2 seconds and are therefore outside the frequency range of the brain-generated EEG. Salt bridge artefact differs from the perspiration artefact by its lower amplitude, lack of low-frequency oscillations and the fact that it typically includes only one channel. It may appear flat and close to the isoelectric.
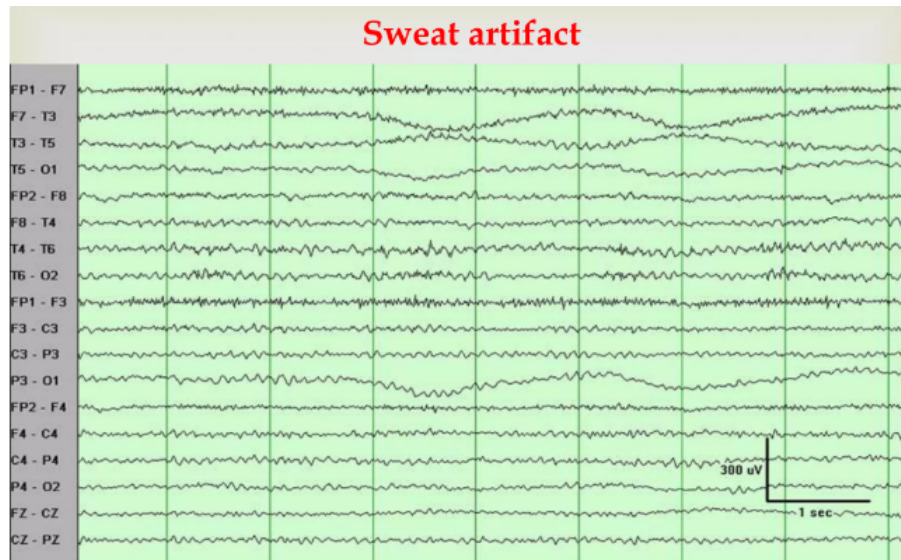
Figure 1.16: This artefact is characterized by very low frequency (0.25 to 0.5 Hz in this specific case) oscillations. Here the distribution (midtemporal electrode T3 and occipital electrode O1) suggests that there is sweat on the left side of the scalp [13].
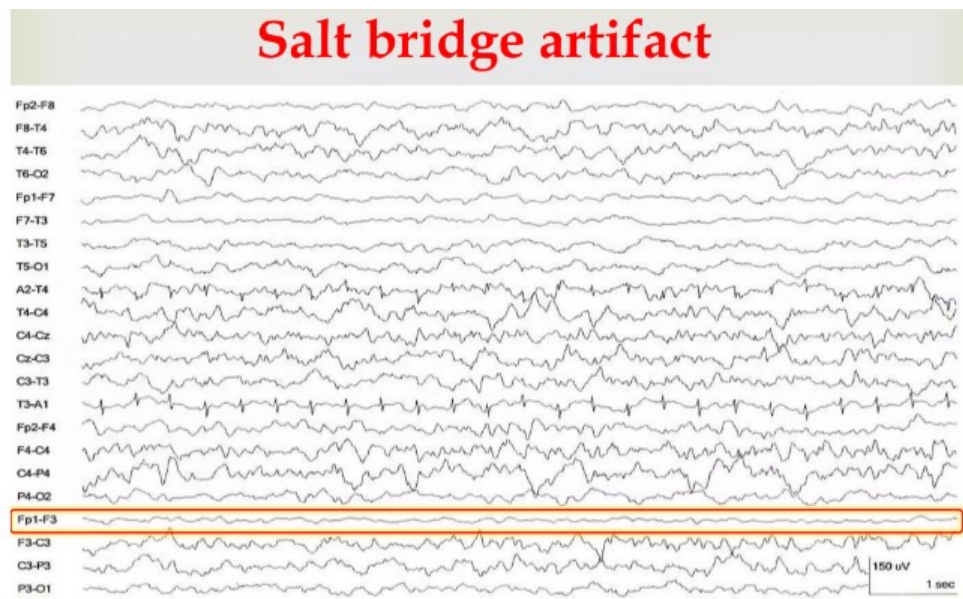
Figure 1.17: The activity in the red-framed channels (those including the left frontal electrodes) is much lower in amplitude and frequency than in the remaining background. The absence of these results, when observed in a referential montage, confirms the presence of an electrolyte bridge between the electrodes involved [13].

External device artefact

The main artefact due to external devices is the 50/60 Hz ambient electrical noise (Figure 1.18). Several types of external devices produce EEG artefacts and they do so either through the electrode fields they generate or through the mechanical effects they produce on the body. The absolute most common external artefact is the one due to the alternating current present in the electrical power supply. The sound usually has a medium to low amplitude and has the monomorphic frequency of the current, which is 50 Hz (60 Hz in North America). This artefact may occur in all channels or only in those channels that include electrodes with poorly matched impedances. Within a hospital environment where, in addition to the EEG acquisition device, many other medical equipment and instruments are used, other forms of noise are easily generated, that in turn produce other artefacts.
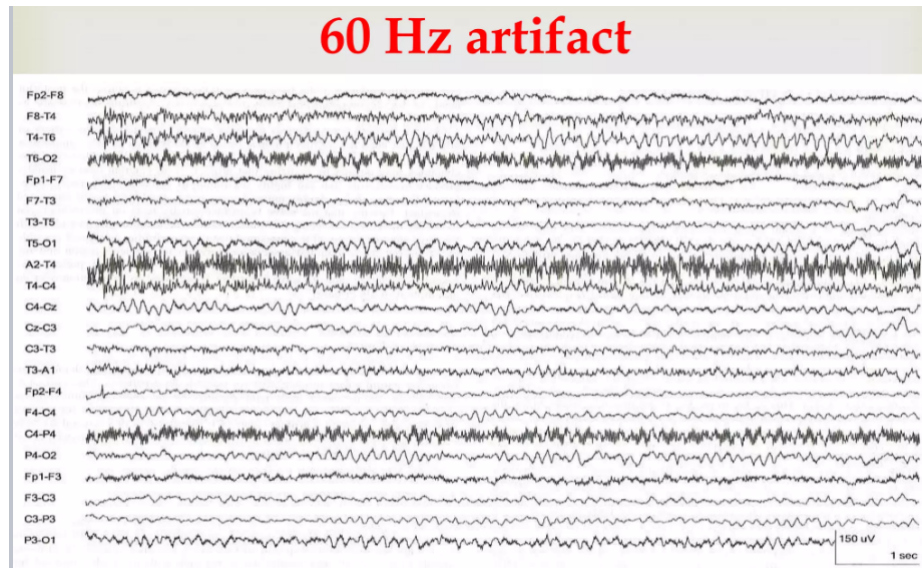
Figure 1.18: The very high frequency of this artifact does not vary. This artifact can be eliminated introducing a Notch filter that rejects the specific frequency band (50 Hz or 60 Hz) [13].

In study situations such as that of this work, there is no need to worry about these types of artefacts.

Muscle artefact

Three types of muscle artefact can be listed:

- Glossokenetic (chew/swallow)

- Photomyogenic (photomyocloinc)

- Surface electromyography (scalp/facial muscle)

During an EEG recording, movement may cause artefacts through the electric fields generated by the muscle and through the movement effect created on the electrode contacts and their leads (Figure 1.19). Indeed, EMG activity is the most significant source of noise in an EEG.
 The frequency of this artefact is higher than that of the clinical EEG. On a morphological level, it may either appear very regular and thus be confused with beta-band activity or it may appear as repetitive spikes if the low-pass filter is set at 35 Hz or below. Without this filtering, the EMG artefact usually has a more disorganised appearance because individual myogenic potentials overlap each other and are rarely distinguishable. This happens in conjunction with the activity of involuntary motor units such as from fibrillations and has a classic EMG wave appearance. The duration of the EMG artifact varies depending on the duration of the muscle activity, so from less than one second to the entire EEG recording.
Logically it appears in regions below the muscles, so on the channels comprising the frontal and temporal electrodes.
The photomyogenic artifact (Figure 1.20) may appear, on the frontal and periorbital regions bilaterally, with photic stimulation as a response of the facial muscles to the flash of light. This response has a latency of 50 ms from the stobe flash and can occur with both eyes open and closed, but more frequently in the latter case. It obviously disappears consistently with the stop of photic stimulation. Also swallowing and speaking produce EMG artifacts. This is called glossokinetic artifact and it has a wide field with a maximum frontal amplitude and may comprise either isolated slow waves at delta-band frequency or, more typically, slow waves with overlapping faster frequencies.
As the frontal muscle extends over the central frontal region, the EMG artifact often co-localises with the region of maximum beta activity resembling its characteristic frequency over 25 Hz. The main characteristic to distinguish the two of them is the morphology: EMG artifact has a sharper contour and less rhythmicity.
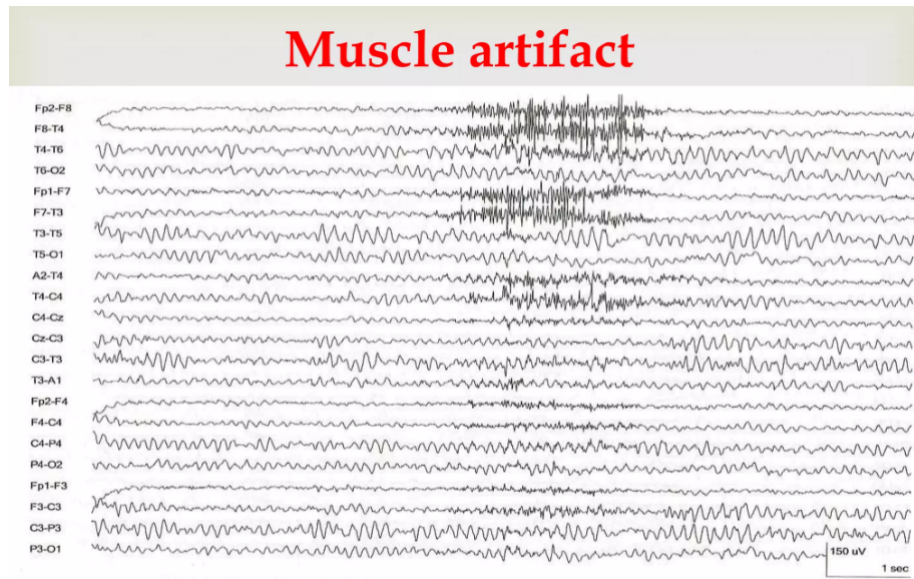
Figure 1.19: The fast, high-amplitude activity across the anterior region is due to the contraction of the facial muscles and has a distribution that reflects the position of the muscles that generate it. Typical of muscle artefact, it begins and ends abruptly [13].
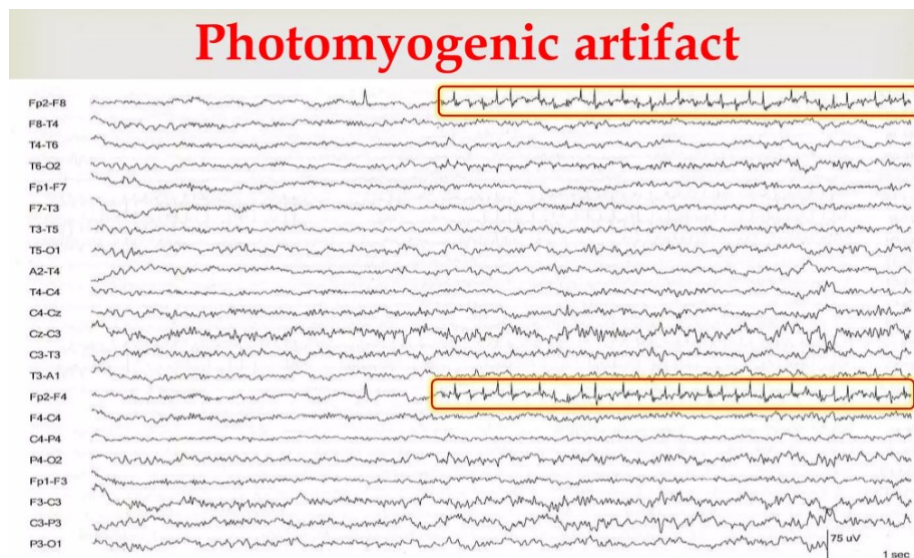
Figure 1.20: Activity contemporaneous with 6 Hz stroboscopic stimulation is evident in the frontal region reflecting involuntary muscle contraction [13].

Ocular artefact

There are many types of ocular artefacts, the most important and frequent of these is the eye blinking artifact.

Most ocular artefacts are related to the electric dipole of each eye. This dipole is oriented along the cornea-retina axis and is positive if oriented towards the cornea and negative if oriented towards the retina. The dipole begins to be relevant in the EEG field when it becomes a moving electric field, thus when there are changes in gaze and eye opening and closure. The vertical movement of the eye (opening and closing) creates an upward deviation called Bell's phenomenon.

Blinking artefact (Figure 1.21) appears on the EEG as a bifrontal, diphasic, synchronous slow wave with a field limited to the frontal region.

Another fairly frequent artifact is what is called eye flutter (Figure 1.22). This type of artefact is also related to the vertical movements of the eye, however it differs from eye blinking in that it is faster and has a smaller amplitude. Due to these characteristics, it is very reminiscent of delta activity.

19
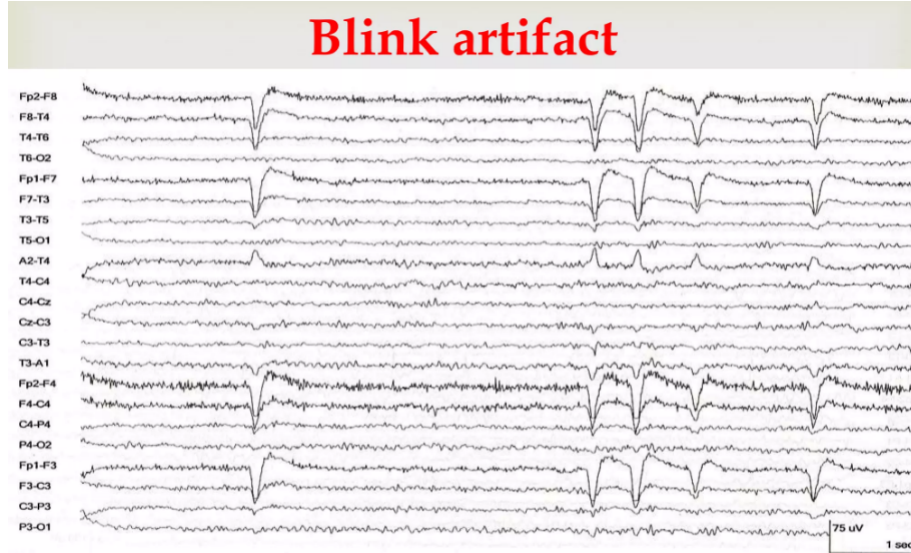
Figure 1.21: Potentials like the ones shown here, bifrontal, biphasic and with this specific morphology are undoubtedly eye blinking artifacts [13].
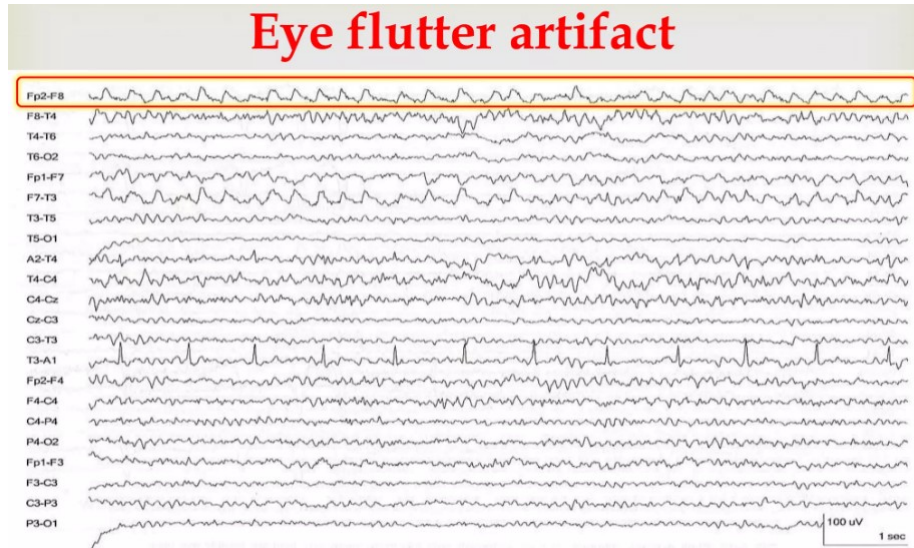
Figure 1.22: The morphology characterized by medium amplitude and low frequency activity confined to the frontal poles identifies the ocular artifact. Compared to the blink artifact, the flutter artifact is distinguished by its typically lower amplitude and more rhythmic appearance [13].

Lateral-gaze ocular artefact appears most during drowsiness, when the eyes make slow, repetitive lateral movements. This generates slow, rhythmic artefacts anteriorly with a field that has its maximum at the frontal poles and remains within a frequency below 1 Hz. It may appear to be an unstable baseline of EEG activity but the opposite polarity slowing allows to distinguish them. This artefact usually occurs intermittently and is accompanied by slowing of the alpha rhythm.

1.3   Cardiovascular system

In the following sections, we will briefly describe the anatomical structure of the heart, its main functions and how the cardiac cycle works. Then a description of the ECG signal follows.

The cardiovascular system contributes to maintain homeostasis of the body's internal environment by ensuring, through blood circulation, the rapid transport of nutrients and oxygen to cells throughout the body and by ensuring the transport of waste products and carbon dioxide to the organs responsible for
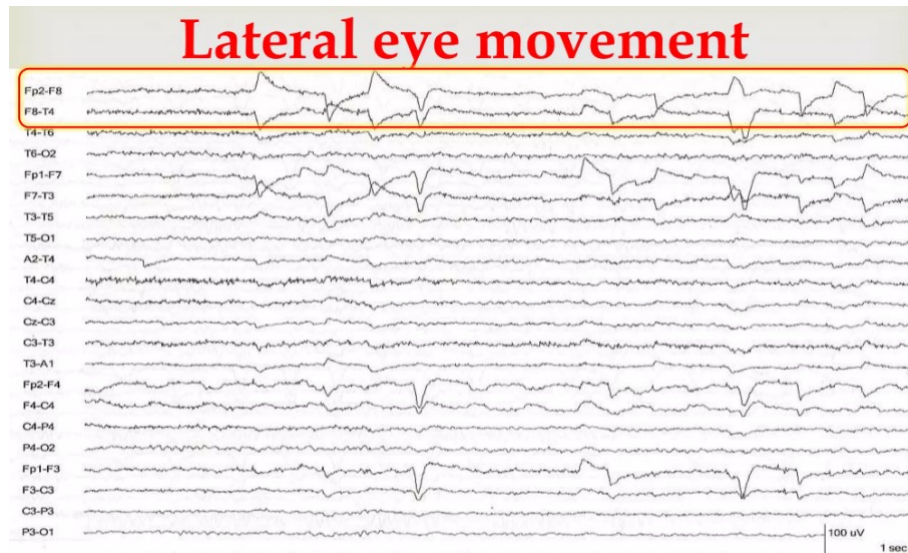
Figure 1.23: Positive and negative phase inversions are observed on electrodes F7 and F8. The frontal horizontal dipole is what characterizes lateral eye movements, but the artefact is also distinguished by its morphology, having a more abrupt transition between positive slopes and negative slopes than blinks and most flutters [13].

their elimination.

The cardiovascular system consists of three elements: the heart, blood vessels and blood. The heart is not only a muscle that pumps blood through blood vessels to various organs to bring oxygen and nutrients to the tissues and remove carbon dioxide and waste products; the heart also has sensory and endocrine functions that help regulate cardiovascular parameters such as plasma volume and blood pressure. Blood vessels are not merely conduits for the passage of blood, but are also important sensory and effector organs that regulate blood pressure and the distribution of blood to various parts of the body. The blood not only carries nutrients and catabolites, but also transports hormones from one part of the body to another and, acting as a communication system, works in cooperation with the nervous system.

1.3.1   Heart anatomy

The heart is a muscle located in the centre of the thoracic cavity (Figure 1.24), just above the diaphragm; it is surrounded by a membranous sac, called the pericardium, containing the pericardial fluid that lubricates the heart during beats. The heart is made up of four chambers: the two upper chambers, the atria, receive the blood returning to the heart from the venous vessels, while the two lower chambers, the ventricles, receive the blood from the atria and generate the pressure needed to push the blood out of the heart into the great arteries.

The heart can be functionally divided into a left and a right half: the left atrium and ventricle constitute the left heart, while the right atrium and ventricle constitute the right heart. The portion of the septum separating the two atria is called the interatrial septum, while the interventricular septum separates the two ventricles.

The cardiac chambers are engaged in repeated phases of contraction and release that constitute the cardiac cycle. Blood is pushed from the atria into the ventricles, and from them into the arteries downstream thanks to a pressure gradient between cardiac chambers.

Blood flow in the opposite direction must be prevented. Four heart valves ensure the right flowing:

- the atrioventricular valves (AV valves): they allow blood to flow from the atrium to the ventricle, preventing reverse flow. These valves open and close in response to the cyclical variations in pressure that occur with each heartbeat. They are open when atrial pressure is higher than ventricular pressure, and are closed in the opposite case. The left AV valve has two flaps, or cusps, and is called the bicuspid valve (or mitral valve), while the right AV valve has three cusps and is therefore called the tricuspid valve.

- the semilunar valves: these are located between the ventricles and the arteries. The aortic valve is located between the left ventricle and the aorta, while the pulmonary valve is located between

21

the right ventricle and the pulmonary trunk. The principle of operation is the same as the other two valves, i.e. they open when the ventricular pressure exceeds the downstream arterial pressure, allowing blood to leave the ventricles and enter the arteries; in the opposite situation they close, thus preventing blood from flowing backwards from the arteries into the ventricles.
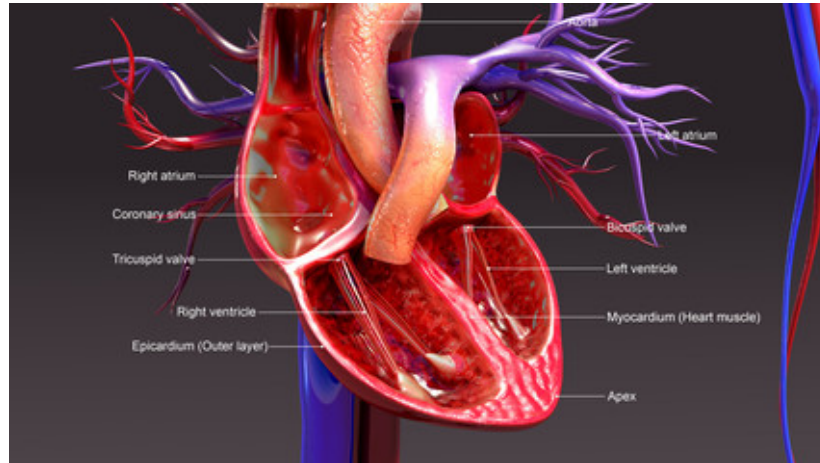
Figure 1.24: Section of the anatomy of the heart [15].

1.3.2 Heart electrical activity and autorhytmic cells

In order to adequately pump blood into the circulatory system, the heart muscle must contract synchronously, i.e. first both atria contract, then both ventricles in succession. The cardiac contractions are coordinated by an elaborate conduction system that determines the sequence of excitation of the cardiac muscle cells. The heart is an autonomous muscle; it does not receive commands from the central nervous system to contract, but its contractions are generated by signals originating within the muscle itself. The heart's ability to generate signals that periodically activate its contractions, generating its own rhythm, is called autorhythmicity. The heart's autorhythmicity is due to the action of the autorythmic cells that do not generate a contractile force, but initiate and coordinate the rhythm of the heartbeats. There are two types of autorhythmic cells:

- *pacemaker cells*: they initiate action potentials and establish the heart rhythm by generating the regular discharge of action potentials. These cells are mainly concentrated in two specific areas of the myocardium: the sinoatrial node (SA node), located in the upper wall of the right atrium, at the outlet of the superior vena cava, and the atrioventricular node (AV node), located near the tricuspid valve in the interatrial septum. The spontaneous discharge frequencies of the cells of the two nodes are different. In fact, those of the SA node have a higher discharge frequency and the heartbeat is almost always generated from there. In contrast, the AV node only rarely generates cardiac muscle contractions, acting as an emergency system if the SA node ceases to generate impulses or if it slows down excessively.

- *conduction fibres*: they conduct the action potentials generated by the pacemaker cells and propagate them in a highly coordinated manner to all other regions of the heart. Although all cardiac muscle fibres are capable of transmitting action potentials, conduction fibres differ from those of the common myocardium in that they are larger in diameter and can therefore conduct action potentials more rapidly (at a speed of more than 4 m/s as opposed to 0.3-0.5 m/s for the other cardiac fibres).

These two types of cells constitute the conduction system of the heart. The propagation of impulses in the heart muscle occurs in an orderly manner, producing a kind of depolarising wave front, referred to as an 'excitation wave'. The flow of electrical current through the heart during a cardiac cycle is recorded by the electrocardiography (ECG). In the following sections we will describe the characteristics of the ECG signal and how it is acquired.

1.4 ECG signal and cardiac cycle

The ECG is the recording of the electrical activity generated by the cells of the heart that reaches the body surface. Electrocardiography is the word derived from *electro* (greek for electricity), *cardio* (greek for heart), *graph* (greek for "to write").
Originally the ECG signal was printed on graph paper and was displayed normally sliding it with a speed of 25 mm/s (standard speed). Today the ECG signal is shown on video on specific displays, scrolling it at the same speed, or multiples of it (50 mm/s or 100 mm/s) . Time is represented along the horizontal axis and the amplitude of the signal along the vertical axis. Each small box (1 mm x 1 mm) corresponds to 40 ms time and 0.1 mV, so that the 5 mm x 5 mm box amplitude represents 200 ms time and 0.5 mV amplitude (Figure 1.25). The isoelectrical line represents the resting potential of the heart, the
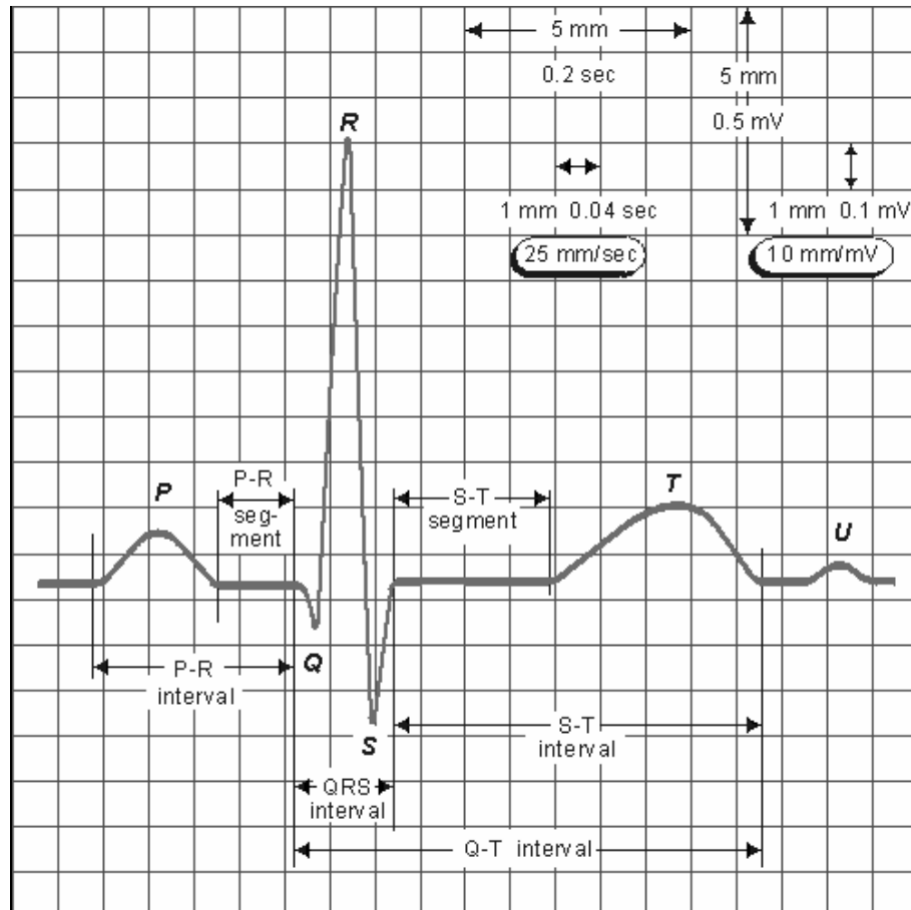
Figure 1.25: Electrical events of a single cardiac cycle and its representation on ECG paper [16].

electrical events are represented by deflection away from this line. Cardiac cycles are initiated by the depolarization of the SA node, which is the instant when the cell from being negatively charged becomes positively charged. The cells that are present at SA node depolarize by themselves and this property is called *automaticity*. From this moment all the neighboring cells are going to depolarize and the wave of electrical depolarization is conducted through the cardiac muscle of both the atria. This is called **Atrial Depolarization** and it represents the **P wave**. The P wave must have an amplitude ranging from 70-80 μV to 150-160 μV. The depolarizing wave causes contraction of the atria pushing blood into the ventricles. The wave of depolaritazion from SA node reaches the atrio-ventricular node through the internodal pathways. AV node then depolarizes and conducts, creating also a delay between the atria and the ventricles. Both atria and ventricles contract the same number of times, but not at the same moment of time, there is a slight delay (about 0.1 s). If atria and ventricles contract simultaneously, then they be passing the blood against each other and this will not move the blood in the right direction. So, by creating the delay, atria can contract first, passing the blood to the ventricles, and then, after 0.1 s, the ventricles can contract and move the blood onwards. The **Atrial-Ventricular (AV) node Depolarization** represents the **PR-interval.**
AV node conducts the depolarization to the Bundle of His, and this represents the **QRS complex**. The

wave moves quickly through the specialized conducting tissue and at this point the electrical signal can spread in all directions through Purkrinje fibers. The coordinated, synchronized depolarization produces an effective contraction of both ventricles. The **Q wave**, which marks the beginning of depolarization of the ventricles, should never be present in first derivation, it should always be below 50-60 μV. The **R wave** (peak of the QRS complex) marks the point of maximum depolarization of the ventricles, the **S wave** marks the end of the ventricular depolarization event. The duration of the QRS complex indicates the conduction time of the depolarization, therefore it gives a functional indication.

After depolarization and the contraction, the ventricle re-polarizes, returning to the resting potential. The **Ventricle Repolarization** represents the **T wave** [17].

The U wave is still not interpreted in a safe way today, it is present in children, it disappears in adults in 80-90% of cases. Since its physiological meaning is not well known, normally this wave is neglected.

1.4.1   ECG Leads

Leads are used to acquire the ECG signal. An ECG lead is a graphical description of the electrical activity of the heart and it is created by analysing the electrical currents detected by several electrodes.

Every leads represents difference in electrical potentials measured in two points in space. The simplest leads are composed using only two electrode. The electrocardiograph defines one electrode as exploring (positive) and the other as reference (negative) electrode. In most leads, however, the reference is actually composed of a combination of two or three electrodes. Regardless of how the exploring electrode and the reference is set up, the vectors have the same impact on the ECG curve. A vector heading towards the exploring electrode yields a positive wave/deflection and vice versa (Figure 1.26). Electrical potential
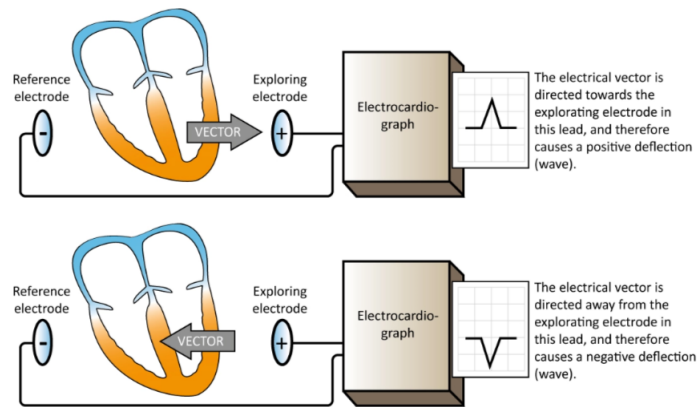
Figure 1.26: Positive and negative deflection depending on the electrical vector direction [18].

difference arises as the electrical impulse travels through the heart and it is defined as a difference in electric potential between two measurement points (skin electrodes).

Numerous ECG lead systems have been tested but the **standard 12-lead ECG** is still the most used and the most important lead system to master. The 12-lead ECG displays, as the name implies, 12 leads which are derived by means of 10 electrodes. Three of these leads are simply the result of comparing electrical potentials recorded by two electrodes; one electrode is exploring, while the other is a reference electrode. In the remaining 9 leads the exploring electrode is still just one electrode but the reference is obtained by combining two or three electrodes. These 12 leads consist of two sets of ECG leads: 6 limb leads and 6 chest/precordial leads. In particular the 6 Limb Leads, which include 3 Standard Limbs leads (Lead I, II, III) and 3 Augmented Limb leads (aVR, aVL and aVF), have the exploring electrode and the reference point placed in the frontal plane. On the other hand, the 6 Chest/Precordial Leads (V_1-V_6) have the exploring electrodes located anteriorly on the chest wall and the reference point located inside the chest.

The axis of a particular lead represents the viewpoint from which it looks at the heart.

In 10 electrodes, 4 are limb electrodes and 6 are chest electrodes. Speaking of the 4 limb electrodes, they are placed as follows:

- RA on the right arm, at the level of the wrist

- LA on the left arm, at the level of the wrist

- RL on the right leg, at the level of the ankle

- LL on the left leg, at the level of the ankle

Note that the electrode on the right leg is not included in any lead, but serves as a ground wire.

Leads I, II and III are *Einthoven's original leads*, and they can be presented with the *Einthoven's triangle*. Leads aVR, aVL and aVF were constructed by *Goldberger*; their reference point is the average of two electrodes. Lead aVR can be inverted into lead -aVR which is recommended as it may facilitate interpretation. The Figure 1.27 shows how the electrodes are connected in order to obtain these six leads. Lead II, aVF and III are called **inferior limb leads**, because they primarily observe the inferior wall of
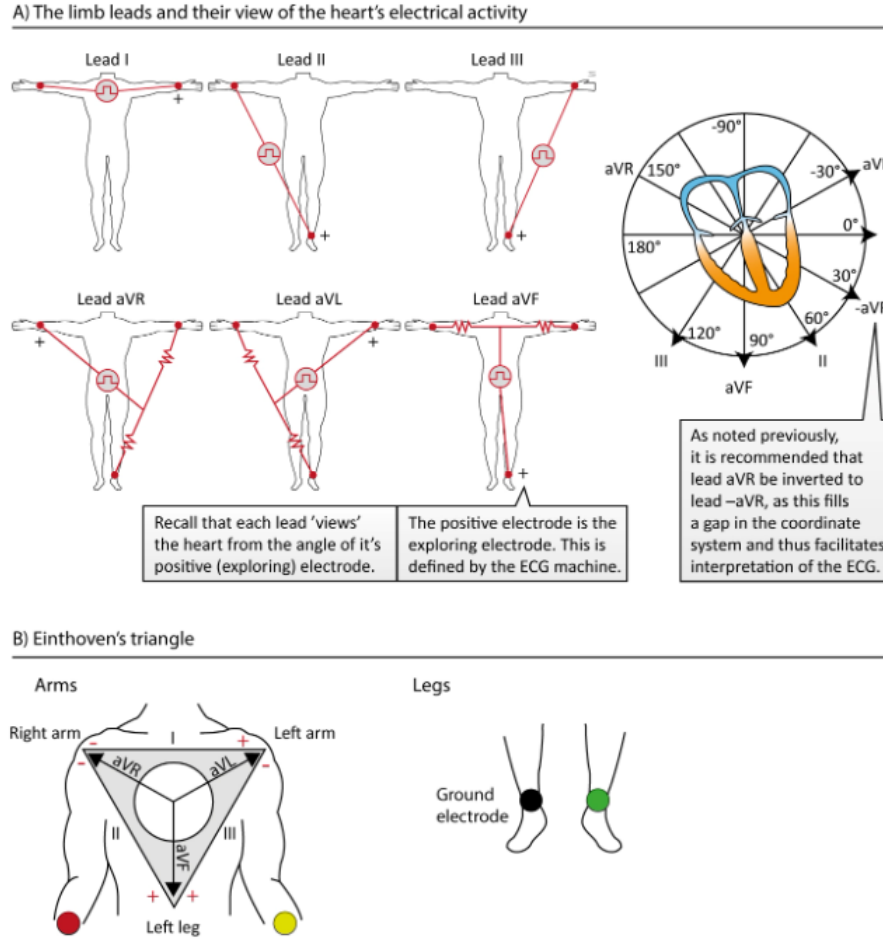
Figure 1.27: The organization of limb leads [18].

the left ventricle. Lead aVL, I and -aVR are called **lateral limb leads**, because they primarily observe the lateral wall of the left ventricle. All six limb leads are presented in a coordinate system; there is 30° distance between each lead, except from the gap between lead I and lead II. To eliminate this gap, lead aVR can be inverted into lead -aVR, and this is actually meaningful as it facilitates ECG interpretation. Here a more detailed explanation of the leads follows.

Leads I, II and III compare electrical potential differences between two electrodes. Lead I compares the electrode on the left arm with the electrode on the right arm, the first of which is the exploring electrode. It is said that the lead I observes the heart "from the left" because its exploring electrode is placed on the left (at an angle of 0°). Lead II compares the left leg with the right arm, with the leg electrode being the exploring electrode. Therefore, lead II observes the heart from an angle of 60°. Lead III compares the left leg with the left arm, with the left leg electrode being the exploring one. Lead III observes the heart from an angle of 120°.

Lead I, II and III have a spatial organization that forms a triangle in the chest (**Einthoven's triangle**). This triangle can be seen as a circuit, so the Kirchhoff's law should be applyied, resulting in:

$$LeadI + LeadIII = LeadII \tag{1.1}$$

It follows that we need only to know the information in two leads in order to calculate the exact appearance of the remaining lead. Hence, these three leads actually carry two pieces of information, observed from

three angles.

The augmented leads (the letter **a** stands for **augmented**, **V** for **voltage** and **R** is **right arm**, **L** is **left arm** and **F** is **foot**) were originally constructed by Goldberger, and in this leads the exploring electrode is compared with a reference which is based on the average of the other two limb electrodes.

In aVR the right arm is the exploring electrode and the reference is composed by averaging the left arm and left leg. In lead aVL the left arm electrode is exploring and the lead views the heart from -30°. In lead aVF the exploring electrode is placed on the left leg, so this lead observes the heart directly from south. Since Goldberger's leads are composed of the same electrodes as Einthoven's leads, it is not surprising that all these leads display a mathematical relation. The equations follow:

$$aVL: \frac{LeadI - LeadIII}{2} \tag{1.2}$$

$$-aVR: \frac{LeadI + LeadII}{2} \tag{1.3}$$

$$aVF: \frac{LeadII + LeadIII}{2} \tag{1.4}$$

This means that the augmented leads do not offer any new information, but instead new angles to view the same information. Speaking of the **Chest Leads**, they are derived by comparing the electrical potentials in WCT to the potentials recorded by each of the electrodes placed on the chest wall. The **WCT** is the **Wilson's central terminal** (Figure 1.28), which is a theoretical reference point located approximately in the center of thorax, or more precisely in the centre of Einthoven's triangle. WCT is computed by
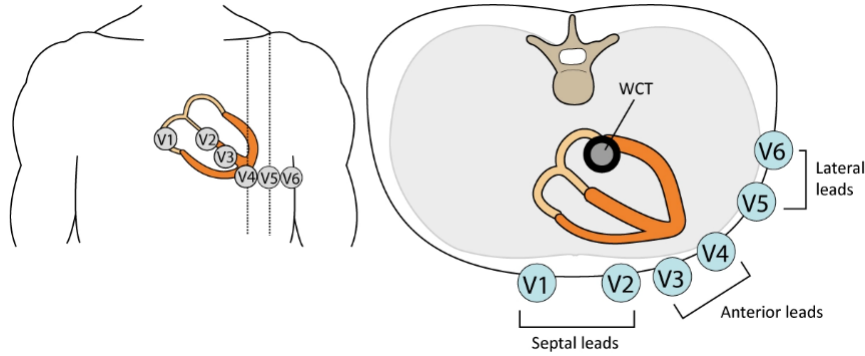
Figure 1.28: WCT: Wilson's central terminal [18].

connecting all three limb electrodes to one terminal which will represent the average of the electrical potentials recorded in the limb electrodes. WCT serves as the reference point for each of the six electrodes placed anteriorly on the chest wall. There are six electrodes on the chest wall and thus six chest leads (Figure 1.29). Each chest lead offers unique information that cannot be derives mathematically from other leads. Since the exploring electrode and the reference are placed in the horizontal plane, these leads primarily observe vectors moving in that plane.

The chest/precordial electrodes are placed as follows:

- V1: fourth intercostal space, to the right of sternum

- V2: fourth intercostal space, to the left sternum

- V3: placed diagonally between V2 and V4

- V4: between rib 5 and 6 in the midclavicular line

- V5: placed on the same level as V4, but in the anterior axillary line

- V6: placed on the same level as V4 and V5, but in the midaxillary line
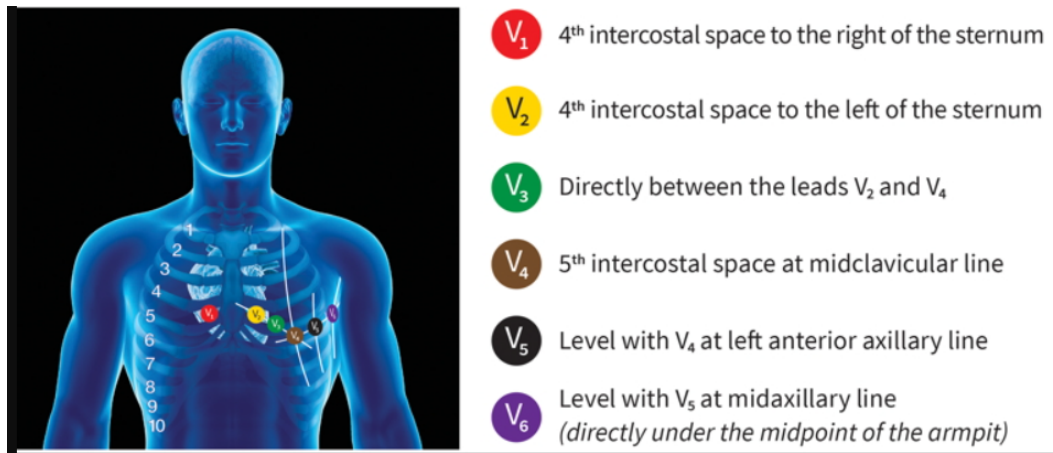
Figure 1.29: The chest (precordial) leads [19].

Chapter 2

Biofeedback, Neurofeedback and Brain Entrainment

2.1 Storical Overview

Behaviour medicine is the field relating to the development of behaviour science knowledge and techniques. This field is relevant to understand physical well-being and discomfort. The application of this science and techniques is essential to the fields of diagnosis, prevention, treatment and rehabilitation. Behavioural medicine also emerged because traditional medical approaches were not sufficient to handle and treat many chronic disorders, conditions and maladaptive or health-damaging behaviours. Behavioural medicine places great emphasis on the patient's role in both prevention and recovery from organic issues.

This same emphasis is also placed by applied or clinical biofeedback. In fact, clinical biofeedback is regarded by many practitioners as a major speciality of behavioural medicine, but with a broader scope. An important branch of behavioural medicine focuses on researching the effects of stress in causing physical symptoms and altering the immune system. But in reality, stress research began long before the development of behavioural medicine or biofeedback, in fact both fields have their roots partly in stress research.

Physicist Claude Bernard developed the concept of physical 'homeostasis' as the major process the body uses to maintain its equilibrium. Physical and mental disorders are thought to occur due to malfunctions in certain homeostatic feedback mechanisms, and one of the major effects of these homeostatic imbalances would be stress. The focus of biofeedback on detecting and generating changes in the body's processes contributes to the development of new behavioural techniques to alleviate the effects of stress.

Many methods of stress relief have been developed over decades, but without high-quality instrumentation that accurately and reliably measured physiological events, the emergence of biofeedback would not have been possible. Progress came after the war. Biomedical engineers developed technology that is both non-invasive and highly sophisticated; surface recordings used to acquire biomedical signals allow feedback within many different physiological activities. Thanks to this instrumentation, it has been possible to constantly monitor and amplify electronic and electromechanical signals to transform them into visual or auditory feedback, therefore into understandable information.

The term *biofeedback* is a shortcut for referring to external psychophysiological feedback and increased proprioception. The basic idea is to provide the user with precise information about what is happening inside their body, including the brain. The field that comes closest to information processing and feedback is cybernetics. A fundamental principle of cybernetics is that a variable cannot be controlled until the information is made available to the controller, and this information provided is called 'feedback'. Another important principle of this science is based on the fact that feedback makes learning possible. In applied feedback, individuals receive clear and direct feedback concerning their physiological functions, and this helps them to increase, reduce or possibly adjust the specific parameter in question.

The workhorse of biofeedback has long been electromyography. Several uses of EMG feedback for the rehabilitation of patients after strokes have been reported since 1964. These studies have been instrumental in the development of applied biofeedback, especially for the field of neuromuscular rehanilitation, gaining great support among clinicians and researchers.

Many studies on altered states of consciousness have pushed the use of electroencephalography into the field of biofeedback, leading it to focus on the functional relationship between the brain and behaviour. In the early 1960s, studies on the relationship between alpha wave activity on the one hand and emotional

states and certain states of consciousness on the other began to appear. Alpha-wave biofeedback received more attention in the late 1960s, and most clinical applications were focused on general relaxation. Many researchers and practitioners continued to support the value of alpha rhythm biofeedback into the early 1980s, despite recognising that "there was no clear-cut and concrete rationale to explain why it should help patients".

Meanwhile, other researchers investigated specialised learning processes and other EEG parameters, such as theta waves, evoked cortical responses, and the synchrony of EEG phases on different areas of the cerebral cortex. At that point, the different brain areas and EEG parameters became the focus of well-conducted studies. These studies were continued and emerged as effective therapies for carefully selected patients with CNS disorders such as epilepsy, as well as patients with attention deficit and hyperactivity disorders. [20]

2.2 Types of biofeedback

Biofeedback (BFB) and neurofeedback (NFB) procedures are performed on the basis of the "physiological mirror" principle, whereby the patient has the opportunity to see, hear and receive updates on changes in his various physiological processes.

Functional biocontrol based on biofeedback involves training of psychic self-regulation capabilities. The various biofeedback trainings aim to normalize the functional state of various body systems such as the CNS, the ANS, the cardiovascular system, the respiratory system, the locomotor system and others. This is done by developing relaxation skills, reduction of muscle tension, normalization of heart rate and heart rate variability, reduction of the tone of vessels of different calibers, normalization of blood pressure and cerebral and central hemodynamic parameters, change in the ratio of EEG rhythms and their topical characteristics [21]. Biofeedback learning shares at least three important aspects related to classical conditioning: generalization, extinction and discrimination.

- *Generalization* in the sense that the new conditioned stimulus must be activated in more than one place so that learning is not restricted to the experimental condition alone. It must be ensured that the relaxation, learnt during the experimental procedure through the apparatus, continues and is put into practice in everyday life situations.

- *Extinction* refers to the gradual loss of the effect. In biofeedback, it is important that the training is continued even after the goals have been achieved to ensure a solidification of the learning. Hence, it is necessary to have extra sessions after achievement in order to prevent or limit extinction.

- *Discrimination*, in the sense that stimuli are customised to the subject and his or her physiological responses [22].

A more detailed analysis of the different types of biofeedback training that are used today follows.

2.2.1 Temperature Biofeedback

The main goal is to correct changes in functional status associated with increased tone of the sympathetic nervous system, which can be manifested by emotional stress and increased tone of blood vessel smooth muscles. There are now numerous indications on the possibility of normalizing blood pressure by regulating local temperature by reducing vascular tone as a consequence of changes in the general functional state of the central nervous system. Trainings on skin surface temperature accelerate and increase the efficiency of teaching mental relaxation skills.

In humans the temperature of the so-called "core" of the body (internal organs, brain and blood) is normally maintained at a constant level of about 36.6° with the help of thermoregulation. The normal temperature of the fingers, on the other hand, is considered 25-34°; the temperature of the fingers reflects the intensity of blood flow in the subcutaneous vessels and depends on both internal and external factors. External stimuli or internal stimuli, such as fear or negative thoughts and emotions, lead to the activation of the sympathetic nervous system and a decrease in peripheral temperature. On the other hand, external stimuli such as feelings of calm and safety lead to the activation of the parasympathetic nervous system and an increase in peripheral temperature.

When you start a temperature relaxation biofeedback training, the relaxation effect is able to expand towards the whole body creating a general relaxation sensation. In self-regulation of the involuntary thermoregulatory function and in achieving relaxation, autogenic training is often used. Autogenic training

aims to restore the dynamic balance of the homeostatic mechanism of the human body, which is disturbed by stressful situations, by increasing the tone of the parasympathetic division of the autonomic nervous system. In temperature biofeedback training, visualization techniques in which the client uses mental representation of heat are used. The moment he manages to increase the temperature of his hands, a temperature graph appears on the computer monitor, as in a "physiological mirror", and at that point the client must pay attention to the internal sensations that have accompanied this change, learning, thus a self-regulation. Only an adhesive sensor on the finger is used for this type of training; there is no need to attach a neutral electrode. Usually the control parameter (the one through which the feedback is provided) is an average temperature value. Two sensors, one on the right hand and the other on the left hand, can also be used to control and train the thermal balance between the two hands. [21]

2.2.2   Electrodermal Biofeedback

Electrodermal activity is one of the most reliable signals correlated to states of neurophysical stress and emotional responses to external stimuli. Galvanic Skin Resistance can be considered as a sensory indicator of emotional intensity, an indicator of an orientational or defensive response to external stimuli and a marker for emotional distress. (CITE: mnanuale rehacor 2) In fact, the electrodermal activity (EDA) resides under the control of the sympathetic nervous system; when a person is in a state of stress due to external stimuli or internal emotional stress, the eccrine sweat glands located on the palms of the hands and soles of the feet come into activity causing the pores to dilate and consequently decreasing resistance of the skin to the possible passage of current.
EDA manifests itself by showing two specific components: a component called "phasic" consisting of spikes evoked by external stimuli, therefore from instantaneous situations, and a component called "tonic" which appears as a baseline and represents long-term tendencies of changes in EDA, characterizing changes in the activation of the autonomic nervous system [21].
The sensors used to record the electrodermal activity are two: a galvanic skin response (GSR) sensor which allows to record only the phasic component of the response, and the skin conductance (SkC) sensor which allows to record both a phasic and longer changes, hence the tonic component of the response. This type of training can have several objectives, the main ones being the extinction of the bursts of the phasic response to the stress-generating model in the form of various graphs and sound images of a stress-generating nature. This means training the skills to manage one's psychoemotional state in the face of stressful situations. Another important goal of prolonged training could be to have better management of anxiety and stress over the long term, thus improving the tonic component of one's electrodermal response.
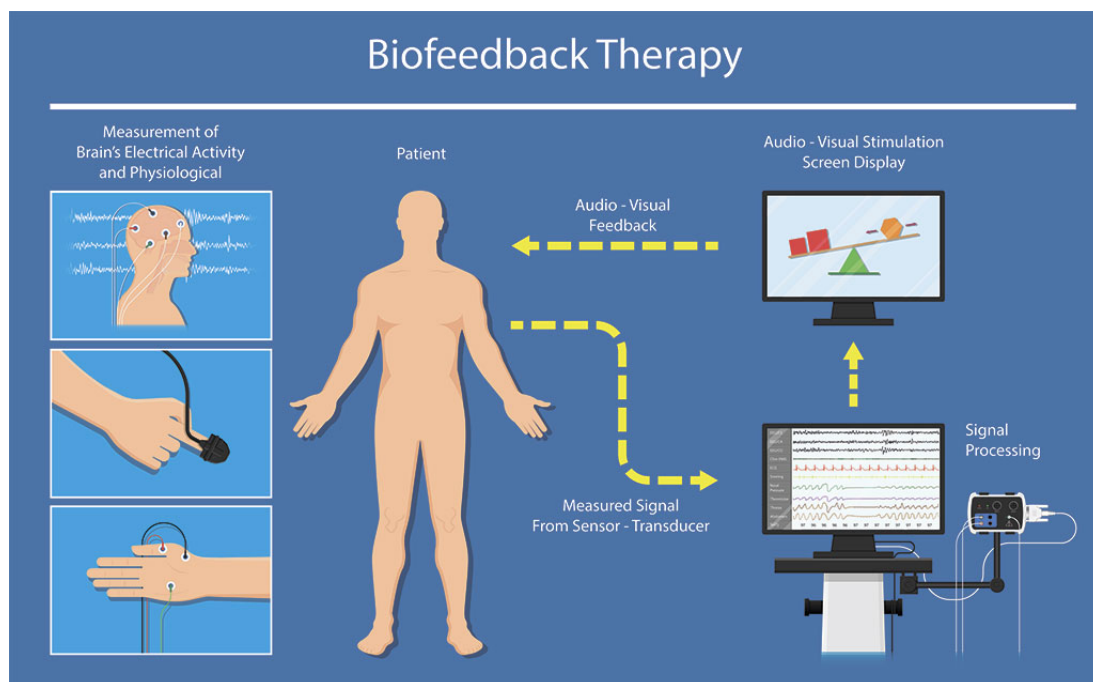
Figure 2.1: Scheme of a Biofeedback training protocol [23].

2.2.3 Electromiographic Biofeedback

EMG training is used to solve two types of problems. The first concerns a decrease in general, psycho-emotional stress and anxiety, by reducing excessive muscular activity. Trainings of this type are indicated for a wide variety of functional disorders (neurotic disorders, tension headaches, pain syndrome, etc.), when, in the absence of organic damage to the nervous or muscular system, functional disorders of muscle activity are observed, more often in the form of chronic unconscious increase in muscle tone. The second problem concerns the correction of central and peripheral motor disorders of various origins by improving voluntary motor activity, reducing spasticity, hyperkinetic activity and pathological reflexes. [21]
During this type of training, surface EMG electrodes are placed in different muscles of the body, depending on the purpose (mainly trapezius muscle) of the training. The electrodes, connected to an EMG device, pick up a signal whose envelope is calculated, reflecting the dynamics of muscle tension.

2.2.4 Pulse and heart rate biofeedback

Heart rate training is indicated in cases of decrease in the level of the body's defenses, with stress reactions accompanied by functional disorders of the cardiorespiratory system. It can be recommended in cases of increased resting heart rate, decreased heart rate variability, or to increase the body's functional reserves and general health level.
Heart rate control using BFB is an important connection in the prevention and correction of some functional disorders of the cardiovascular system. By reducing or accelerating the rate of heart contractions by weakening or strengthening the effect of the sympathetic and parasympathetic parts of the nervous system on the heart, a person is able, to various extents, to affect the contractility, excitability and conduction functions of the myocardium.
A typical pattern of electrodes used during heart rate BFB training includes the standard first lead ECG, in which the ECG is recorded between the left and right hands, with an additional neutral electrode placed on the left wrist. The goal of this lead is to receive an ECG signal with a well-pronounced QRS complex and a clearly visible R wave. [21].
In a more complex heart rate training, patients might also wear a device connected to sensors in either the ears or fingers or sensors placed on the wrists, chest, or torso.
Starting from the analysis of the acquired signals, statistical methods are used to determine quantitative indicators which, mainly starting from the duration of the RR intervals, allow to obtain control parameters for biofeedback and secondary parameters to control the combined dynamics of cardiac cycles and of respiratory cycles.

2.2.5 Respiratory biofeedback

Breathing trainings are aimed at training and consolidating relaxation diaphragmatic breathing skills to increase lung ventilation, normalize the autonomic balance of body nervous regulation, and achieve mental relaxation of the client.
This type of training is designed to correct pathological conditions such as hypo- or hyperventilation syndrome, with the ultimate goal of normalizing the respiratory cycle. All this is obtained by learning from biofeedback signals which are based on a gradual increase in respiratory depth and decrease in frequency of breathing, simultaneously switching to the diaphragmatic type of breathing. This reorganization is aimed not only at improving the functioning of the lungs, but also at affecting other aspects, including the mental one, increasing the overall vitality of the body. The respiratory training performed by the client, when the execution becomes automated, leads to persistent changes in the mode of ventilation towards the desired direction. The pathologies for which this type of training is indicated are post-traumatic, neurotic and neurotic-like syndromes, hyperventilation of various origins and a number of other functional disorders of the respiratory system.
Abdominal or diaphragmatic breathing, compared to chest breathing, helps reduce heart rate, cardiac output, and peripheral blood vessel expansion. Diaphragmatic breathing, with an increased respiratory cycle period and an emphasis on exhalation, creates the conditions for the respiration rhythm to resonate with a person's other physiological rhythms, which is great and ensures that normal homeostatic functions of the body are maintained.
For respiratory training, belted respiratory sensors (Figure 2.2) are used which are tied around the torso at different levels (chest and/or abdomen). The two sensors are used simultaneously when determining the degree of participation of the thoracic and abdominal regions in the general breathing pattern. [21].
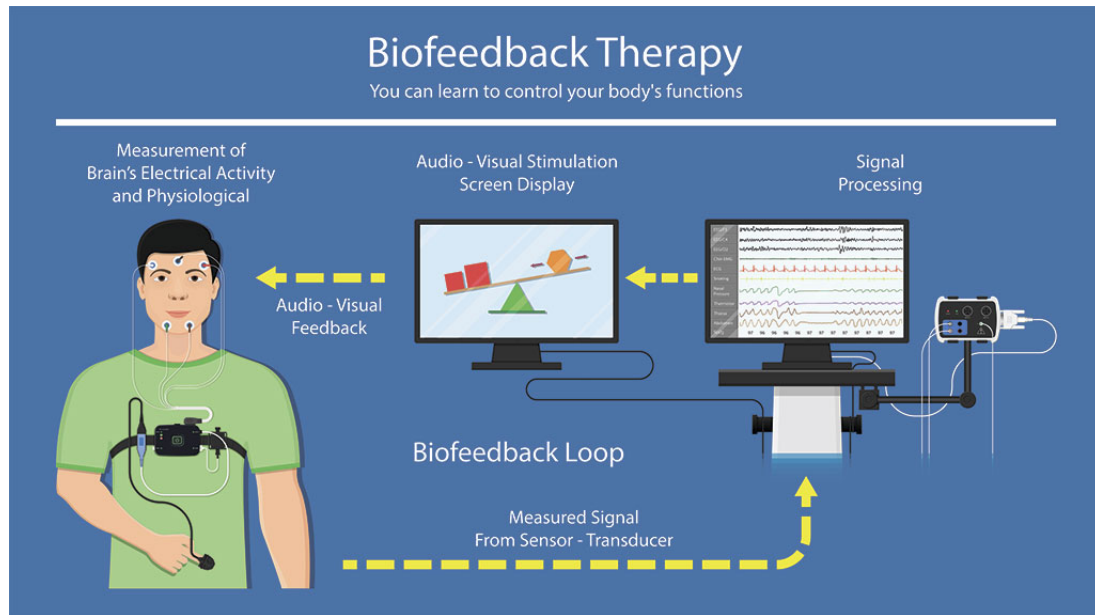
Figure 2.2: Scheme of a Biofeedback training protocol [23].

2.2.6 Blood circulation Biofeedback

The main objective of this type of training is to increase peripheral blood flow and decrease arterial tone, which is characteristic of a person's relaxed state. These things contribute to the normalization (decrease) of blood pressure, correction of functional disorders, for example peripheral angiospasm (impaired peripheral circulation), imbalance of the autonomic nervous system. In fact, this type of training can be used to learn specific skills such as:

- relaxation using peripheral circulation indicators

- improvement of the blood volume pulse (BVP) and reduction of the tone of the main arteries

- lowering of systolic blood pressure in the initial form of arterial hypertension

For this type of training, sensors of various types are used, mainly electrodes for measuring the ECG signal and a photoplethysmograph (PPG). This last sensor is widely used because it is not bulky and very functional; in fact, the PPG indices adequately characterize the pulse volume and tone of the main arteries and reflect their changes in the biocontrol process. Simultaneous monitoring with PPG and ECG allows to control both the chronotropic mechanism (heart rate regulation) and the regulating vascular mechanism. The main parameter acquired by the PPG is the systolic wave amplitude (SWA) which characterizes the blood volume pulse at the point where the sensor is applied. As a rule, the PPG sensor is attached to the terminal phalanges of the fingers, where small arteries and arterioles dominate, whereby the extracted parameter characterizes the tone of peripheral vessels [21].

2.2.7 EEG feedback or Neurofeedback

Neurofeedback is based on the concept of neuroplasticity, i.e. the brain's ability to change its structure over time in response to experience. Our brain is designed to always learn and face new challenges and neurofeedback challenges the brain to become more efficient and effective.

Neurofeedback provides the subject with real-time information about their brain rhythms and brain functioning through sounds, graphics or even vibrations. The brain takes note of this information and gradually modulates its activity in response to it. The training promotes efficiency in utilizing the brain's energy resources and promotes self-awareness (Figure 2.3).

The main point of difference between neurofeedback and traditional drug-based medicine lies in the fact that the first requires consciousness and awareness, while the latter does not; a drug works indiscriminately, with or without the conscious cooperation of the patient. Another major difference is that a drug has an immediate but not a permanent effect because no learning process has taken place, the brain has not learned on its own how to behave differently in order to change its situation and state. On the other side,

biofeedback requires involvement and awareness: the subject has to be in a comfortable situation, he has to sit, concentrate on the feedback and allow the change within his body to take place. Neurofeedback is a kind of experiential learning, it does not come from a single event, but needs to be supported by training that is often required to be done also as homework.

It is a kind of computer-guided learning: information about the brain's electrical activity and metabolic fluctuations is taken from instrumentation and returned to the subject in real time in the form of comprehensible feedback. The aim is to promote awareness so that this leads to functional changes. It is about acquiring a skill of self-regulation, in fact subjects are empowered to regulate their specific functions, event-related potentials, slow cortical potentials, infra-slow frequencies and even regional cerebral blood flow [22].

At the neuronal level, neurofeedback training teaches the brain to modulate excitatory and inhibitory patterns created by specific groups of neurons and to regulate specific neuronal pathways based on the details of the positioning of capture sensors and the feedback algorithms used, thus increasing the flexibility and self-regulation of relaxation and activation patterns. During the procedure the subject becomes aware of the changes that occur within the training and is able to evaluate his progress to achieve better performance.

The Neurofeedback Therapy process involves sensors placed on the scalp to measure the electrical activity of the brain. The positioning of the electrodes is established according to the specific neuronal functions and according to the specific symptoms. Also other methods of monitoring brain activity, such as functional magnetic resonance imaging (fMRI) or hemoencephalography (HEG), can be used [24]. More details will be given in the following paragraphs.
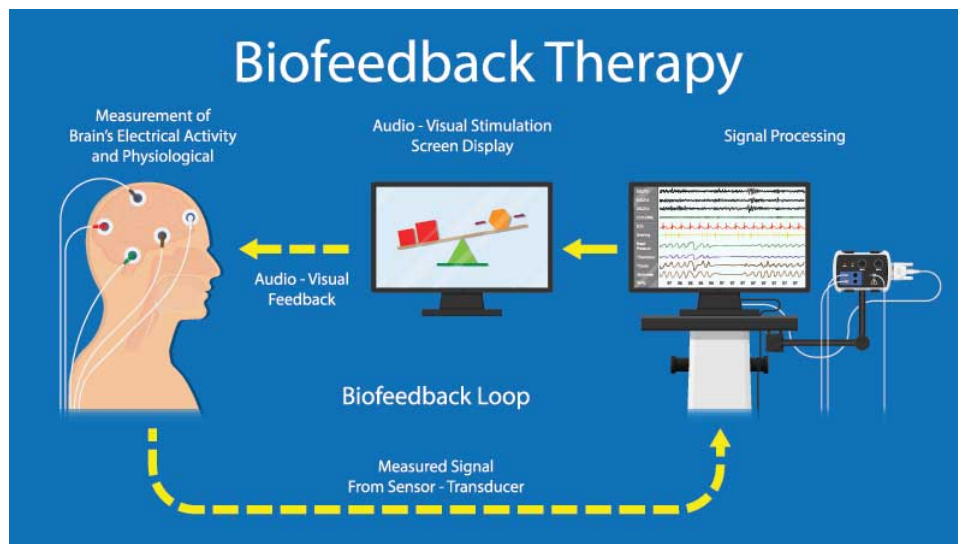
Figure 2.3: Scheme of a Neurofeedback training protocol [23].

Neurofeedback applications: how to establish the area of treatment

It has been found that neuronal lesions located in specific regions of the brain generate symptoms related to these same regions. Each area of the cortex is devoted to a specific skill and/or feeling, so the identification of these regions is crucial for accurate neurofeedback treatment. For example, the frontal lobes are responsible for immediate and sustained attention, emotions, social skills, working memory, and time management and planning. The parietal lobes are responsible for solving problems that were conceived by the frontal lobes: grammar, sentence construction, and mathematical processes are handled by the left parietal lobe, while spatial orientation, right and left recognition are functions of the right parietal lobe. The temporal lobes are responsible for different tasks, the left hemisphere is entrusted with reading, learning memory and functions associated with a positive mood, while the left hemisphere has functions related to music, facial recognition, and anxiety. The occipital lobes are responsible for visual memory, accurate reading, traumatic memories accompanied by visual flashbacks, but also for localising objects in the environment, recognising colours and drawings, reading, writing, and spelling. Finally, the sensorimotor cortex (C3, C4, Cz) is in charge of the control of all skeletal movements, thus writing, typing, playing an instrument, manual operations, speaking, and the ability to recognise the

origin of body sensations. In this regard, the motor cortex helps the cerebral cortex to encode physical and cognitive tasks, so, for example, neurofeedback training on the left hemisphere of the sensorimotor cortex can help individuals who have problems following the logical sequence of cognitive tasks. Training on the sensorimotor cortex is applied for the treatment of epilepsy, paralysis, stroke, attention-deficit hyperactivity disorder (ADHD), and other disorders of sense-motor integration.

Electrodes are usually placed so that a specific EEG channel is positioned on one side of the brain; switching to the opposite side may lead to undesirable results, so the location of the EEG electrodes during neurofeedback training is crucial [25].

Types of Neurofeedback and Treatment Protocols

There are 7 different types of Neurofeedback used to treat various disorders:

1. Frequency/power neurofeedback: is the most widely used type. This technique involves the use of two or four surface electrodes and aims to change the amplitude or speed of specific neural waves, especially brain locations for the treatment of ADHD, anxiety and insomnia. This type is the one used in this study.

2. Slow cortical potential neurofeedback (SCP-NF): it is used to improve the direction of slow cortical potentials for the treatment of ADHD, epilepsy and migraines.

3. Low-energy neurofeedback system (LENS): in this treatment, a weak electromagnetic signal is released to change the brain waves when the patient is motionless and with eyes closed. This treatment is used for insomnia, anxiety, depression, anger, ADHD, fibromyalgia, and head trauma.

4. Hemoencephalographic (HEG) neurofeedback: the feedback returned by this treatment is on cerebral blood flow for the treatment of migraines.

5. Live Z-score neurofeedback: provides continuous feedback by comparing variables of the brain's electrical activity with a systematic database, and is used for the treatment of insomnia.

6. Low-resolution electromagnetic tomography (LORETA): this type is used to treat addictions, depression and obsessive-compulsive disorder and uses 19 electrodes to monitor phase, power and coherence.

7. Functional magnetic resonance imaging (fMRI): is a novel form of neurofeedback that utilizes feedback from deep subcortical regions of the brain to regulate brain activity.

The various protocols are distinguished according to the frequency band to be treated. The alpha band is associated with a calm and pleasant mood, all alpha frequencies are related to the creative activity of the brain, it is the band associated with the process of muscular relaxation that then leads to sleep but also to meditation phases. Alpha band training is used for various treatments such as reducing stress and anxiety, improving memory and mental performance, and treating brain injuries. The most widely used band range is 7-10 Hz, used for meditation, sleep and to reduce anxiety and stress, but treatments as low as 10 Hz also help in deep muscle relaxation, regulation of breathing and heart rate.

Beta activity is an excellent indicator of mental performance, beta waves are associated with problem-solving ability, strong concentration and accuracy. Beta rhythm training is aimed at improving reading skills, attention and concentration, improving cognitive processes, reducing over-thinking, obsessive-compulsive disorder, alcoholism and insomnia.

The alpha/theta ratio is an index between awareness and sleep. Trainings to train this ratio are among the most popular for stress reduction, but they are also used to combat severe depression, addictions and anxiety, increasing relaxation, creativity and promoting healing from trauma reactions.

Delta waves have the lowest frequency and are associated with the third and fourth stages of sleep. Delta protocols are used to relieve headaches, traumatic brain injury and acute muscle contraction.

Gamma waves, on the other hand, are the highest frequency waves, they are the waves linked to cognitive processes and memory, they are responsible for neural connections and the transfer of information to the outside world. Gamma protocols aim to improve cognition, mental clarity and organisation, speed of information processing and short-term memory.

Theta waves are associated with various activities such as emotion, memory, sleep, meditation and hypnosis; they are the typical waves of the first phase of sleep. Theta protocols help reduce anxiety, depression, emotional disorders, day dreaming and ADHD.

To sum up, we can say that there are two macro-directions of neurofeedback training: the one focused

on low frequencies (alpha or theta) that increases relaxation and focus, and the one focused on high frequencies (beta and theta) that improves activation, organisation and inhibits distractibility [25].

Neurofeedback applications: who might benefit from Neurofeedback therapy

Neurofeedback training is now used in the treatment of many disorders and diseases, many of them related to low anterior brain lobe activity.

For example, ADHD is due to a malfunction of the right frontal lobe. The rehabilitation approach with neurofeedback aims to provide an opportunity that has a lasting effect and deviates from treatment with drugs that can lead to heavy side effects. For this type of disorder, the aim is to decrease brain activity in the theta band and increase the activity in the beta band (theta/beta training) on Cz.

Neurofeedback has also been shown to be effective on people with schizophrenia, making them able to adjust their activity to specific frequencies. It is also very effective on insomnia by teaching patients to distinguish precisely the phase associated with the waking state and the phase associated with the sleeping state, so they learn to prepare their bodies for sleep more quickly.

Neurofeedback has created a huge change in the treatment of learning disorders such as dyslexia and dyscalculia by increasing alpha wave activity in these patients. Cocaine addiction can also be alleviated through this treatment, along with addiction to alcohol and computer games.

Patients with autism spectrum disorder, on the other hand, have been shown to have high anxiety-related beta activity, a high delta/teta ratio confirming lack of attention, impulsivity and hyperactivity, and abnormal EEG seizure activity. The efficacy of neurofeedback in autistic children has been well confirmed by numerous studies and is primarily aimed at inhibiting the theta/alpha ratio and improving the beta wave.

Approximately one third of epilepsy patients are immune to medical treatment. Many studies on neurofeedback treatments have shown that continuous SMR training reduces the frequency of seizures in severe and uncontrolled forms of epilepsy.

Further applications of neurofeedback include recovery from injury or stroke, eating disorders, mental health treatment, but it is also used by artists and surgeons to increase their musical and surgical performance, respectively [25].

Side effects

Neurofeedback is considered an evidence-based intervention as it integrates clinical experience with the best available research in order to manage and address behavioural, cognitive and subjective functions related to brain activity.

Neurofeedback is non-invasive, does not involve surgery or drugs, is not painful and has no long-lasting effects.

The FDA attributes risks and benefits to all interventions. In the case of neurofeedback, it is clear that the benefits far outweigh the risks, although mild adverse events can sometimes occur as a form of biofeedback. For these reasons, it falls into the category of other low-risk activities such as progressive relaxation, hypnosis, breathing exercises, meditation, yoga and massage.

Neurofeedback training can on certain occasions provoke adverse responses that temporarily increase the symptoms generally associated with the calm and relaxed state of the central nervous system such as fatigue, headaches, dizziness, irritability, moodiness, crying, insomnia, agitation, concentration difficulties and anxiety. But these reactions turn out to be rare and, if they do occur, they are temporary, lasting only 24-48 hours. Moreover, they generally only occur in the first few training sessions, in fact as soon as the subject becomes more relaxed and aware of the procedure, they tend to integrate past emotional problems and the above-mentioned symptoms subside [24].

In addition, there are methodological limitations and ambiguities regarding the treatment, especially regarding the number of sessions required for a certain type of learning to take place or for the expected result to be achieved; another doubt lies in how long-lasting the effect can be once the treatment is over. Finally, an important limitation of this methodology is certainly the cost; these are expensive procedures, not supported by most insurance companies [25].

Neurofeedback Softwares

The software used for Neurofeedback follows the principle of brain-computer interface (BCI) systems, which are already widely used in clinical and research applications. A BCI is a communication tool that uses the EEG signal of a human subject to make a computer do something. The new frontier in this

field is the virtual environment, i.e. a human-computer interface system that allows the user to virtually move their point of view in real time with the aim of generating natural interactivity and creating a real sensation due to mutimodality. This type of setting is created in both 2D and 3D, the latter being much more attractive and immersive [25]. The subject may be asked to play and complete interactive games by manipulating virtual objects or simply to immerse himself in the virtual world and follow the various procedures involved in the specific protocol. A more detailed description of these aspects will be made in the chapter on Virtual Reality.

2.3   Brain Entrainment

Brain entrainment describes the brain's electrical response to rhythmic sensory stimuli, such as sound and visual impulses. When provided with a sensory stimulus, i.e. a stimulus that the body receives through the eyes, ears or another sense, the brain emits an electrical charge as a response, called Cortical Evoked Response [26].
Since the beginnings of the study of the electrical activity of the brain and the EEG signal, it has been noted that a repeated sensory stimulus at a fixed frequency can selectively modulate brain oscillations, activating or inhibiting populations of neurons and thus generating a change in the voltage amplitude of the electrical activity recorded by the EEG. In this regard, three types of oscillations are distinguished:

- Evoked oscillations: responses to an individual stimulus that are synchronised in time, they are said to be "phase-locked" to the stimulus.

- Induced oscillations: also responses to a stimulus, but they are not bound to it in time.

- Entrained oscillations or steady-state evoked potentials: these are responses elicited by repeated visual or auditory stimuli. The interesting note is that these responses reveal resonance frequencies that are similar to the spontaneous EEG frequencies; this is an indication that this type of stimulation does not generate oscillatory responses ex novo but rather re-emerges the activity of its own intrinsic oscillator. One could say that this type of stimulus evaluates the brain's ability to generate endogenous oscillations that are synchronised with the frequency of the external stimulus.

These three types of oscillations reflect different neuronal processes and mechanisms.
Speaking of brain entrainment, the main feature is that as soon as the frequency of the external stimulus matches the frequency of one's own intrinsic oscillator, an alignment of the two signals occurs over time, i.e. an increase in phase-locking between the EEG signal produced by the subject and the signal related to the external stimulus. An effective phase reset of the current oscillations may also occur at the moment the external stimulus is experienced. A further representation of brain entrainment is the increase in signal amplitude (power) at the frequency of the intrinsic oscillator (which coincides with that of the external stimulus) because more and more neurons are aligned in phase with the driving stimulus.
From a more strictly theoretical point of view, Arnold's tongue appears to be an efficient method of assessing the degree of entrainment by varying the amplitude of stimulation at different frequencies. The result is that as the stimulus amplitude increases, the window of phase-locking activity of the response widens around the frequency of the intrinsic oscillator. Plotting the results of this theory on a two-dimensional graph as a function of stimulation frequency and stimulation amplitude, it results in an inverted triangle called Arnold's tongue. Stimulation frequencies far from the intrinsic frequency need an increasing amplitude in order to achieve a good degree of entrainment (Figure 2.4).
At the boundary of Arnold's tongue, entrainment is interrupted by unpaired periods of time, called "phase shifts". That is, the intrinsic oscillator is initially coupled to the phase of external stimulation for a given period of time, after which, continuing with constant stimulation, the internal oscillator slips back to its intrinsic frequency and is then entrained again by external stimulation.
Rhythmic auditory stimuli far above the threshold of audible perception have been shown to generate a high degree of brain entrainment at the frequency of stimulation; but an alignment of the intrinsic oscillator has also been demonstrated in the case of stimulations that are not consciously perceptible, demonstrating that a marked perception of the stimulus is not a requirement for neuronal entrainment [27].

Several studies have been conducted over the years showing that the state of brain entrainment can affect behaviour and cognition in different ways.
These studies have been carried out using sound stimuli, whereas very little can be found in literature on visual stimuli. Brain entrainment underwent its greatest development from 1973 with Oster's findings on binaural waves, while studies on medical applications began in 1980, mainly for the treatment of anxiety,
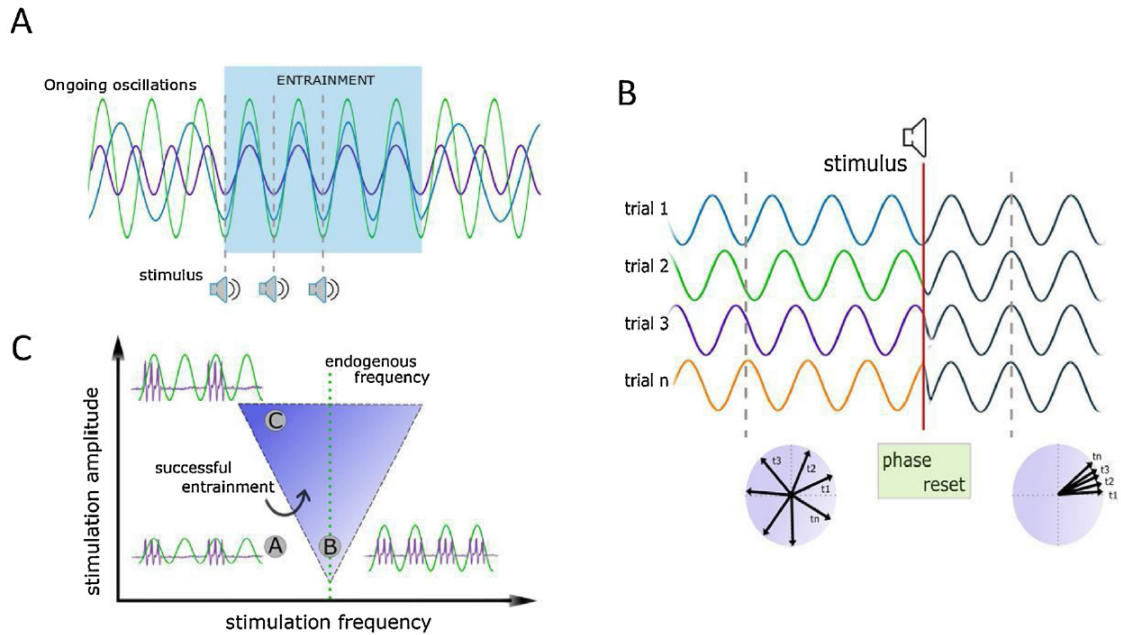
Figure 2.4: A. Temporal phase synchronization. **B.** Phase resetting fenomenon. The polar diagrams show the phase synchronisation of the signal between trials after the external sound stimulus occurs. **C.** Arnold's tongue, it shows the area where successful brain entrainment can be achieved by changing amplitude and frequency of stimulation [27].

stress, headaches, migraines and pain.

To date, the most common methods are to stimulate the subject's brain at the desired frequency (depending on the objective of the study) with flashing lights, different sound tones or a combination of the two. As regards auditory stimuli, binaural waves are used in the first instance, and for the past few years, monaural waves and isochronic waves are also beginning to be evaluated. Listening to binaural waves generates the illusion that the sound comes from inside one's head, producing a relaxing and hypnotic effect. On the other hand, according to Papagiannakis and his collaborators [26], this type of waves are unable to produce any brain entrainment; in their study (one of the very few in the literature on isochronic tones), they verified, indeed, that isochronic tones are the most effective method of auditory stimulation for brain entrainment as they provoke a strong auditory evoked response.

Stimulation with monaural waves is performed by applying the same amplitude-modulated signal simultaneously to both ears; in this way, sound perception does not require information integration by the two ears. On the other hand, in binaural wave stimulation, two close-frequency sine waves are generated separately to each ear; this requires information integration and results in a perceived wave at the frequency equal to the difference of the two. The sensation of the binaural waves (sensation of sound localised within the head) is modulated in the brainstem at the level of the superior olivary nuclei, while the information of the monaural waves is modulated at the level of the cochlea. The effect of binaural waves as a form of anxiety reduction, as a tool to increase creativity, attention control, and cognitive flexibility, working on the gamma band, has been confirmed in several studies. Nevertheless, Chaieb and his collaborators [28] in their study obtained more pronounced responses in the case of monoaural waves than binaural waves on all three stimulation frequencies in their experiments. Thus, it could be hypothesised that the reduction of anxiety states using brain entrainment with monaural waves at alpha-band frequencies produces similar or even more pronounced results than those obtained in the literature with binaural waves with frequencies below the alpha band (the theta band was often used).
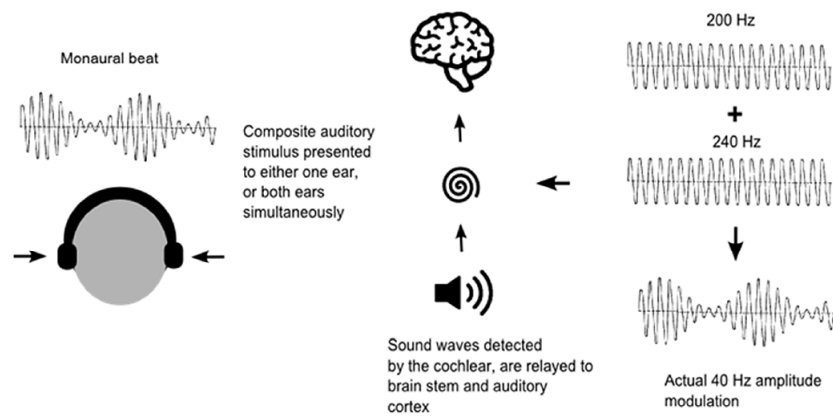
Figure 2.5: Monaural beats can be created by the superposition of amplitude-modulated signals of neighbouring frequencies transmitted to only one ear or to both ears [28].

Chapter 3

Virtual Reality and its applications

Virtual reality (VR) is a 3D computer-generated simulation that allows the user to interact with fictitious environments using specific electronic equipment. A desktop or a Head-mounted display (HMD) shows the user a virtual environment. An HMD includes a head tracking system to ensure six degrees of movement while hand tracking systems are engaged to enable the user to manipulate and interact with objects in the virtual environment.

In addition to virtual reality there is augumented reality (AR). The main difference lies in the concept that in VR the user is immersed in a completely simulated scenario whereas AR auguments the real world by adding virtual elements (Figure 3.1).
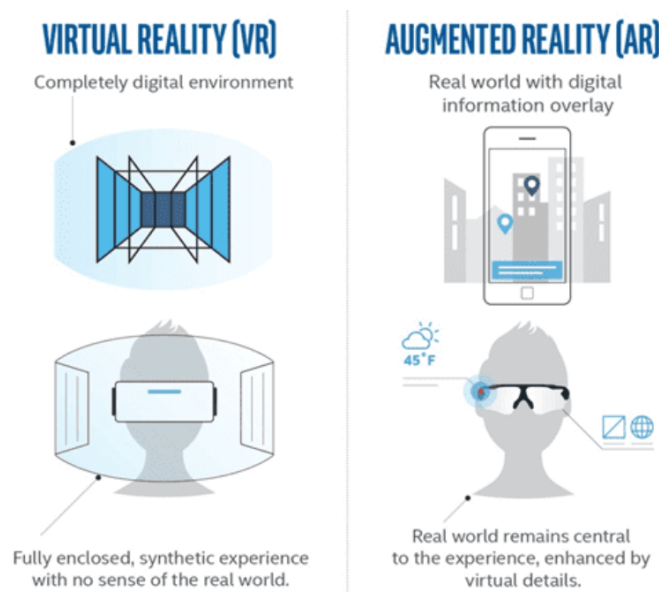
Figure 3.1: Comparison between VR and AR [29].

VR systems can be classified according to the grade of immersivity [30, 31]:

- Non-Immersive: provides to the user the lowest level of immersivity. In this case, a virtual scenario is showed on a simple desktop. The user can only interact with the scenario but is not immersed in it. Non-immersive VR is also called Window on World (WoW) (Figure 3.2).

- Semi-Immersive: provides to the user a partially immersive scenario. These systems use standard 3D monitors supported by head tracking system. They give the feeling of being immersed in a different reality but do not support any type of sensory output (Figure 3.3).

- Immersive: provides to the major level of immersivity. These systems use an HMD to fully immerse the user in a virtual environment through the use of 3D stereoscopic lenses. They may be integrated with audio, haptic and sensory interfaces (Figure 3.4).

Figure 3.2: Non-Immersive VR [32].

Figure 3.3: Semi-Immersive VR [33].

Figure 3.4: Fully-Immmersive VR [32].

3.1 History of Virtual Reality

The very first idea of virtual reality dates back to 1957 when the Sensorama Machine (Figure 3.5) was designed in New York by the director Morton Heiling. He wanted to reproduce a realistic and immersive simulation of riding a motorcycle. A prerecorded film in stereo was integrated with sensory feedback as wind or vibration.

Figure 3.5: Sensorama [34].

In 1965, the first HMD, called "The Sword of Damocles" (Figure 3.6), was created. It supports head tracking and the images were projected by using two cathode ray tubes. This HMD was extremely expensive and heavy, thus making the experience uncomfortable.

In '90s the main videogame companies began to produce the first devices for VR. In 2012, Oculus Rift (Figure 3.7), a HMD that allows a 90-degree field of view, was presented for the first time. In 2014, Mark Zuckerberg, the owner of Facebook, bought Oculus VR. In 2015, Google presented Cardboard (Figure 3.8), a low-cost stereoscopic viewer. In 2016, HTC developed HTC Vive StreamVR headset (Figure 3.9), the first HMD that allowed free movement to the user in a defined space. In 2019, Oculus released Oculus Rift S and Oculus Quest.

3.2 Main application of virtual reality

Gaming was the pioneering field for development of virtual reality application. In the present days, VR has tons of applications:

- In automotive industry, VR allows engineers and designers to simulate test drive, also in particular road scenarios. Rendering prototypes in 3D allows a detailed visualization from the inside of the vehicle and a complete interaction with them. Both advantages makes the design process much easier and cost-effective due to the fact that is no more necessary to manufacture a large number of prototypes. Some companies are also starting to offer recorded virtual drive-test to let customers see the final product in a test condition [39].

Figure 3.6: The sword of Damocles [35].

Figure 3.7: Oculus Rift [36].

Figure 3.8: Google Cardboard [37].

Figure 3.9: HTC Vive StreamVR headset [38].

- Due to the pandemic situation, VR has now several applications in the tourism sector. People can access virtual tours of hotels and landscapes so that they can choose the best for their vacation. VR also allow virtual tour of fictional place from films [40].

- Virtual reality technology has enabled the consumption of news stories and documentaries in a more immersive way. With the New York Times VR app, users can experience stories as if they were standing next to the journalist at the scene [40].

- In addition, VR retail experiences and body-scanning technology will allow consumers to try on clothes in a virtual world, giving them a sense of what the clothes would look like in person. This not only saves shoppers time, but it is also a more sustainable option. By allowing customers to know whether an item fits before they order it, the environmental cost of production and shipping for fast fashion can be significantly reduced [40].

- In space and military industry is mostly used to simulate situation that can't be easily accessed, so it allows training with minimal risks. Is it possible to simulate real weapons and vehicles and to add haptic feedback in order to have a simulation that is as close as possible to reality for military training. Instead, astronauts need to go through different types of complex training in order to go for a space flight. VR allows to make training for complex specific activities related to space mission [41].

- In architecture, VR has a great impact. It allows architects to render in a 3D simulation a building and experiences how it feels and to make real-time changes without building the structures.

- VR has also great influence in instruction. Toyota developed a VR simulation to teach young people about the risks of distracted driving. Through another simulation project, vocational school students were able to experience the operation of cranes and other heavy construction equipment. The National Football League and some of the most advanced university teams use VR to improve game strategy and athletic training.

- Through the aid of VR is possible to attend rock concerts and sporting events, watch music videos. It is possible to relive important events in first person. It is also possible to experience film and art at 360 degrees.

3.3 Virtual reality in medicine

Medicine also benefits from virtual reality in several areas:

- One of the main use of VR in medicine is for virtual surgery. By the use of virtual reality, the surgeon can see inside the three-dimensional image of a patient having the opportunity to simulate surgery procedure reducing time and risk. During operation, VR technology yields a precise image of the patient and this could also be certainly useful for training new doctors and nurse providing a new innovative and stimulating way of teaching, which students can practice without the burden of a surgery (Figure 3.10) [42].

Figure 3.10: VR in surgery [43].

- Rehabilitation through VR is a health technology that is used to recover motor or sensory ability lost due to accident or illness [44]. VR system can help patient to engage intensive training. This treatment has been proved to be very efficient for stroke rehabilitation. Being immersed in a virtual scenario allows patients to complete tasks they are not able to execute, or generates a simulation where the patient is most involved and makes the task easier to complete. It also provides very specific treatments for the individual patient in which he has the ability to modify the activity's difficulty. Studies demonstrates that VR therapy lead also to an improvement in motor skills (Figure 3.11) [45].

Figure 3.11: VR in leg rehabilitation treatment [46].

- In both clinical settings and experimental studies, VR has been utilized to manage pain and discomfort related to various painful medical procedures. Participants who were immersed in VR reported reduced levels of pain, general discomfort, and a desire to use VR again during future procedures. Researchers have theorized that VR acts as a non-pharmacological form of analgesia by affecting the body's pain modulation system through emotional, cognitive, and attentional processes.

Although the precise neurobiological mechanisms of VR effect remain unclear, ongoing investigations are studying the intricate interplay of cortical activity associated with immersive VR [47].

- Detection of mental disorders is one of the major issue in medical research. According to World Health Organization, 35.5-50.3% of mental disorder cases in developed countries and 76.3%-83.4% in less-developed countries are not detected on time [48]. Several studies confirm that the use of VR treatment can lead to improve treatment and diagnosis of mental disorders. Traditional exposure treatment for anxiety disorder shows situations, objects or people that are the main reason of anxiety for the patient, making therapy difficult to accept, thus leading to an abandonment of treatment. The great advantage of VR is that the patient can perceive anxiety scenario more safely (Figure 3.12). He is fully immersed in a virtual scenario but he perceives it to be real, thus making the treatment more acceptable. In Post-traumatic stress disorder (PTSD), VR is used to re-create the traumatic situation. VR treatment is also used for eating disorders, social anxiety disorders, obsessive-compulsive disorders, dementia, ADHD, depression, autism spectrum disorders, schizophrenia and addiction disorders [49, 50].

Figure 3.12: VR for fear treatment [51].

- A further application field of VR is improvement of cognitive functions. VR has the ability to enhance neuroplasticity, leading to the formation of new neural connections. So VR could be used to recover lost cognitive functions in elderly subjects or to accelerate learning process. There are several studies that confirm that learning with the use of VR leads to a better performance in examination tests [52].

3.3.1 Virtual reality in Biofeedback and Neurofeedback

The majority of bio and neurofeedback treatment uses visual feedback that mostly consists of bars whose height changes in response to changes in brain activity. The main problem of this treatment is that simple and uninteresting designs can demotivate and exhaust patient in feedback sessions. Thereby it is of great relevance to develop more engaging feedback designs [53].

Virtual reality has shown to be a useful tool in the creation of realistic and immersive virtual scenarios. Immersion is a key element in order to evoke emotions, allowing for exploration and training of emotion regulation competences. VR games are increasingly being employed in therapies for anxiety. In biofeedback treatment, players are encouraged to maintain a desired physiological condition by playing games that monitor their physiology state and adjust the game (e.g., difficulty, mechanics) in function of a specific biological parameters. As a result, due to the challenging character of these games, they might be useful for neurofeedback training, behavior monitoring, motivating patients to attain minor goals, aiming to develop self-regulation competences, as well as applying newly learned behaviors in daily life [54].

Chronic strokes patients with motor disability received NF in VR and expressed high levels of enjoyment and a desire to continue training even after the fixation time. This effectively demonstrates how the right kind of feedback may raise training enthusiasm and enjoyment, both of which have a beneficial impact on NF performance. In addition, patients said they felt more in charge and were more interested than those who trained using the conventional 2D paradigm [55].

The use of VR in NF not only has benefits in terms of the pleasantness of the treatment. Several studies demonstrate that it also increases performance on the individual treatment. The aim of a study conducted by Berger et al. was to analyze the positive effects of the use of VR. They compare a standard

visual feedback scenario (vertically moving bars) with a 3D VR scenario (moving ball in forest environment in a 3D scenario). Within a single training session, participants who received feedback through 3D VR exhibited a steady rise in SMR power during the feedback session. Conversely, the group that received the traditional bar feedback in 2D showed no alteration in SMR power throughout the feedback runs. This study emphasizes that the choice of visual feedback modality can impact NF training performance, and that the use of 3D VR-based feedback provides benefits over conventional 2D feedback [53].

3.3.2   Effects of natural environment

Exposure to nature is proven to have a number of positive effects on people physical and mental wellbeing (e.g. improve emotional states, reduce the risk of mental health issues, and benefit cardiovascular functions). Several studies demonstrate that immersive and interactive virtual environments that simulate natural elements like a beach or mountain scenery, are effective for relieving stress and promoting relaxation. The use of virtual nature environments in BF applications may be particularly effective because is possible to replenish attentional resources in an enjoyable and calming way, while also offering immersive and relevant feedback opportunities [56, 57].

Yeo et al. [58] classified virtual environment simulations into two main types: real-scene-based 360-degree videos and computer-generated (CG) scenarios. While the former offers a more realistic experience, the latter enables greater interaction with the virtual environment. Interactive virtual reality is considered a highly engaging and motivating tool for promoting subject engagement in rehabilitation therapy.
The advantages of using virtual nature environments in biofeedback applications are similar to those of real nature. Browning et al. [59] found that virtual nature environments and actual nature can both lead to similar positive effect and restorative outcomes. Previous research suggests that both visual and auditory stimuli are key factors in obtaining the benefits of nature exposure. With current VR devices delivering vivid audiovisual experiences, users can feel as if they have been transported into a virtual world, which in turn enhances their presence in a restorative natural environment and provides psychological benefits [60].

The quality and structure of the environment are important factors in determining the restorative and relaxing benefits of nature. Virtual nature environments are typically designed to feature high-quality and aesthetically pleasing landscapes, providing viewers with an optimal experience that can lead to improved psychological and physiological outcomes.
According to a review [61], researchers has examined the effects of different types of forest environments on stress relief, including those with high or low levels of openness, the presence of water, and comparisons between forests and golf courses. The results suggest that the stress-relieving effect of a natural environment is enhanced by the presence of significant amounts of trees, shrubs, water, and other natural elements, with minimal evidence of human influence.
Xiaobo Wang et al. [62] investigate the effects of seven different VR forest resting environments (Figure 3.13). They show that different types of forest resting environments can have varying effects on stress relief. While the natural environment is more effective at relieving stress physiologically, the artificial environment can lead to psychological recovery. Surprisingly, the forest resting environment that provides the best stress relief is not always the most natural. A natural environment with some human-made facilities can be more effective in relieving stress than a pure natural environment with no such facilities. Additionally, a water landscape, particularly a dynamic one, has a positive effect on stress relief, providing benefits for both physical and psychological well-being.
A second study, conducted by Anderson et al. [63], evaluates relaxation by comparing a neutral scenario, an empty Australian beach, and an Irish countryside with animals and human intervention. Once again, a greater degree of relaxation is observed in the case of natural environments, particularly in the case of the Australian beach.

Regarding the use of VR combined with biofeedback for relaxation, two illustrative studies are reported. The purpose of the first study [64] is to induce patients to relax quickly. The technique of Sophrology is used, which is a method of dynamic relaxation that includes physical and mental exercises to promote health and well-being.
A Virtual Sophrology protocol was created with three key components: VR environments, Sophrology instructions, and EEG feedback. The subject is given the opportunity to choose between three environments: the sea, a Japanese garden with the sound of a river in the background, and waterfalls, while the feedback is displayed on a screen through an index (Figure 3.14).

Figure 3.13: Natural scenarios evaluated in Xiaobo Wang et al. study [62].

The results obtained show a decrease in the index used to evaluate relaxation and a reduction in the time required to reach the maximum state of relaxation.
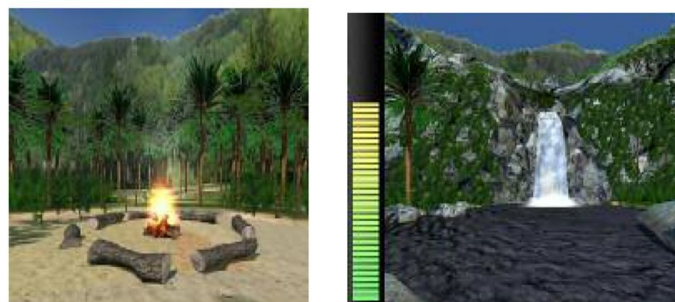

Figure 3.14: The scenarios presented in the sophrology protocol [64].

The purpose of the second study [65] is to implement a protocol to combat Generalized Anxiety Disorder (GAD) or anxiety symptoms in general.

In the VR environment, the patient is on a tropical island and walks along paths under the guidance of a voice that leads to 4 different scenarios in which the elements of the environment are directly modified by the physiological parameters registered as feedback (Figure 3.15).

In particular, the intensity of a fire, waves, and the intensity of the waterfall are modified in the first three scenarios, while the fourth scenario consists of visualizing a stressful element for the patient that is reduced in size as relaxation increases, making the treatment customizable to the user.

Figure 3.15: Two of the four scenarios presented in the INTREPID project [65].

Chapter 4

Materials and Methods

4.1 Instrumentation employed

In this study, the Enobio 8 sampling system from Neuroelectrics was used for the acquisition and management of the EEG and ECG signals, and the NIC2 software that allows Neuroelectrics systems to communicate with computers. An Oculus Meta Quest 2 was used as a HMD and the scenarios reproduced by it were created with the Unity graphics platform. Finally, the signals were processed using Matlab R2020b.

4.1.1 Enobio 8 Neuroelectrics

Enobio 8 is a portable 8-channel EEG signal monitoring system. It is equipped with battery-operated and wireless (data rate of 921 kbps) electrophysiological sensor systems that allow data transmission within a range of 10 metres from the computer running the NIC2 software. The sampling system has a dynamic resolution of 24 bits (0.05 μV), a bandwidth of 0 to 125 Hz (DC coupled), a sampling rate of 500 SPS and all data are stored at sample precision. The system integrates markers from external data sources via LSL, TCP or triggers from hardware. The equipment also allows data to be recorded from a triaxial accelerometer and to acquire ECG and EMG signals.

In this study, 5 channels of the 8 available were used, 4 of which were used to take the EEG signal and one to take the ECG signal from the subject's wrist via an extension cable. The sampling system included a Neuroelectrics Control Box (Necbox), which would be Enobio's control unit, a neoprene Pro headcap in which a 64-position grid of the EEG 10-10 system is traced through holes, representing a precise electrode positioning system (Figure 4.1). The electrodes used are dry Ag/AgCl electrodes filled with conductive electrolyte gel placed in contact with the skin to lower impedances as much as possible and improve signal quality. Finally, adhesive disposable electrodes were used for reference, placed behind the two ears at the level of the mastoid bone, and a slightly larger adhesive disposable electrode for taking the ECG signal.

4.1.2 NIC 2 Software

NIC (Neuroelectrics Instruments Controller) is the software interface of the medical device, managing both wired and wireless connections. This software connects the Necbox Enobio with a neighbouring computer and allows EEG data to be streamed and analysed in real time. NIC 2 corresponds to the second generation of the NIC software. It has a graphical user interface that is easily understood by both clinicians and researchers and simplifies interaction with the technology embedded in the device. The software can be downloaded free of charge from the Software section of the Neuroelectrics website for both Windows and Mac OS X systems. The software allows connection to the Enobio via Wi-Fi or Bluetooth. Once the device is connected, there is the possibility to enable a line noise filter (50 Hz or 60 Hz) to remove the main line artefacts from the EEG data and to enable default filtering to display the signal in the bands of interest.

In this study, both the 50 Hz filter and a 3-40 Hz bandpass filter were enabled. These filters are only retained for signal display, while the recorded data is raw data, i.e. unfiltered. The software makes it possible to create precise acquisition protocols in which the timing must be reported and all the channels used must be specified manually, i.e. the position of the channel and the corresponding connector number (Figure 4.2). It is possible to divide the protocol into different phases, each of which can have different timing parameters and channels. The NIC allows the files to be saved in different formats (.nedf, .easy,

Figure 4.1: Enobio 8 Neuroelectrics. In this figure a different type of electrodes is shown [66].

.edf, .sdeeg) depending on the signal processing requirements, and in this study all files were saved in .easy format, as this is a format compatible with Matlab. During the protocol creation phase, the LSL connection was also enabled, which allowed the transmission of data in real-time to Matlab. Once the
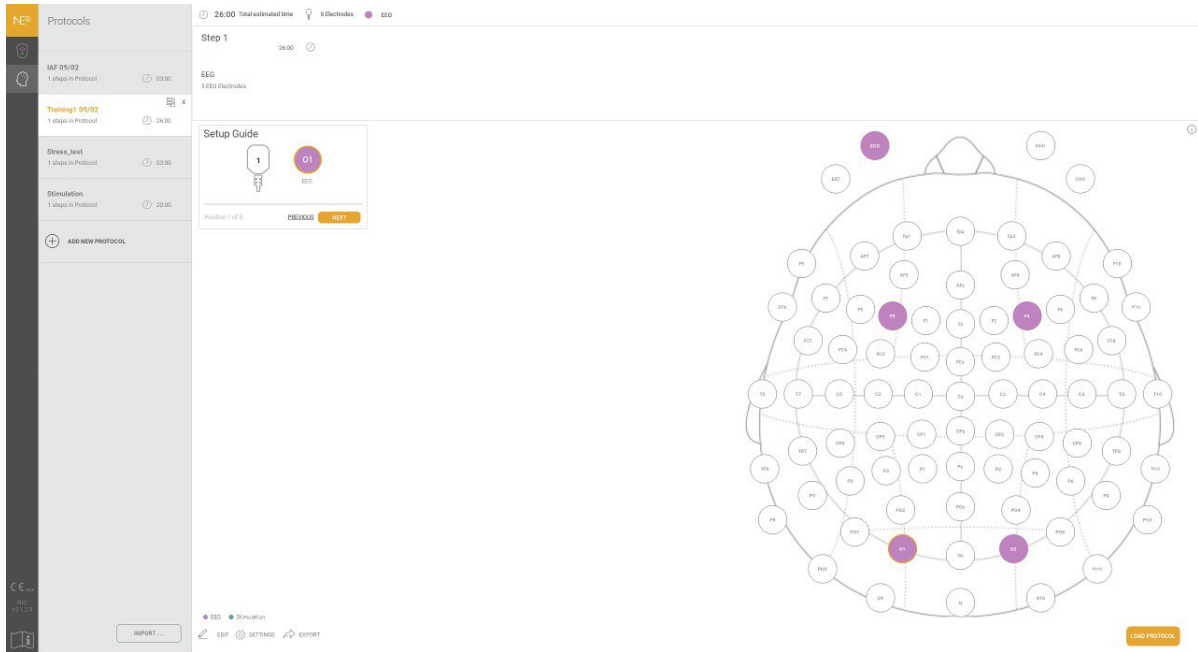

Figure 4.2: Protocol creation panel: this is the training protocol used for this study.

protocol is loaded, a panel is displayed where the multi-channel signal is plotted for all previously defined positions. It is possible to change both the time scale and the voltage scale at which the signal is displayed. During acquisition, it is possible to use the computer keyboard keys to enter markers; when these keys are pressed during the experiment, the marker number is added to the corresponding sample. This makes it possible to mark time references instantaneously and then retrieve them during visualisation and processing by matching them to the sample. In this study, the markers were used throughout the training to distinguish the various phases from each other, but also occasionally to mark a particular artefact (such as a sneeze during acquisition) and later determine how to deal with it. There are six different Liveviews in the NIC2 for visualising the EEG signal in real time (Figure 4.3):

- EEG plot: temporal plot of one of the channels in the created protocol.

- Accelerometer: real time display of the triaxial accelerometer data.

- Spectrum: display of the Fast Fourier Transform (FFT) or Power Spectrum Density (PSD) of the selected channel.

- Spectrogram: shows, via colour map, the frequency content of the signal on a specific channel over time.

- Band Power: shows in real time the power on the different EEG bands (Delta, Theta, Alpha, Beta, Gamma) on a specific channel.

- Scalp Map: shows, via colour code, the spatial distribution (μV^2) for the selected band or band ratio.
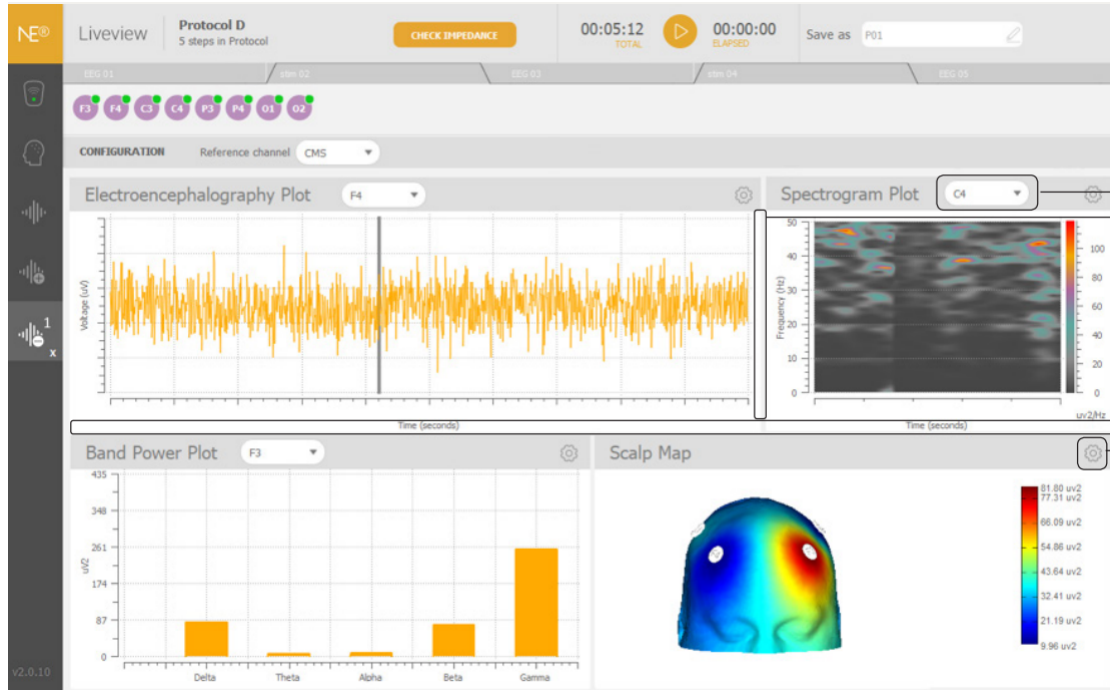
Figure 4.3: Example of customized liveview [67].

In the display panel it is also possible to choose a specific channel as reference, otherwise by default all signals are referred to the CMS channel.

In the NIC, the quality of the EEG signal is assessed by means of a quality index (QI), which is calculated every 2 seconds and depends on four parameters:

- Line Noise: signal strength (μV^2) in the standard line noise frequency band.

- Main Noise: signal strength of the standard EEG band (1-40 Hz).

- Offset: average value of the waveform.

- Drift: it is measured but not included in the QI calculation because it has a high inter-subject variability. A high drift does not imply a bad signal.

Each channel shown in the signal display panel appears with a colour code based on its QI (Figure 4.4):

- Green (QI: 0.0 - 0.5)

- Orange (QI: 0.5 - 0.8)

- Red (QI: 0.8 - 1.0)

It is possible to display on each channel the value of each of the four parameters mentioned above, with the parameter that most affects the signal being shown in bold. The quality of the signal depends mainly on the type of electrodes used, the values of the impedances and thus the quality of the contacts, and the reference CMS channel, so it is a good idea to check these three factors when the QI of any channel is not optimal [67].
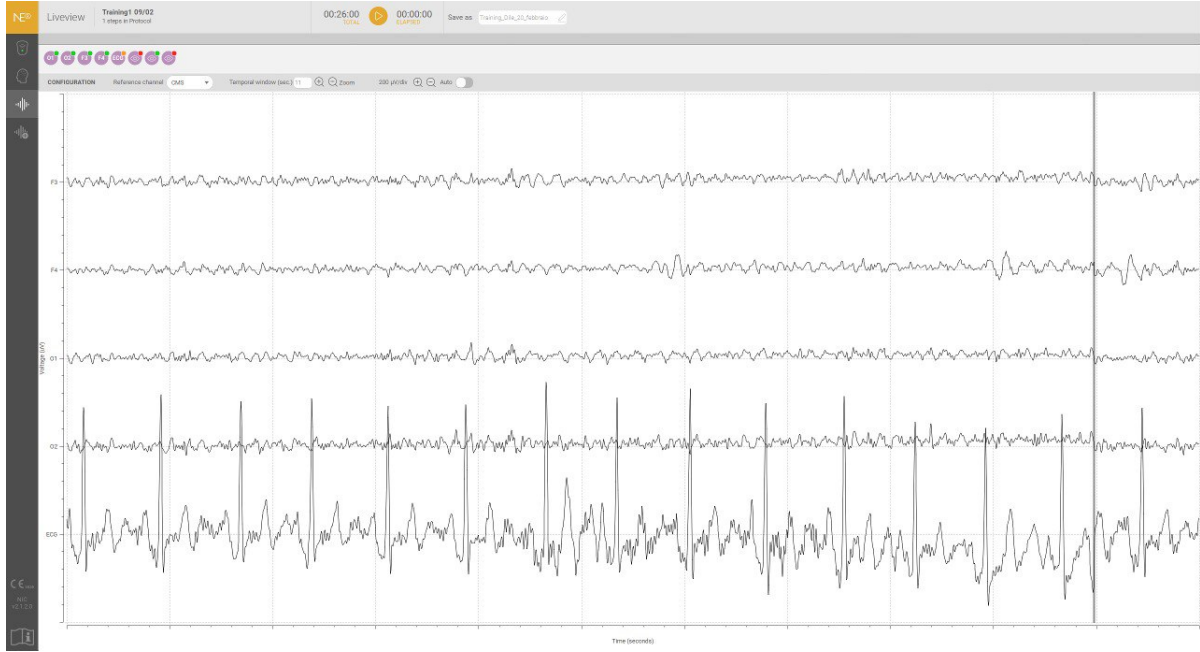
Figure 4.4: Display screen of the acquired signal in our training protocol: the channels used with their colour code are shown at the top left. By positioning the cursor over the coloured dots, a drop-down menu opens with information about the QI.

4.1.3   NIC real-time interaction with Matlab: LSL Connection

Creating a Neurofeedback protocol entails creating a closed-loop study protocol. This means transmitting and processing data in real-time, returning the result of the processing also in real-time and managing the subsequent changes. NIC software is able to transmit data acquired in real-time to Matlab via a Lab Streaming Layer (LSL) connection.

LSL is an open source networked middleware system for streaming, receiving, synchronising and recording streams of physiological, behavioural and neural data acquired from different sensor hardware [68]. It is a low level technology for exchange of time series between programs and computers. At the bottom of the whole stack as a protocol there is a library called "liblsl" and that's what allows the communication between machines and programs. There are some wrappers on top of that for various languages (C, C++, Matlab, Python, Java and other languages) and the same system can be used from all these languages for the same protocol. LSL software distribution includes documentation, user guides, example programs, acquisition programs and generic tools, and everything is open source. Neuroelectrics Enobio is in the list of the EEG devices that support LSL.

Reading data fundamentally starts with discovering a stream on the network, no IP addresses are needed, so you only need to specify the type of data your are waiting for (in this specific case, type: eeg). Once you have found a stream, you open an inlet and then you pull in your samples; streaming can take place sample by sample or through chunks of samples.

In the case of the software used in this study, NIC creates an outlet with the following settings [69]:

- Name: (choosen in NIC EEG settings)

- Type: EEG

- Channel count: 8, 20 or 32 depending of the Enobio NIC handles (8 in this specific case)

- Nominal sample rate (SPS): 500

- Channel format: float32

- Unique source ID: The Enobio/Starstim type plus its mac address

4.1.4 Oculus Meta Quest 2

The VR-HMD Meta Quest 2, previously known as Oculus Quest 2, was created by Meta Platforms, formerly Facebook, Inc in 2020. Meta Quest 2 has the same features as its predecessor, Oculus Quest, in that it can be used as a standalone headset with an internal operating system based on Android or with VR software compatible with Oculus Rift and operated from a desktop computer. However, the updated version has a refreshed design, weighs less, has advanced internal specifications, a higher refresh rate display, per-eye resolution, and longer battery life for the Oculus Touch controllers.

The Quest 2 is equipped with the Qualcomm Snapdragon XR2 SoC, which is a Snapdragon 865 version designed specifically for VR and augmented reality devices. It also has 6 GB of LPDDR4X RAM, which is 2 GB more than the first-generation model. The previous dual OLED displays were replaced by a single fast-switch LCD panel with a per-eye resolution of 1832×1920 and a refresh rate of up to 120 Hz, reducing the screen-door effect and improving image clarity. The Quest 2 also has physical interpupillary distance adjustment and can be set to 58 mm, 63 mm, or 68 mm by moving the lenses.

The Quest 2 operating system is based on Android and requires the Meta Quest app to set up. In February 2021, an update allowed up to three additional accounts to be logged in to a single headset, with the ability to share purchased software. In April 2021, system software version 28 introduced experimental Air Link wireless streaming, and in July 2021, experimental APIs were added to the Passthrough feature to enable augmented reality features. The third-generation Oculus Touch controllers have four times the battery life of the controllers included with the first-generation Quest.

Figure 4.5: Meta Quest 2 and its controllers [70].

The Quest 2 also integrates Oculus Link, a software that connects the device to a PC, using the PC processing power to replicate the Oculus Rift performance. With Oculus Link, users can use the Quest 2 like an Oculus Rift, while taking advantage of their PC processing power to create and experience more advanced VR simulations and games.

4.1.5 Alienware 17 R5 Laptop

To use Oculus Link, a high-performance PC is required. In this study, an Alienware 17 R5 (i7-8750H, GTX 1070, QHD) hired from the Visionary Lab at Politecnico di Torino with the following specifications was used.

- Processor: Intel Core i7-8750H 6 x 2.2 - 4.1 GHz, Coffee Lake-H

- Graphics adapter: NVIDIA GeForce GTX 1070 Mobile - 8 GB VRAM, Core: 1480 MHz, Memory: 8000 MHz, GDDR5, ForceWare 389.12

- Memory: 16 GB, 2x 8 GB SO-DIMM DDR4-2400, dual channel, all slots occupied, max. 32 GB

- Display: 17.30 inch 16:9, 2560 x 1440 pixel 170 PPI, JYWWF_B173QTN (AUO1496), TN, QHD, 120 Hz, G-Sync, glossy: no

- Mainboard: Intel CM246

- Storage: SK hynix PC401 HFS256GD9TNG, 256 GB, NVMe−SSD + HGST Travelstar 7K1000 HTS721010A9E630, 1 TB HDD, 7200 rpm. Slots: 2x M.2 Type 2280 & 1x 2.5 inch

- Weight: 4.416 kg (= 155.77 oz / 9.74 pounds), Power Supply: 798 g (= 28.15 oz / 1.76 pounds) [71]

Figure 4.6: Alienware 17 R5 Laptop [71].

4.1.6   Unity

Unity is a cross-platform game engine developed by Unity Technologies, first announced and released in June 2005. Unity in mainly used to develop 2D and 3D videogames and interactive simulation. The engine supports various operating system (Windows, Linux and Mac) and the application supports mobile (Android, iPhone, Windows mobile . . .), console (Xbox, PlayStation, Wii, Nintendo . . .), desktop and virtual reality platform. The engine offers a primary scripting API in C#, both for the Unity editor in the form of plugins, and for the games themselves, as well as drag and drop functionality. In 2D games, Unity allows the import of sprites and an advanced 2D world renderer. For 3D games, Unity allows to specify texture compression, mipmap and resolution settings for each platform that the game engine supports, and provides support for bump mapping, reflection mapping, parallax mapping, screen space ambient occlusion , dynamic shadows using shadow maps, render-to-texture and shadow maps, render-to-texture and full-screen post-processing effects.

4.1.7   TCP/IP connection

A TCP/IP connection is used for Matlab and Unity real time communication.
The Transmission Control Protocol (TCP) is a standard for communication that allows the transmission of data over a network between computing devices and applications. TCP ensures the successful delivery of data and messages between a server and a client, and it guarantees data integrity throughout the process. It establishes a connection between the source and the destination before transmitting data, and it organizes large amounts of data into smaller packets.
The Internet Protocol (IP) is the standard for transmitting data between devices on the internet. Each device is identified by a unique IP address that allows it to communicate with other devices on the internet. IP defines the modality for exchanging data and messages between devices and applications. It is a crucial component of the Internet Protocol Suite (TCP/IP), which consists of a set of communication protocols organized into four abstraction layers.
IP is one of the main protocol within the internet layer of the TCP/IP, and its primary function is to deliver data packets from the source device or application to the destination by adding tags, such as address information, to the packets. IP ensures that data packets are transmitted in the correct order and that they reach their intended destination.
TCP and IP are two separate protocols that work together to ensure data is delivered to its intended destination within a network. IP is responsible for obtaining and defining the address of the destination device or application, while TCP is responsible for transporting and routing the data through the network and ensuring its safe delivery to the intended destination. The combination of TCP and IP enables communication between devices over long distances and allows for efficient data transfer. By implementing appropriate security measures, users can use TCP/IP to transfer data between devices in a safe and secure manner.
TCP/IP model organizes communication tasks into layers to maintain a standardized process, which prevents hardware and software providers from managing the process themselves. The data packets go

through four layers before reaching the destination device. TCP/IP reverses this process through the layers to reassemble the message into its original format [72].

The "Client" is the device that initiates the connection, while the "Server" is the computer that is listening for incoming connections. To establish a connection, the Client needs to know the IP address of the Server it wants to connect to, as well as the port number it will use to send and receive data. The Server, on the other hand, simply waits for incoming connections and can choose to accept or reject them.

Once a connection is established, it remains open until either the Client or the Server decides to terminate it. During this time, data can be sent and received between the Client and the Server through the specified port number [73].

The four layers of the TCP/IP protocol are the application layer, transport layer, network layer, and physical layer. The application layer handles data exchange between applications using standardized protocols, while the transport layer maintains communication between hosts and provides flow control and reliability. The network layer handles packet transport across network boundaries, and the physical layer deals with protocols that operate on a link, such as Ethernet and ARP (Figure 4.7) [74].
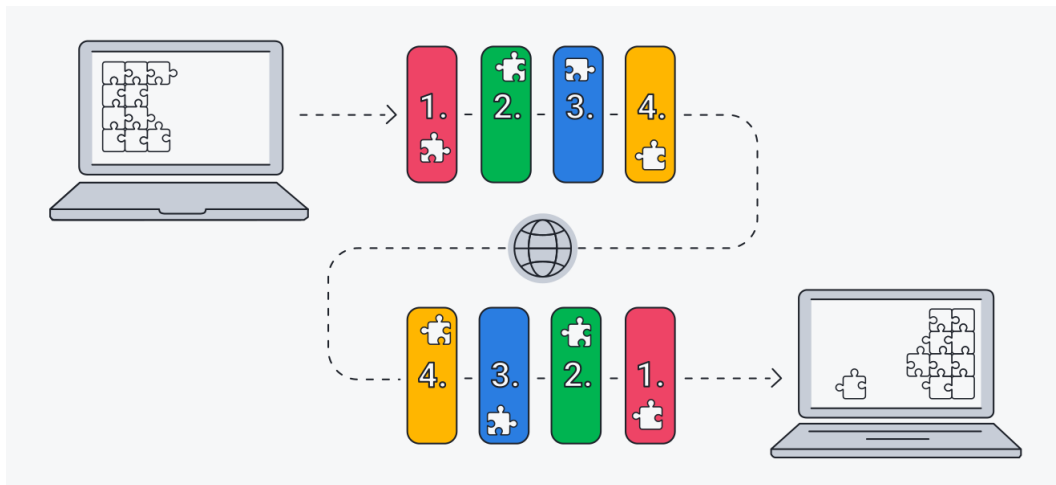
Figure 4.7: A diagram of how the TCP/IP model divides data into packets and sends it through 4 different layers. [75]

In the case of this study, Matlab receives data from NIC2, and establishes a TCP/IP connection with Unity, that only receives data. So Matlab is set to Client and Unity is set to Server.

4.2 Study protocol

Starting from this paragraph, a complete description of the protocol will be provided, from the training organization to the creation of the different scenarios in Unity.

In this study, a complete sample of subjects for conducting a comprehensive analysis was not available. Therefore, initial training sessions were carried out on both authors of this thesis, followed by a single training session on three external subjects. Subsequently, the decision to conduct a Single Case Study on one of these subjects was taken.

The protocol in organized in three main phases: a baseline phase in rest conditions, a stress test and a relaxing phase.

During the training sessions, modifications were made to the stress test phase to increase its intensity. Then, official training was initiated, and it was realized after the first three sessions that the baseline phase was not suitable for the study. As a result, the baseline scenario was modified. Further details regarding the description and modifications of the scenarios will be provided in Chapter 4.

The entire training was held at LED5 of Politecnico di Torino.

Here the official protocol description follows: the subject is sitting in a quiet room, the EEG helmet of the 8-channel Enobio device connected to the NIC2 software is mounted on his head. Then the Oculus Meta Quest 2 is mounted and earphones are connected to it. The NIC2 software communicates via the LSL protocol with Matlab platform, transferring the user's EEG signal to it in real time. Matlab, in turn,

communicates via TCP/IP protocol with the Unity graphics engine by sending it the control parameter extracted from the EEG signal, i.e. an index of the subject's relaxation. Unity modifies the displayed scenario according to this parameter, and sends the scene via Oculus Quest Link to the Oculus Meta Quest 2 so that it can represent it in a virtual reality environment. The various steps of the training that the user has to undergo are listed below. The entire duration of the acquisition protocol is approximately 30 min.

1. IAF (Individual alpha frequency) calibration (3 min): The subject sits comfortably in a chair wearing the HMD and EEG helmet. In this first phase the Oculus is switched off and the subject is asked to keep his/her eyes closed for the entire duration of the phase. At the end of 3 minutes, the trainer performs a quick calculation on Matlab to determine the subject's initial IAF which will be used as the frequency of the visual and auditory stimuli in the relaxation phase. During this phase, only O1, O2 and Pz channels are used; no ECG signal is taken.

2. Baseline 1 (3 min): the subject wears the Oculus on and holds the controller. A neutral screen is shown, this is a simple scenery with a brown tiled floor, seen from an elevated point of view and therefore appears very wide. The subject has to simply remain in a resting state during which his EEG baseline is acquired. This baseline serves to compare the subject's activation during the before and after training session. From this second phase, channels O1, O2, F3, F4 are used and the ECG signal is taken from the subject's wrist.

3. Stress test (3 min): the subject is shown an unrealistic scenario, he is inside a small room in a castle and on the screen appears a mathematical operation to be performed and two buttons, a TRUE button and a FALSE button. An anxiety-inducing music plays in the background. The subject must engage in the mathematical operations (additions, subtractions, multiplications and divisions) that are proposed to him, and he will use the controller to click on the TRUE button or the FALSE button, having 10 seconds to answer each of the operations. When he gives the wrong answer, on the scenario an explosion will be presented, emphasising the stress condition that will develop in the subject. A further explosion will also be presented when the subject fails to give an answer within the 10 seconds available. Throughout the test a timer is shown to indicate the time remaining, and at 30 seconds to the end of the three minutes a red light flashing at 1 Hz starts. The subject's EEG signal is recorded throughout the test and indices are extracted during post-processing.

4. Relaxation phase (15 min): The subject is shown a naturalistic setting. The subject finds himself in front of a small lake over which a waterfall cascades, surrounded by hills, trees and flowers. In the background he/she listens to relaxing music accompanied by sounds of nature and the sound of the waterfall. Two types of stimuli are inserted into the scenario to help the patient relax: a visual stimulus, represented by three trees, placed in three different areas of the scenario, flashing with a point light at a frequency equal to the subject's IAF, and an auditory stimulus consisting of monaural waves at a delta frequency equal to his IAF. Both stimuli are inserted with a low amplitude so that they are easily confused within the scenario, thus hardly perceptible to the user and well integrated. Two feedback elements for the patient are also inserted within the scenario: a text that prints on the screen the value of his relaxation parameter extracted from the EEG signal in real time and some fog that thickens as this parameter increases and weakens as it decreases. During this last task, the subject is asked to try to relax as much as possible and follow the two feedback elements that give him feedback on his mental state. The aim is to focus on the mental connection between the physical efforts he makes to achieve greater relaxation and the feedback he obtains so as to move in the direction of actually learning and acquiring a greater perception of his body. His EEG signal, again, is taken during the entire duration of the task and related features are extracted from it.

5. Baseline 2 (3 min): same as step 2.

6. Final IAF (3 min): In this final step, the final IAF is recalculated as in step 1. At the end of this final step, the subject is released from the instrumentation and is free to return home.

The protocol involves three sessions per week, for three weeks (nine sessions in total).

Figure 4.8: The subject during Stress Test phase.

Figure 4.9: The subject during Relax Phase.

4.3 Virtual Reality Scenarios design

The entire protocol is carried out using the Oculus Link software so that it can take advantage of the specifications of a high-performance PC to display fairly realistic scenarios that would otherwise not be rendered smoothly with the graphics card of the Meta Quest 2.

Unity provides the ability to create 3D projects. Interaction with virtual reality was achieved through the use of XR Plugin Management and XR Interaction Toolkit libraries.

The XR Interaction Toolkit bundle is a component-based interaction system that enables the creation of VR and AR experiences. It offers a framework that allows for 3D and User Interfaces (UI) interactions via Unity input events. The foundation of this system is comprised of two types of components: Interactor and Interactable, as well as an Interaction Manager that links them together. Additionally, it includes components for locomotion and visual rendering.

The XR Interaction Toolkit offers components to support various interaction tasks, such as cross-platform XR controller input, object hover, select and grab, haptic feedback through XR controllers, visual feedback to indicate possible and active interactions, basic canvas UI interaction with XR controllers, and an XR Origin utility to handle stationary and room-scale VR experiences [76–78].

A detailed description of the scenarios developed for this study follows.
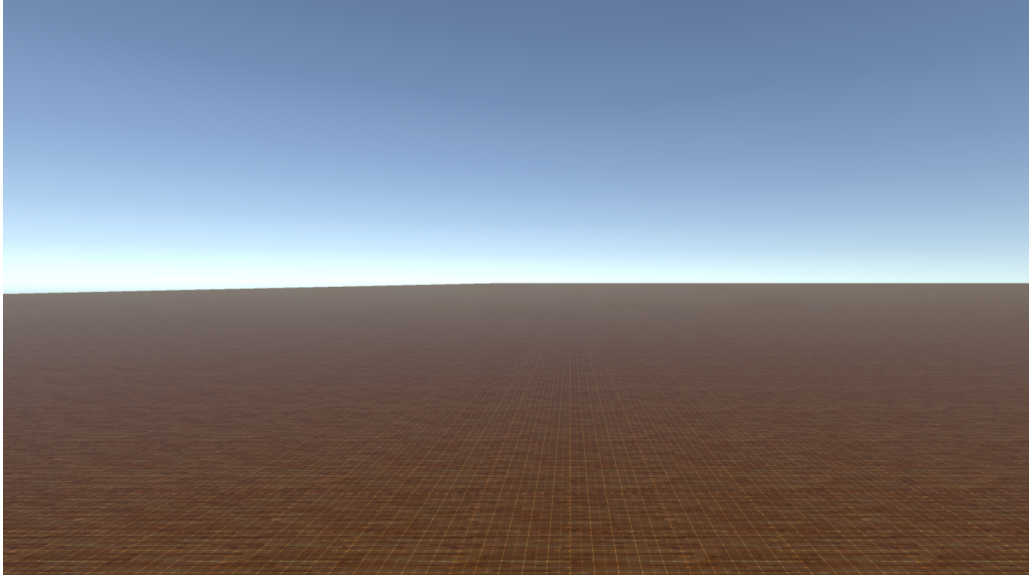
4.3.1 Baseline

The Baseline scenario was initially designed with a completely white screen. However, this scenario proved to be slightly uncomfortable for the patient. The EEG signal showed very pronounced alpha rhythms; therefore, it was replaced with the baseline previously described (Figure 4.10).

4.3.2 Stress Test

The stress test setting was downloaded from the Decrepit Dungeon LITE by Prodigious Creations free asset on Unity asset store [79] and modification were made on it. The interaction with Oculus is handled using the Oculus asset [80, 81]. The explosion was generated using a particle system. A frame of this scenario is shown in Figure 4.11.

The math task is handled by a C# code. Initially, the stress test involved only additions, stressful music

Figure 4.10: Final Baseline Scenario.

in the background, and an explosion when the subject provided an incorrect answer. The operations were displayed on the screen every 10 seconds, and each time a response was given, regardless of whether it was correct or not, a second operation was generated only after the 10 seconds had elapsed. This made the task easy, boring, and not so much stressful. In the last few minutes, the subject tended to lose concentration and randomly insert answers, resulting in EEG signals that showed no significant variations. After two trials, modifications were made:

- The type of operation is randomly generated between addition, subtraction, multiplication and division.

- The chance of an operation with a TRUE outcome being generated is the same as the chance of an operation with a FALSE outcome.

- In the case of an operation with a FALSE outcome, to make sure that the result shown on the screen is plausible, a result in a range of $\pm$ 20 from the hypothetical correct result is given.

- To make the operations as difficult as possible, but still simple enough to be performed in 10 seconds, they are generated between two-digit integers.

- Operations are generated every time the subject provides an answer or after 10 seconds have elapsed, thereby avoiding periods where no mathematical task is being performed.

- Two different timers are added, the first being 10 seconds and being reset every time a new operation is generated, indicating the remaining time to perform a specific operation. The second timer starts at the beginning of the stress test and lasts for 3 minutes, indicating the remaining time until the end of the trial.

- The explosion is triggered even if the patient does not provide an answer within 10 seconds, and not only if the subject provides an incorrect answer (Figure 4.13).

- At 30 seconds before the end of the stress test, an alarm red light is shown on the screen to increase the subject's agitation (Figure 4.12).

- A clock ticking sound is added to mark the passing of time, and the outcome of the response is displayed on the screen as "Correct!" or "Error!".
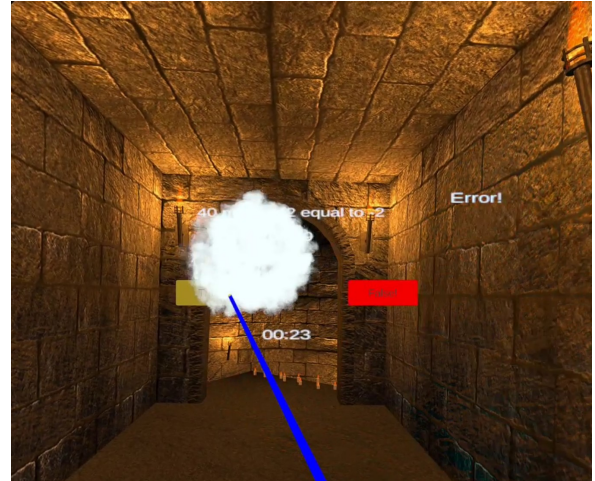
As a result of these changes, the test was much more difficult and stressful, and the EEG signal also showed the expected trends. It was therefore kept that way until the end of the training.
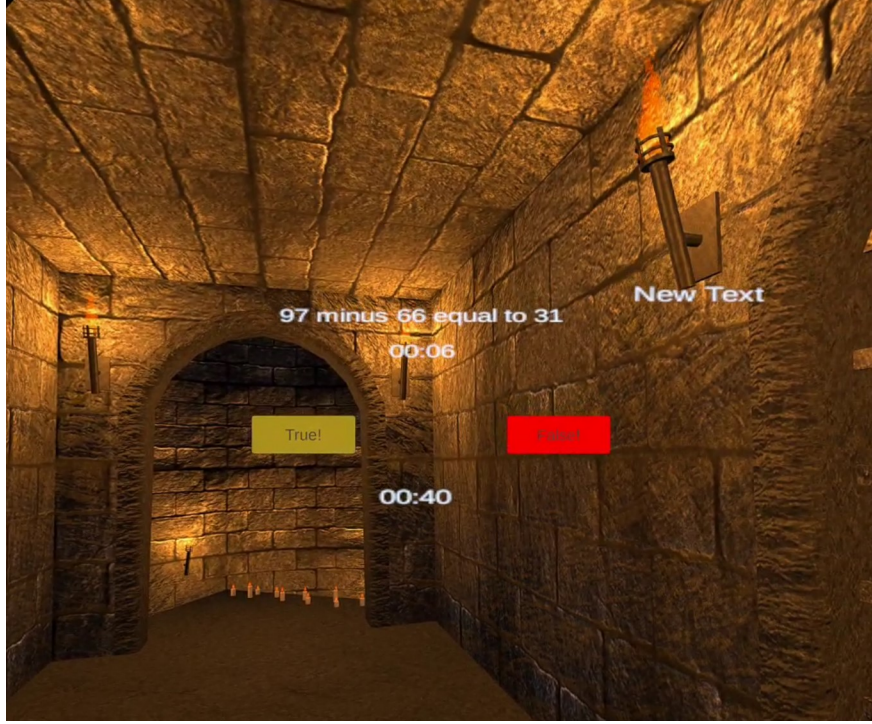
Figure 4.11: Stress test scenario.
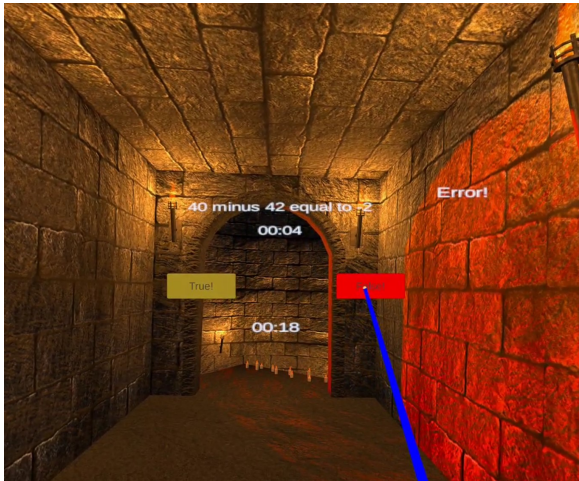
Figure 4.12: Alarm red light in the last 30 seconds.

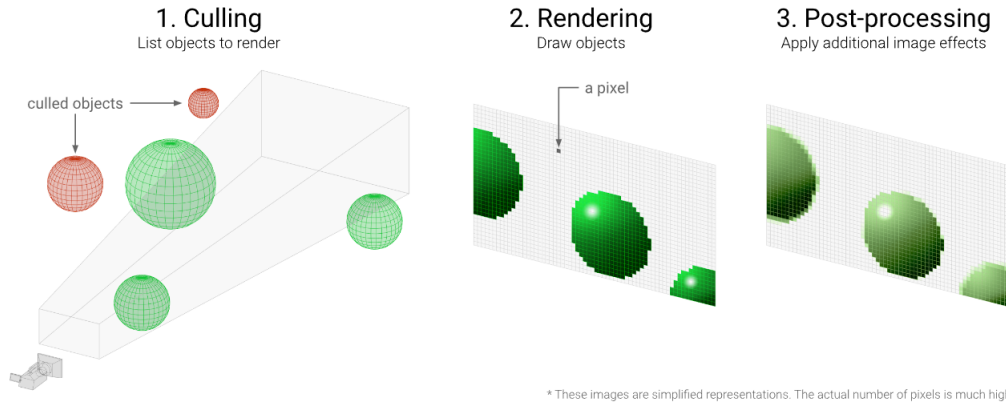**Figure 4.13:** Explosion appears after providing a wrong answer.

4.3.3 Naturalistic Scenario

The aesthetic design of the scenario is not of primary importance for this work, therefore it is described in a concise manner. Prefabricated scenes of a naturalistic setting were searched. However, many of these scenarios were not realistic enough, so it was decided to look for more complex graphical settings.

The purpose of a render pipeline is to perform a series of steps to process the contents of a scene and display them on the screen. Unity offers three pre-built render pipelines with varying capabilities and performance, but also the option to create a customized pipeline using the Scriptable Render Pipeline (SRP) API. A reder pipeline involves three main stages (Figure 4.14) that are repeated according to the frame rate [82]:

- Culling determines the objects to be rendered

- Rendering draws these objects with appropriate lighting and properties into pixel-based buffers

- Post-processing applies operations on these buffers to produce the final output frame sent to a display device.

1. Culling
List objects to render

2. Rendering
Draw objects

3. Post-processing
Apply additional image effects

culled objects →

a pixel

* These images are simplified representations. The actual number of pixels is much higher.

Figure 4.14: Steps of a Renderer Pipeline [83].

Different render pipelines use different shader outputs, giving them unique capabilities and performance characteristics suitable for specific games, applications, and platforms. Understanding the differences between render pipelines is critical to make the right choice for the project in development.

The Built-in Render Pipeline is Unity's default pipeline, offering limited customization options. The Universal Render Pipeline (URP) is a Scriptable Render Pipeline that allows for optimized graphics across a wide range of platforms, from mobile to high-end consoles and PCs. The High Definition Render Pipeline (HDRP) is a Scriptable Render Pipeline that provides cutting-edge, high-fidelity graphics for high-end platforms, but is incompatible with URP (Figure 4.16). When switching the active render pipeline in the Unity Editor or at runtime, developers should ensure that their assets and code are compatible to prevent errors or unintended visual effects.

Terrain URP DEMO scene, a free-download asset by Unity Technology from Unity Asset Store [84], was used and modified to create an initial scenario for the relaxation phase. The main modifications made were:

- Reduction of the size of the scenario.

- Reduction of the material quality.

- Removal of a significant portion of the vegetation, plants, and trees in the scenario.

- Addition of a waterfall, manually created with a particle system.

- Addition of a bridge [85].

The starting scenario (Figure 4.17) and the final scenario (Figure 4.18) are shown.

This scenario, however, posed a problem for creating visual stimulation that would allow brain entrainment. The initial idea was to use light sources that would vibrate at a specific frequency. The first test was done using Directional Light, a type of light source that simulates sunlight and illuminates the entire scenario. The problem in this case is that it is too heavy, so once rendered in Oculus, the stimulus could not withstand the necessary frequencies. Subsequently, other types of light sources were tested that would not affect the entire scenario, but these had problems rendering in URP. Numerous other tests were done to find a stimulus that could withstand the necessary frequencies and, above all, not be annoying for the patient, otherwise the opposite effect of relaxation would occur. The same problems occurred with scenarios in HDRP. The final choice was to completely change the scenario in order to use Build-in RP. Nature Renderer asset is used, which can be downloaded directly from the Asset Store. It is a paid scenario but is available for free in its DEMO, which allows you to use the scenario in Play Mode [86]. In this case, point lights are rendered correctly also withstanding the required frequencies. The scenario was also modified to make it lighter:

- Removal of great part of the vegetation, plants, and trees.

- Addition of a waterfall, manually created with a particle system.
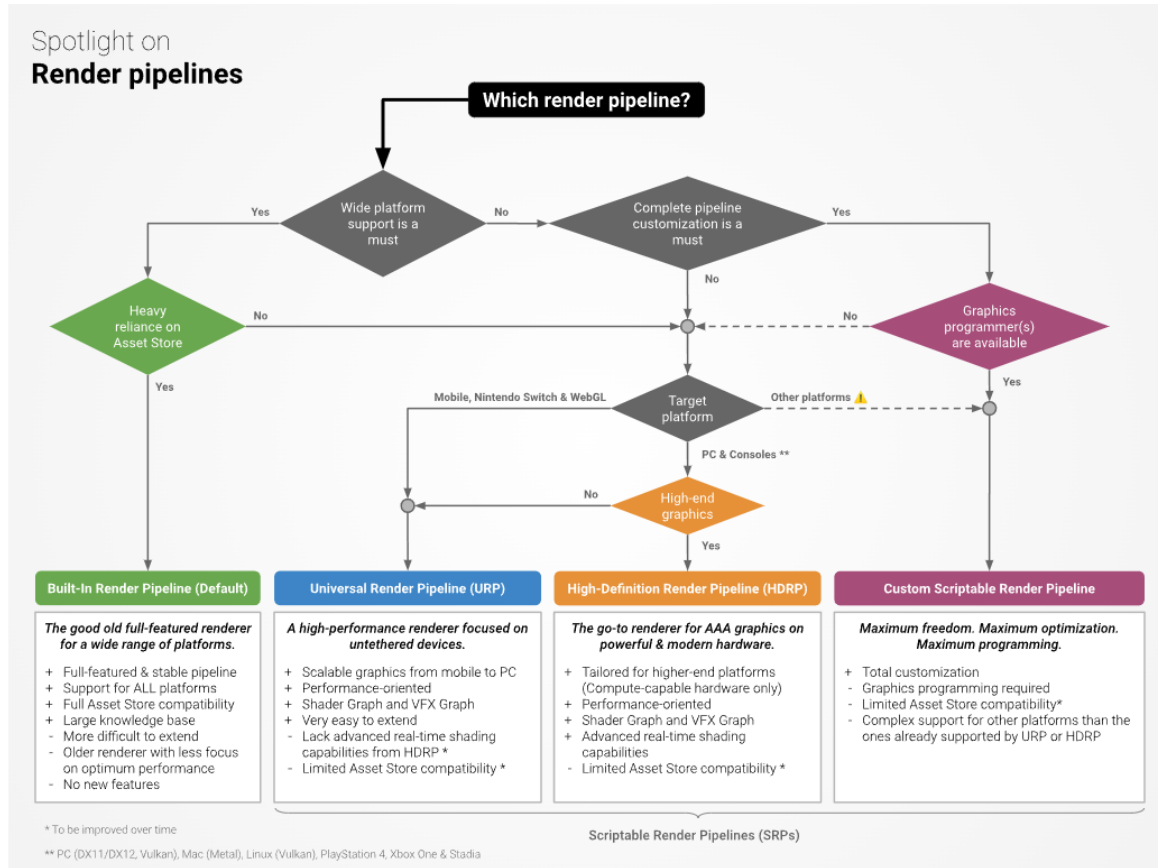
Figure 4.15: Decision chart to find out render pipeline [83].
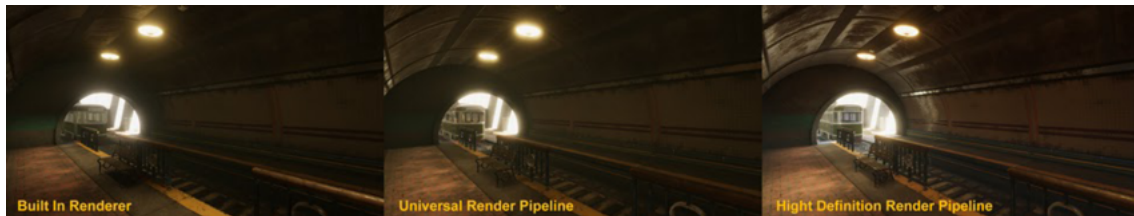
Figure 4.16: Differences between Build-in RP, URP and HDRP [82].

- Addition of a lake using the Standard Assets present in Unity [87].

Figure 4.19 to Figure 4.23 show the chosen scenario at the starting point (with no modifications) and at the final point (with the modifications). This is the final scenario with which the relaxation phase was carried out.

Regarding the audio in the scene, a relaxing music and the sound of a waterfall have been added. The auditory stimulation in the form of monaural beats was incorporated using the Immersive Brain's Level Upper package by Binaural Beat and Monaural Beat by "_chimera0" [88]. Both binaural and monaural beats can be generated interchangeably, and the user can choose to set a default EEG rhythm or generate waves at a specific frequency of their choice (Figure 4.24). The amplitude and sampling frequency of the signal are also parameters that can be adjusted by the user.

A visual indicator displaying the value of the BAR and the intensity of the fog were used as feedback elements. For both of these indicators, a TCP/IP connection was created between Matlab and Unity using C# code. To balance the fog intensity, the BAR value is divided by a constant factor. In Figures 4.25 and 4.26 two situations are shown where high and low BAR is measured.

Figure 4.17: URP demo scene without modification.
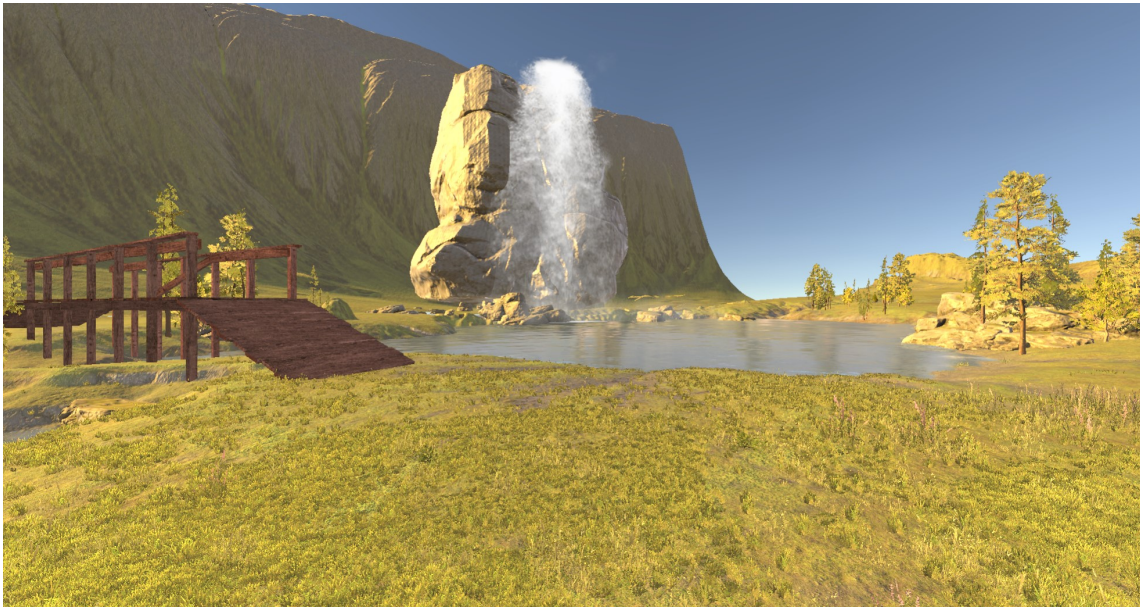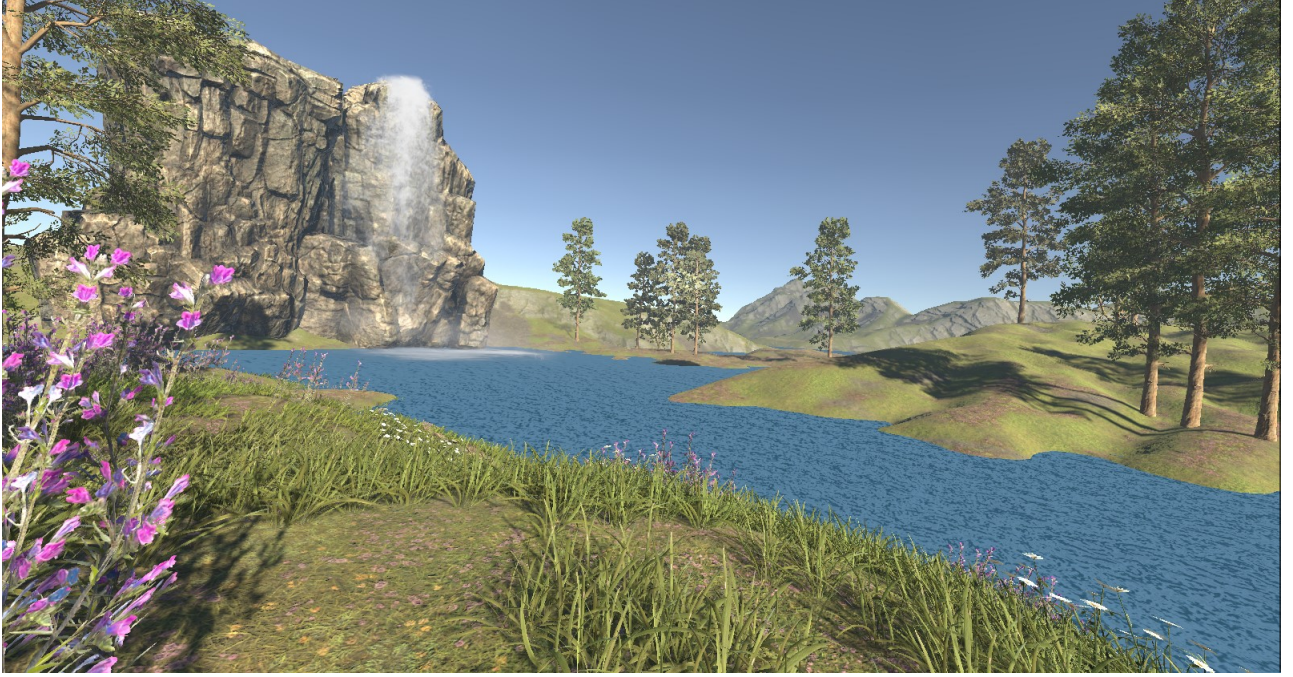

Figure 4.18: Modified URP demo scene.

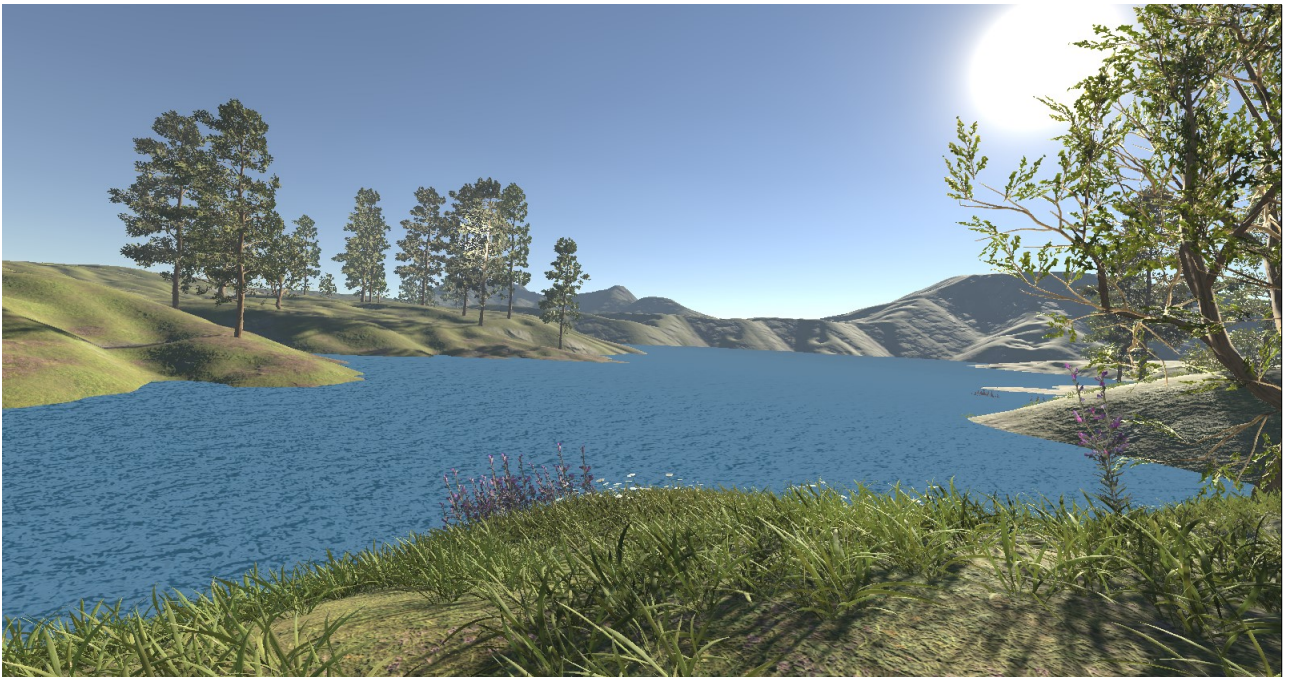**Figure 4.19:** Final scenario without modifications.

Figure 4.20: Final scenario without modifications.

Figure 4.21: Final Scenario for relax phase.


Figure 4.22: Final Scenario for relax phase.

4.3.4 Frequency selection for monoaural beats and light stimuli: brain entrainment.

In this study, in order to promote Brain Entrainment in the alpha band and support the subject's relaxation strategy, it was decided to combine auditory and visual stimulation. Based on the considerations outlined in chapter 2, monaural beats were chosen, supporting the study conducted by Chaieb and colleagues [28]. As explained in the preceding paragraph concerning scenario design, for the visual stimulus, the choice made was to use point lights located on three trees positioned in different areas of the scenario, in order to ensure that the subject always receives a visual stimulus even when turning her head to explore the environment.

Figure 4.23: Final Scenario for relax phase.
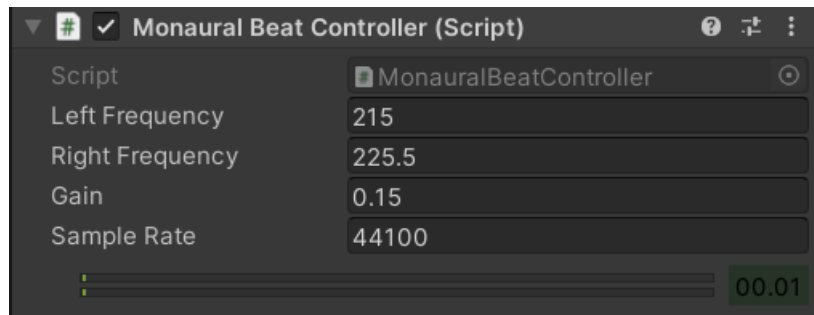
Figure 4.24: Genaration and setting of a monaural beat stimulation. The perceived frequency is the difference between Right Frequency and Left Frequency. The same frequency is provided at both ears.

In order to determine the frequency to set the stimuli, an analysis was conducted that drew from the studies carried out by Notbohm and colleagues in their experiment [89]. They demonstrated that rhythmic visual stimulation can influence brain activity through entrainment, thus supporting Arnold's concept of brain activity. The mechanism underlying the steady-state visual evoked potential (SSVEP) measured through EEG during rhythmic stimulation is not yet fully understood. There are two hypotheses regarding the origin of SSVEP: entrainment of brain oscillations and overlapping event-related responses (ERPs). In Notbohm's study, the entrainment hypothesis, but not the overlapping hypothesis, justifies rhythmic visual stimulation as a means of manipulating brain oscillations, as the overlapping hypothesis assumes a linear sum of individual responses independent of ongoing brain oscillations. It is believed that SSVEP results from the entrainment of an internal oscillator by an external rhythmic visual driving force. In the occipital cortex, this internal oscillator oscillates at the individual alpha frequency (IAF), which is then shifted towards the external frequency during entrainment. In summary, SSVEP would be the result of synchronizing the internal oscillation to an external frequency through entrainment.

In the analysis conducted in this study, a Unity scenario was created to reproduce an intermittent strobe light. In support of the scenario, 35 different combinations of light at different frequencies and amplitudes were generated through a code written in C# (5 amplitude levels, 7 different frequencies). Each combination is maintained for 30 seconds, followed by a 2-second pause that separates it from the next combination. The experiment begins with the first intensity level, and the waves at the 7 different frequencies are generated in turn, followed by the second intensity level, and so on. The scenario is
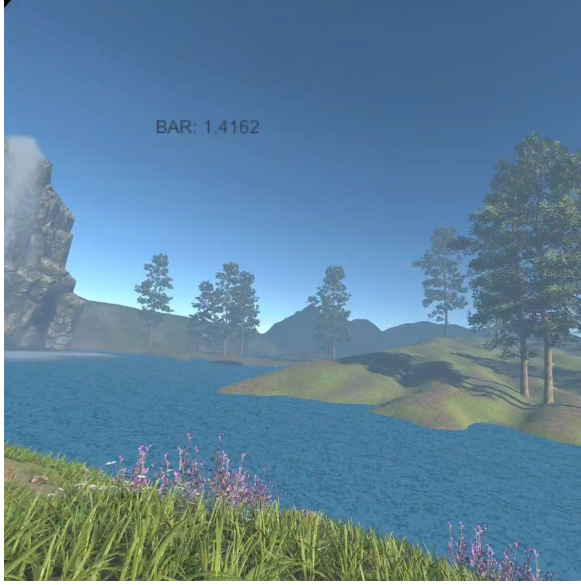
Figure 4.25: Scenario with high BAR values.
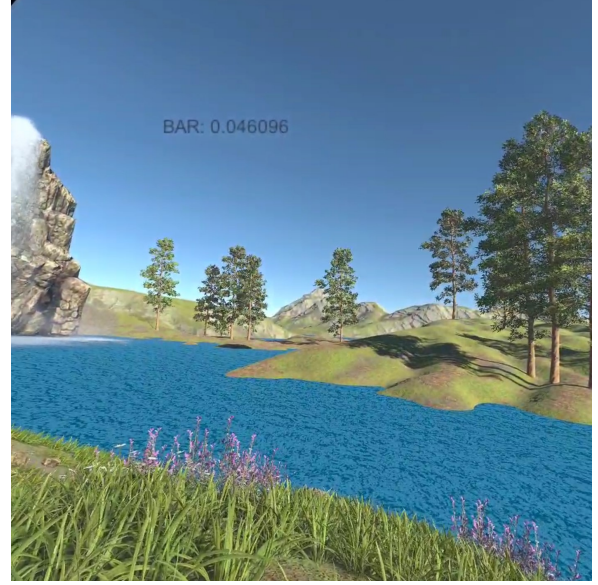
Figure 4.26: Scenario with low BAR values.

displayed on Oculus, and the subject remains with eyes closed for the entire duration of the test.

Before starting the stimulation, the subject's EEG signal with eyes closed is acquired with Oculus turned off in a resting state. From this initial acquisition, the IAF of the subject is determined, which will be used to set the 7 frequency levels of the strobe light test from -3 Hz to +3 Hz around IAF. After calculating the spectral power, IAF was defined as the maximum peak frequency in the alpha range (9-11 Hz) under the eyes-closed condition.

Not having a photostimulator that could generate lights with well-defined voltages, an attempt was made to generate lights on an HDRP scenario, the only scenario in Unity that allows generating amplitude values in lux. In this case, the following amplitudes were used: 1.42 Lux, 8.34 Lux, 52.8 Lux, 326 Lux, 7158 Lux. However, good results were not obtained, as the scenario did not support well the frequencies of the generated lights.

As a second option, it was decided to opt for a standard Unity scenario using directional lights generated as a square wave, with the following amplitudes: I1: 0.3, I2: 0.54, I3: 0.97, I4: 1.75, I5: 3.15. I1 was established as the first amplitude perceivable by the subject with eyes closed, and I5 was established as the maximum tolerable amplitude that was "not too bothersome", and finally, the central amplitudes follow a linear trend.

At the end of the experiment, called "Strobo", the data was post-processed to evaluate the degree of entrainment between the EEG signal and the visual stimulus, demonstrating that it was higher for light combinations at the subject's IAF frequency than for other frequencies.

To do this, 35 different square wave combinations were generated on Matlab, lasting 30 seconds each, at the established amplitudes and frequencies that simulate the light used in the scenario. Both the square waves and the subject's EEG signal were then filtered with a 6th order Butterworth filter with a passband of IAF $\pm$ 3.5 Hz. For each condition, the first and last 2 seconds were discarded to allow for steady-state conditions to be established and to avoid edge effects. To classify the degree of entrainment, phase-locking between the stimulation signal and the EEG signal at occipital channels was calculated. The Hilbert transform was applied to both signals, and the unwrapped phase angle difference was computed. This shift was then wrapped again between -π and +π. To quantify the degree of phase-locking, normalized Shannon entropy was finally calculated for each time point of each combination: the higher the normalized Shannon entropy value, the greater the degree of phase-locking. Normalized Shannon entropy was calculated as follows:

$$\tilde{\rho} = \frac{S_{max} - S}{S_{max}}, \tag{4.1}$$

with

$$S = -\sum_{k=1}^{N} p_k ln(p_k) \tag{4.2}$$

and

$$S_{max} = lnN \tag{4.3}$$

where p_k is the probability density function of the k-th element, N is the number of elements that constitute the signal, and S is the classical Shannon entropy.

Finally, the entropy values were plotted using a colormap. Consistent with expectations, the highest degree of phase-locking occurs for light combinations at the frequency equal to IAF, as shown in Figures 4.27 and 4.28. However, it was not possible to perfectly appreciate Arnold's tongue, according to which the maximum degree of phase-locking is obtained both at frequencies around IAF even at lower intensities, and at frequencies far from IAF as intensity increases, reflecting a sort of triangle. In Notbohm's study, as well as in this one, a perfect Arnold's tongue was not obtained.

In our case, the main problem was probably related to the fact that we did not have suitable instrumentation to generate stroboscopic light with extremely precise amplitudes and frequencies, and certainly to the fact that the post-processing analysis was done by simulating the stimulus signals rather than importing the actual signals, which were not extractable from Unity.

In accordance with this analysis, in our scenario, both for the visual stimulus and for the monaural waves, a frequency equal to the subject's IAF was chosen, calculated anew at the beginning of each training session. The intensity of both stimuli was instead kept fixed for all acquisitions and was determined at our discretion so that it integrated well with the scenario, making the stimuli distinguishable from the rest but not dominant.
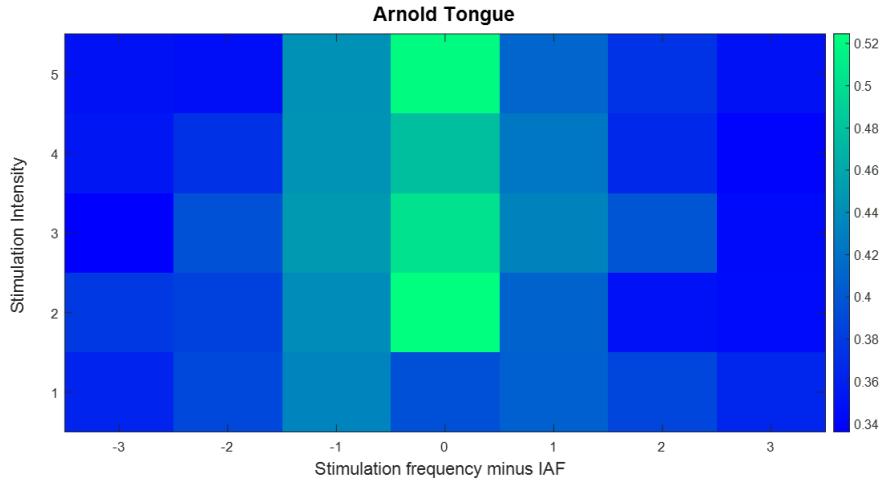
Figure 4.27: Arnold tongue on O1.
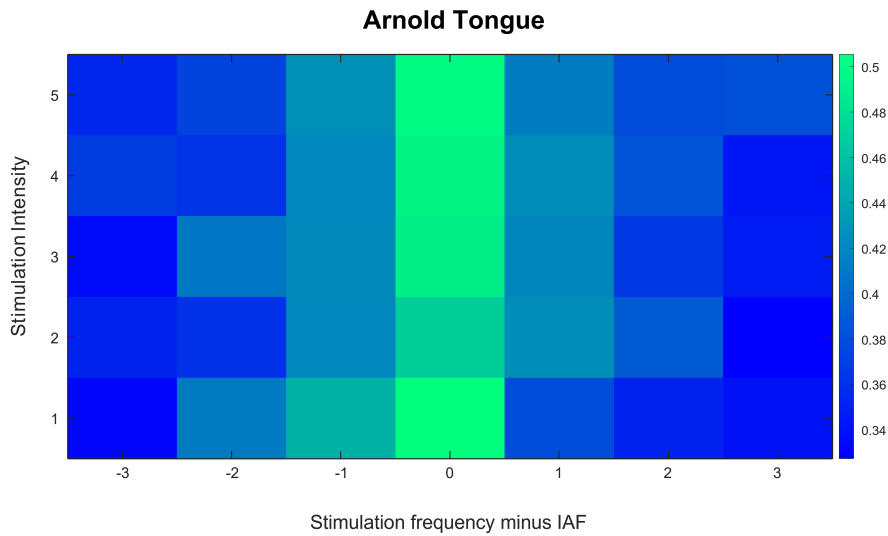
Figure 4.28: Arnold tongue on O2.

Chapter 5

Data Analysis

The processing of data occurred in two distinct phases: in real-time during the various training sessions, and following the training to analyze the results.

5.1 Processing in real time

Through the LSL connection, data is sent from NIC2 to Matlab one chunk at a time every 500 ms. A pre-processing step is performed on each chunk of data to extract an index, which is then sent to Unity. To improve spectral power resolution, upon arrival of each chunk, it is concatenated with the previous 4 chunks to obtain a signal of approximately 1000 samples. This signal is first filtered with a Chebyshev type 1 filter of order 5 with a passband of 4-40 Hz. Subsequently, the Fast Fourier Transform is computed using a Welch periodogram with a window equal to half of the signal length and 50% overlap to preserve information integrity. Based on this, the power spectral density (PSD) is calculated, and the alpha and beta band powers are extracted for each channel. The BAR index is then calculated, for each channel, as the ratio between beta and alpha band powers. To avoid excessive index variability, the BAR is averaged with its previous 3 samples. Finally, the BAR value averaged across the two occipital channels, O1 and O2, is computed and sent via TCP/IP connection to Unity, which will interpret and vary the fog in the scenario based on this value.

5.2 EEG processing off-line and extracted parameters

The subject's EEG signal is acquired during every phase of the training, while the ECG signal is acquired during all phases except for phases 1 and 6 described in Study protocolo paragraph, which involve calculating the IAF. The following EEG channels derived from the 10-10 system were used: O1, O2, Pz, F3, and F4, and the signals were referenced to the CMS channel. All the impedances are mantained below 10 kΩ. The ECG signal was taken from the subject's left wrist. During the acquisition, the trainer, who manages the training session from the computer, inserts markers on the NIC to distinguish the different phases of the acquisition in post-processing.
The EEG signal is acquired at the sampling frequency of the NIC, which is 500 Hz, and is maintained at this frequency even in post-processing. In order to remove low-frequency artifacts and powerline noise, a 6th-order Chebyshev filter with a passband of 4-40 Hz was applied. To extract the PSD, Welch periodogram was used. The periodogram computed by FFT algorithm can be utilized to estimate PSD features of EEG signals, however, the periodogram is prone to large variance and poor statistical accuracy. To overcome these limitations, Welch introduced a modified approach to periodogram averaging that reduces PSD variance. This technique involves segmenting the time-series data, potentially with overlap, then applying FFT, computing the magnitude of each segment, and averaging these spectra [90].

In this study, four different tests were carried out to calculate the periodogram:

- 4-seconds blocks signals without overlap

- 2-seconds blocks signals without overlap

- 4-seconds blocks signals with 50% overlap

- 2-seconds blocks signals with 50% overlap

Tests with 4-second blocks allow for better theoretical frequency resolution, but at the same time do not guarantee the hypothesis of wide stationary signal (WSS).

On the other hand, 2-second blocks signal satisfy WSS hypothesis, but reduce the theoretical resolution. Furthermore, a larger statistical sample is obtained with this option.

The feedback parameter has been extracted from the 4 periodograms calculated. Statistical comparisons (Figure 5.1) were made in order to check whether the value changed consistently over the four conditions. No statistical difference was found, then we chose the condition that fitted our study the best.
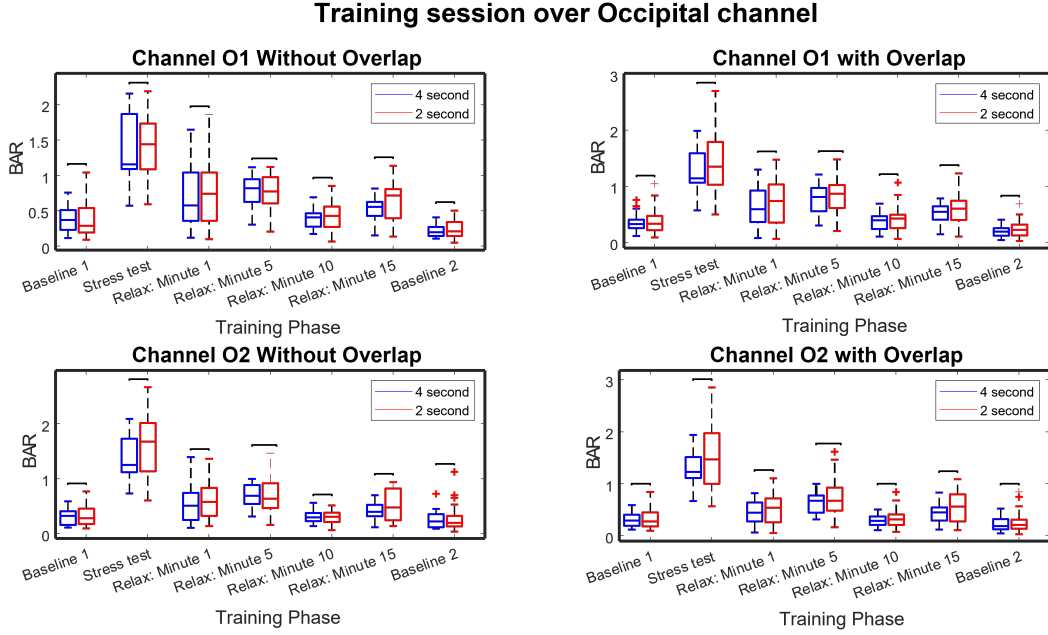
Figure 5.1: Comparison of BAR index boxplots in the same training phase, calculated with different Pwelch conditions. None of the differences was statistically significant. The same test was performed on the frontal channels obtaining similar results.

The final choice was to calculate the FFT using Welch periodogram on 2-second blocks signal without overlap in order to have independent samples of each other. From this, the PSD was extracted, and with it, also the alpha power value, the beta power value, the BAR, and the value of the frontal alpha asymmetry (FAA) were extracted for each 2-seconds block.

$$BAR = \frac{P_{beta_r}}{P_{alpha_r}} \tag{5.1}$$

where P_{alpha_r} is the relative alpha band power and P_{beta_r} is the relative beta band power.

$$FAA = \ln F_4 - \ln F_3 \tag{5.2}$$

where F_4 is the relative alpha power over F4 channel, and F_3 is the relative alpha power over F3 channel. BAR and FAA will be better described in the following paragraphs.

These two computed parameters exhibit a strong variability, therefore, in order to visualize a smoother trend, two steps were performed: removal of outliers and averaging of the samples. The Median Absolute Deviation (MAD) method was used for outlier removal.

This method for identifying outliers involves computing the median of the residuals and subtracting it from each historical value. The absolute values of these differences are then calculated, and a new median is computed by multiplying the original median by a constant that has been empirically determined. This new median, known as the median absolute deviation, is used to set a threshold for outlier detection. Any value that is over the threshold is considered an outlier [91]. By default, this threshold is set at 3 MADs, and this value was mantained for asymmetry (Figure 5.3). However, for BAR parameters, it has been raised to 4 MADs, as it was found to be too restrictive (Figure 5.2).
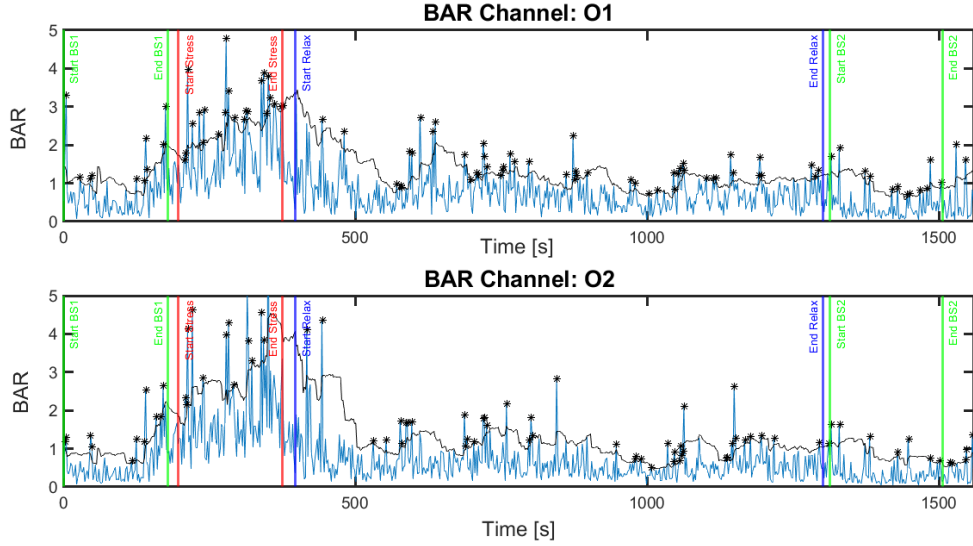
Figure 5.2: Outliers obtained by MAD method are marked with asterisks. The black line represents the threshold used (4 MAD), all values above the threshold are classified as outliers. The coloured vertical lines mark the beginning and end of each phase: in green the two baselines, in red the stress test and in blue the relaxation phase.
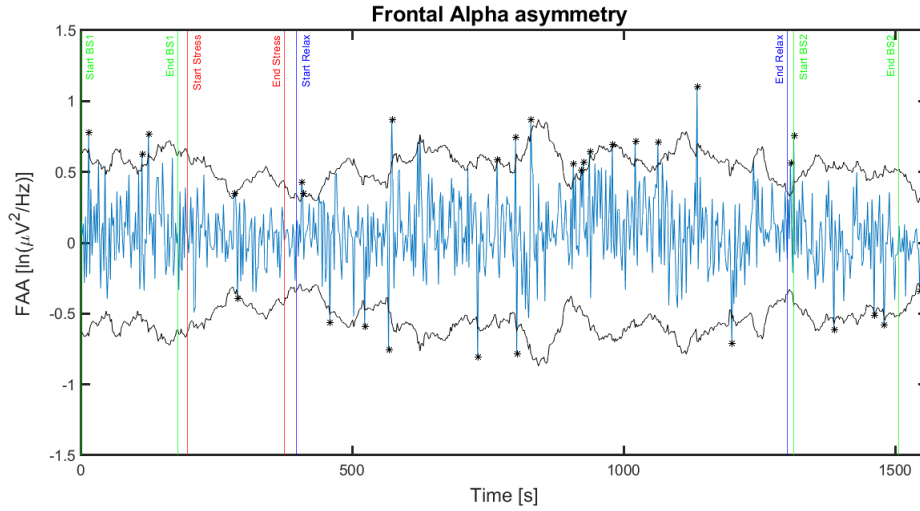

Figure 5.3: Outliers obtained by MAD method are marked with asterisks. The black line represents the threshold used ($\pm$ 3 MAD), all values above the threshold are classified as outliers.

After identifying the outliers (Figure 5.2, 5.3), they were removed and each one was replaced with the mean value of the four preceding samples (Figure 5.4, 5.5). To visualize a smoother trend, each value of BAR and asymmetry was averaged with the previous 5 samples (Figure 5.7, 5.6). However, to process results, no smoothed values were considered.

5.2.1 BAR

The analysis of EEG signals in the frequency domain allows for the detection of stress levels based on the alpha and beta band powers. Band powers were used to extract features that determined the subject's emotional state while performing a stress test and while being engaged in a relaxation task in a naturalistic setting.

One of the techniques employed by researchers to reflect cortical control function over the subcortical is the ratio of slow wave to fast wave (SW/FW) in EEG. Additionally, the Beta/Alpha ratio is utilized to
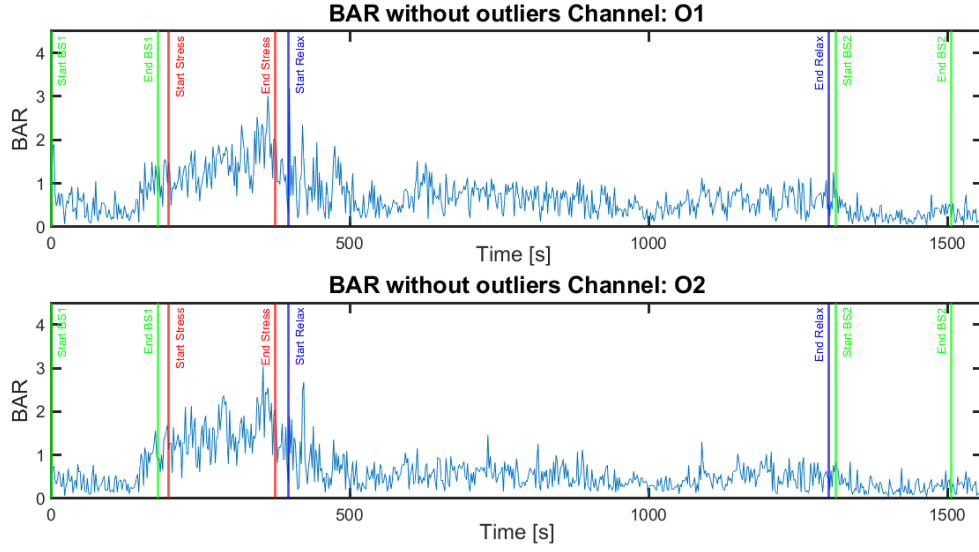
Figure 5.4: BAR trend after outliers removal.
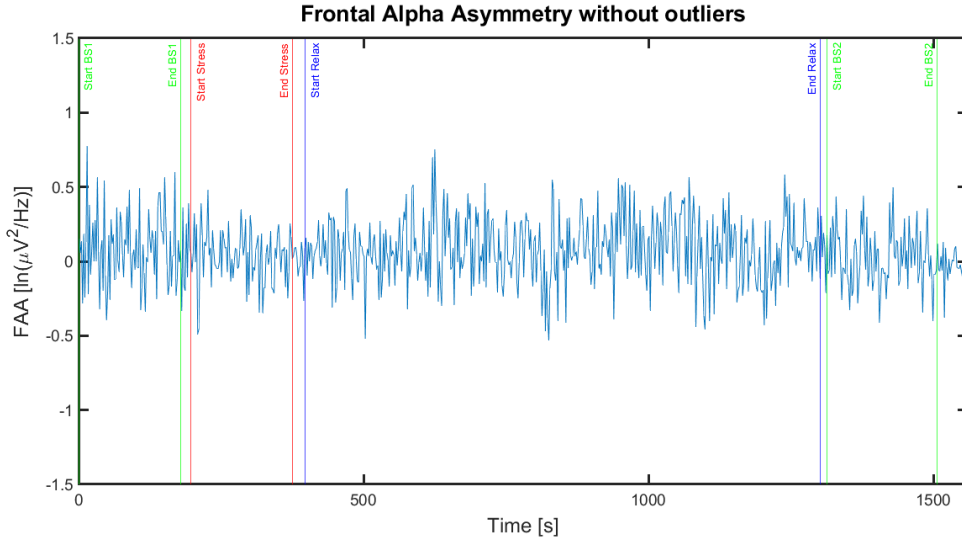
Figure 5.5: FAA trend after outliers removal.

investigate the progression of an individual's cognitive state, including mental attentiveness and fatigue [90].

In particular, the ratio between beta band power and alpha band power (BAR) has been shown in numerous studies to be a reliable index for detecting an individual's stress state.

In conditions of stress, the Beta/Alpha ratio increases, indicating a decrease in Alpha activity and an increase in relative Beta activity. A greater ratio value indicates a greater percentage of Beta activity. Alpha oscillations typically occur when the brain is relaxed, while Beta oscillations are associated with an active and stressful state. Previous studies have found that a lower BAR, which reflects increased Alpha power and/or decreased Beta power, is linked to reduced alertness or arousal, indicating a higher level of fatigue. Furthermore, another study reported that a greater engagement in cognitive processes during decision-making leads to an increase in the BAR, indicating a less relaxed state [90].

This ratio was calculated on the two occipital channels, O1 and O2, precisely because the entire study focuses on visual stimuli in virtual reality. It was used both as a feedback parameter during the various training sessions and as an index of relaxation in post-processing.

Some indices were calculated from the BAR values during the relaxation phase to assess the subject's ability to relax.
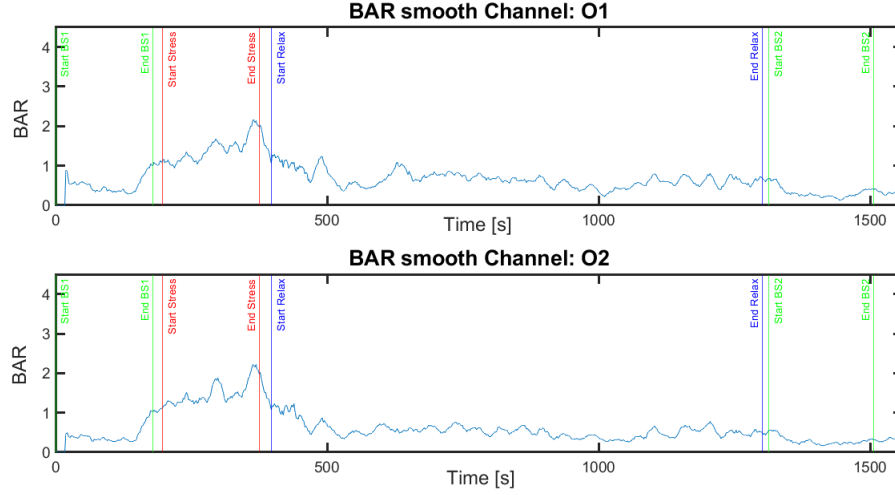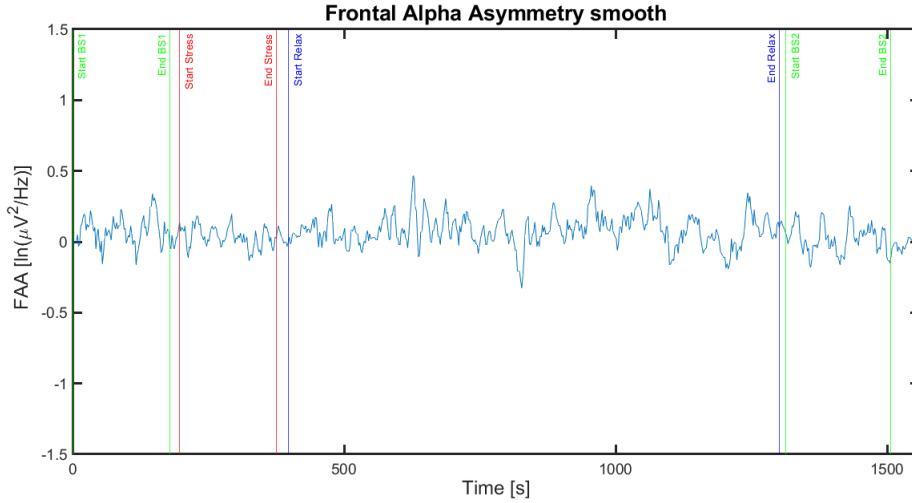
Figure 5.6: BAR smooth

Figure 5.7: FAA smooth

Extracted parameters from EEG

As the first extracted index, a value is calculated that is very close to what Guoxin Gu and Claude Frasson defined as Time Interval to Relaxation (TItR) in their project called "Virtual Sophrologist" [92]. TItR represents the amount of time it takes the subject to reach a certain level of relaxation. A threshold for the BAR value (threshold: 0.6 in this study, i.e. 80% of the BAR values mean in the relaxation phase of the first training session) is established, which is consistently reached by the subject in question in every training session and is close to the minimum values of the BAR reached.

To extract this parameter, all intervals for which the BAR value remains below the threshold for at least 20 consecutive seconds are identified. Then, the first time instant when this condition is achieved is taken as the value of TItR.

The second extracted index is defined as the Max Relaxation Score (MRS). The MRS is the minimum value of the BAR that remains within $\pm$ 5% of its value for at least 10 seconds.

To calculate it, all intervals where the BAR value remained within $\pm$ 5% of its value for 10 consecutive seconds were identified. Within these intervals, the lowest BAR value was taken as the MRS. Finally, another time index, defined as T_{max}, was calculated. To extract this index, all intervals where the BAR remained below the previously established threshold (BAR: 0.6) consecutively were identified. T_{max} was defined as the longest of these intervals, representing the maximum amount of time the subject was able to continuously maintain her BAR below the threshold.

The evaluations regarding the trend of these indices will be presented in the following chapter.

5.2.2 FAA

The FAA theory utilizes EEG recording to differentiate between left and right alpha activity in the frontal regions of the brain. According to this theory, the left frontal hemisphere is associated with the behavioral activation system which is related to positive emotions and approach motivation. Conversely, the right frontal hemisphere is associated with the behavioral inhibition system which is related to negative emotions, withdrawal or avoidance motivation, and comorbid depression and anxiety. In order to measure FAA, Baehr et al. [93] introduced the frontal alpha asymmetry score (A1 score), which is computed by subtracting the common logarithm of left-alpha power from the logarithm of right-alpha power (A1=log F4 –log F3) [94].

As EEG alpha power is an inverse index of cortical activity, frontal alpha power asymmetry is believed to reflect the relative activity levels between the right and left prefrontal lobes. Studies have shown that reduced alpha power in the right frontal sites (i.e., greater right-sided activity) is associated with withdrawal motivation, negative affect, and more intense negative emotions after exposure to unpleasant stimuli such as films. Conversely, reduced alpha power in the left frontal sites (i.e., greater left-sided activity) is linked to approach motivation, positive affect, increased pleasantness after positive film viewing, reward responsiveness, dispositional optimism, greater emotional flexibility, and better emotional regulation [95].

For these reasons, it was chosen to use this parameter as an evaluation tool for the efficiency of the training in this study. FAA should have a lower value during the Stress Test phase, assuming that the subject is experiencing pressure and anxiety, and should increase during the relaxation phase, where positive emotions should increase activity in F4. This was not chosen as a feedback parameter because it is still a highly debated and studied parameter. Additionally, it is more solid when dealing with depressive or anxiety disorders, while there is still very little literature regarding frontal alpha asymmetry for the stress-relaxation combo.

Results were extracted from the trends of these parameters, which will be discussed in the following chapter.

5.3 ECG processing off-line and extracted parameters

Similarly, the ECG signal was acquired at the NIC sampling frequency and maintained at this frequency during post-processing. A 8th-order Chebyshev filter with a passband of 4-100 Hz was applied to the raw signal. The R-peaks were subsequently identified, and the RR interval duration was calculated. From this data, the heart rate parameter and a statistical parameter related to heart rate variability were extracted every 30 seconds.
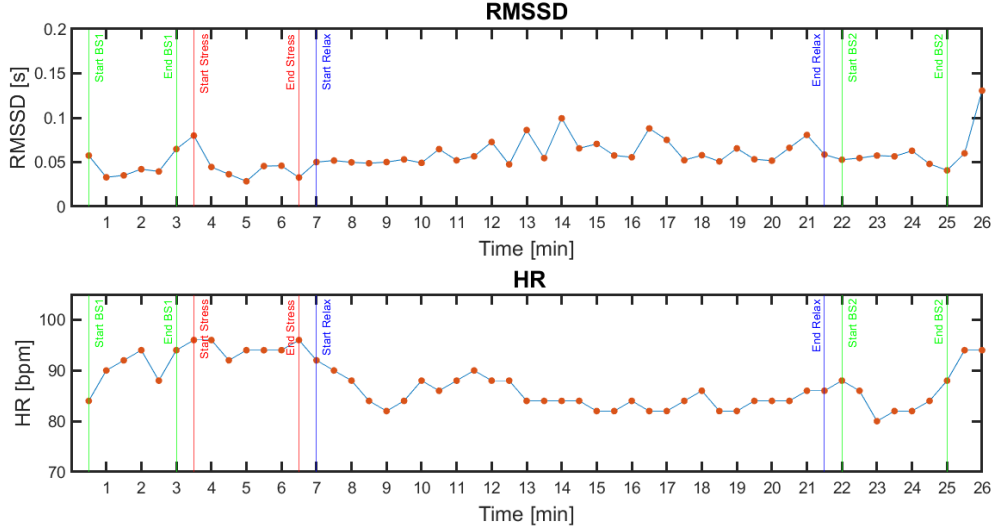
5.3.1 HR and RMSSD

Heart rate (HR) is a physiological response that refers to the number of heartbeats per minute, which fluctuates as the sinus node of the heart activates the autonomic nervous system. During a stable state, HR decreases when the parasympathetic nerve is activated, and increases when the sympathetic nerve is activated. Typically, indices for measuring HR are established using Heart Rate Variabilty (HRV), which reflects the temporal changes in HR, rather than the raw data from HR. Consequently, this study evaluated the subject's stress levels based on her HRV. Generally, HRV refers to minute variations in N-N intervals, i.e. all the intervals between the QRS complexes generated by the sinus node depolarization [96]. The Root Mean Square of Successive Differences (RMSSD) is an index that calculates the root mean square of the difference between two adjacent RR intervals, revealing changes in heartbeat over a short period of time. It provides an indication of the parasympathetic nervous system's activity related to the heart. Specifically, an increase in this index implies that the parasympathetic nerve has been activated, resulting in a reduction in stress levels and improved psychological stability in the subject [96].

HR and RMSSD were calculated for the entire duration of the training sessions. Figure 5.8 shows the trend of the two parameters over a single session.

$$RMSSD = \sqrt{mean[(RRInterval1 - RRInterval2)^2 + (RRInterval2 - RRInterval3)^2 + ...]} \quad (5.3)$$

Figure 5.8: HR and RMSSD trend over a single training session.

Extracted parameters from ECG

Just as in the case of the BAR, indices were extracted from these parameters to reflect the degree of relaxation of the subject. Specifically, firstly, the minimum HR value (HR_{min}) reached in each training session was calculated, sampled every 30 seconds, and the maximum RMSSD value (HRV_{max}). Two temporal indices were then calculated to be consistent with those calculated for the BAR. In particular, a $TItR_{ECG}$ was calculated as the time instant, during the relaxation phase, at which the subject reaches the minimum HR value and maintains it for at least 1 minute. Finally, a $TItR_{ECG}$ with a fixed threshold was also calculated similarly to how TItR is calculated with BAR: intervals of time during the relaxation phase were identified in which the HR remains for at least 2.5 consecutive minutes below a certain threshold value (86 bpm in this study), always reached by the subject in question (except in the third training, for which this value is not calculated) and close to their minimum HR value. Once these intervals were identified, the start time of the first of these intervals was taken as $TItR_{ECG}$ with a fixed threshold. Results of this analysis will be discussed in the next chapter.

5.4 Artifacts Removal: Independent Component Analysis with EEGLAB

As described in Chapter 1, the EEG signal is highly affected by artifacts. Therefore, attempts were made to remove these artifacts. Specifically, the EEGLAB toolbox in Matlab was used to perform an Independent Component Analysis (ICA). ICA is a method for separating data into additive subcomponents, that can be considered statistically independent as possible, enabling, in this way, the rejection of the component of the signal not related to the brain activity. However, due to the limited number of channels available, the efficiency of this procedure was quite low. As a result, a further attempt was made by adding the Fp1 and Fp2 channels, which are the channels most affected by the Eye Blinking artifact, so that this artifact component could be better extracted. This second attempt was more successful than the first, and the number of independent components found was equal to the number of channels used. However, the extracted components were very similar to each other, they were wrongly cassified by the algorithm, and removing them did not produce results that had a substantial effect on the calculation of the EEG parameters considered in this study. Therefore, it was decided to neglect this aspect, which was not particularly impactful in a study where the signals are mainly processed in real-time. Furthermore, a large part of the artifacts was eliminated through the post-processing high-pass filtering at 4 Hz.

Chapter 6

Results and Discussion

From the offline processing of the parameters and the extraction of the indices described above, considerations have been carried out to analyze the effectiveness of the training both in individual sessions and as a whole, by comparing the various sessions with eachother.

6.1 EEG results

The results of the EEG signal processing are shown below.
In order to evaluate the effectiveness of each individual training session, boxplots were created to represent the trends of the main parameters during the different phases of the acquisition. To increase the statistical sample, the parameter values related to the different training sessions were concatenated together over the individual phases. To make the values of the training sessions comparable with each other, each value was normalized by the absolute value of the median obtained in the initial Baseline phase of the same session. This was done for the BAR on O1 and O2 channels and for the FAA, both after removing outliers.
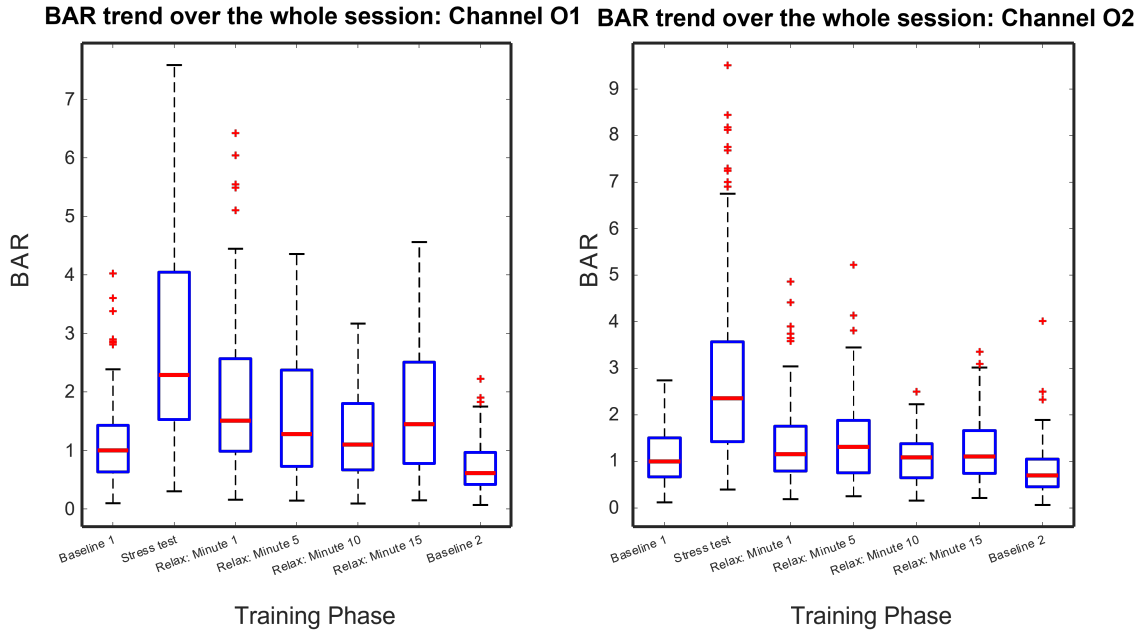

Figure 6.1: Boxplot showing BAR trend on O1 and O2 channels over the whole training session: each box contains 124 samples.

From the image in Figure 6.1, the trend of the BAR can be observed during the various phases of a training session, specifically analyzing the central minute of the first baseline, the central minute of the stress phase, the first, fifth, tenth, and last minute of the relaxation phase, and finally, the central minute of the second baseline.
During the initial baseline, the BAR shows its value within the resting phase, but rapidly increases during

the stress test, demonstrating an increased beta rhythm due to the subject's concentration on calculations and the stress induced by the scenario. The parameter values during the first minute of relaxation phase are slightly influenced by the stress phase, but a clear decreasing trend can be seen in the subsequent minutes, leading to a completely inverted trend in the final phase and second baseline, where the alpha rhythm prevails over the beta rhythm, confirming an increased state of relaxation in the subject.

However, the same results were not obtained for the FAA. In fact, this parameter was expected to show a decreasing trend during the stress test, followed by an increasing trend during the relaxation phase. From Figure (6.2), a slight increase in parameter values can be observed from the stress phase to the relaxation phase, but the finding is not as evident as in the case of the BAR. Reasons for this "negative efficiency" have been identified, primarily related to the placement of the channels used to calculate this value. The frontal channels are strongly influenced by eye blinking artifacts. Furthermore, as expressed in the previous chapter, this parameter is more reliable in studies related to depressive disorders, so it was not expected to yield promising results like those obtained for the BAR. Finally, this was not the feedback parameter that the subject was trained on.
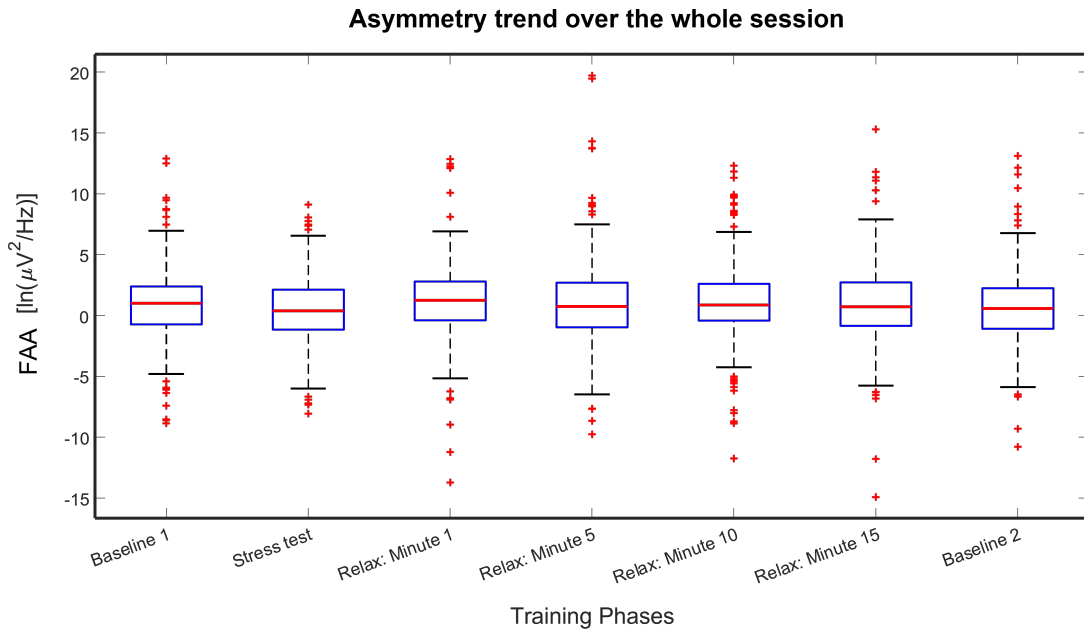
**Figure 6.2:** Boxplot showing FAA trend over the whole training session: each box contains 124 samples.

Results have shown a positive efficiency of Neurofeedback that is maintained over time, even after the relaxation scenario has ended. In this regard, Figure 6.3 shows the comparison of BAR values between the initial baseline and the final baseline. On channel O1, during the initial baseline, the average BAR value is 1.136 ± 0.734, compared to an average value of 0.728 ± 0.444 during the final baseline. On channel O2, instead, the average BAR value is 1.103 ± 0.609 in the initial baseline, compared to 0.804 ± 0.545 in the final baseline.

After the session, the subject experiences a physical relaxation sensation that lasts for several minutes after the end of the session itself. A Student's t-test was performed between the two conditions to demonstrate this result, and a statistically significant difference was found with a p-value of $2.8 * 10^{-7}$ on channel O1 and $6.3 * 10^{-5}$ on channel O2.

The same analysis was performed on FAA, but, for the reasons listed above, the results were not as expected.

A boxplot was also created for the asymmetry parameter comparing the three stress test minutes to minutes from 14 to 17 of the relaxation phase. From Figure 6.5, an increase in the FAA value is observed in the second phase, with a p-value of 0.0016.

For the creation of all these boxplots, the first three trainings were excluded, i.e., those in which the used baseline had problems with the alpha rhythm, as well as the sixth and eighth trainings due to anomalies on the initial and final baseline, respectively. In particular, during the initial baseline of the sixth training, a very high BAR trend is observed compared to the other training sessions. The subject reported that during this acquisition he was counting the squares composing the floor tiles of the baseline
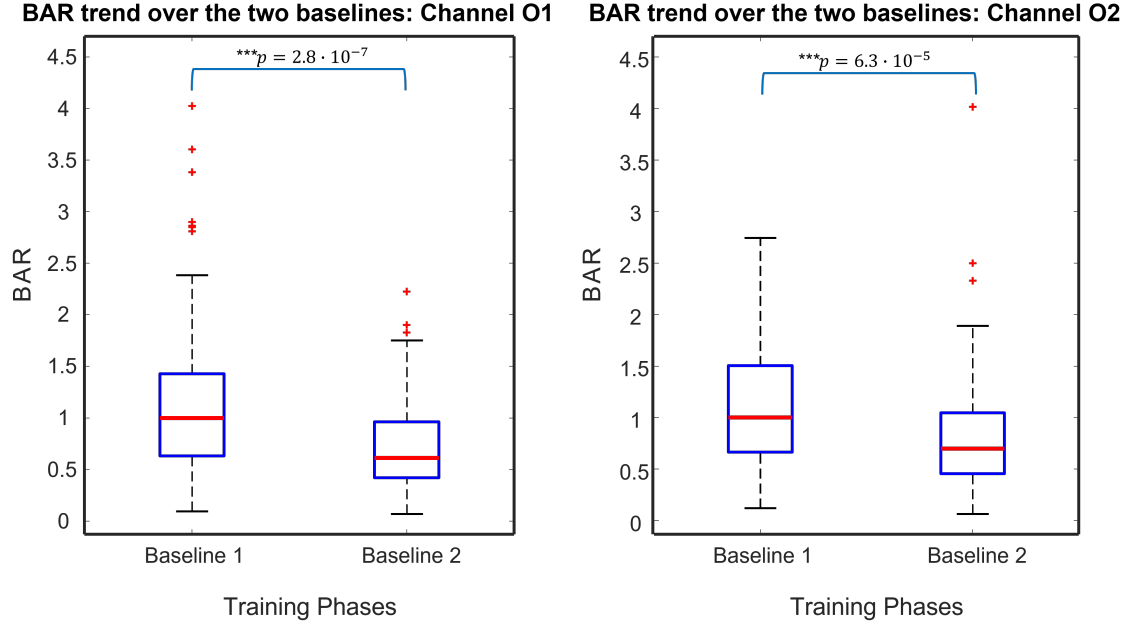
Figure 6.3: Boxplot showing BAR values comparing the initial and the final baseline.
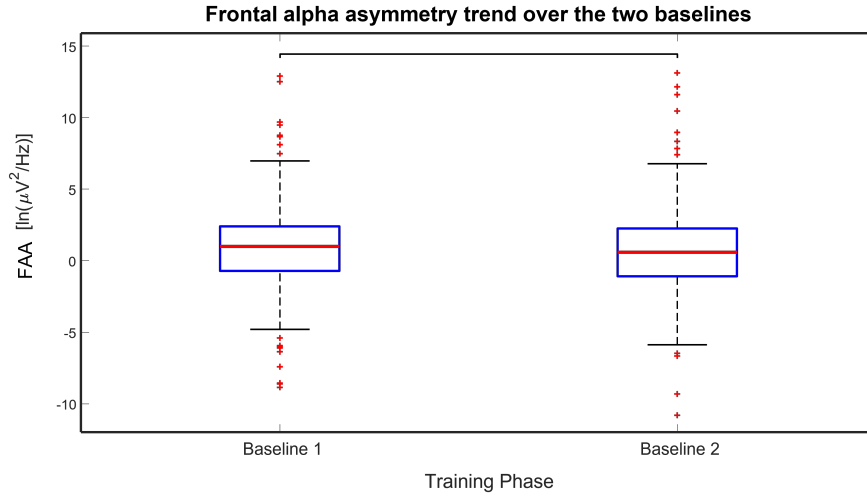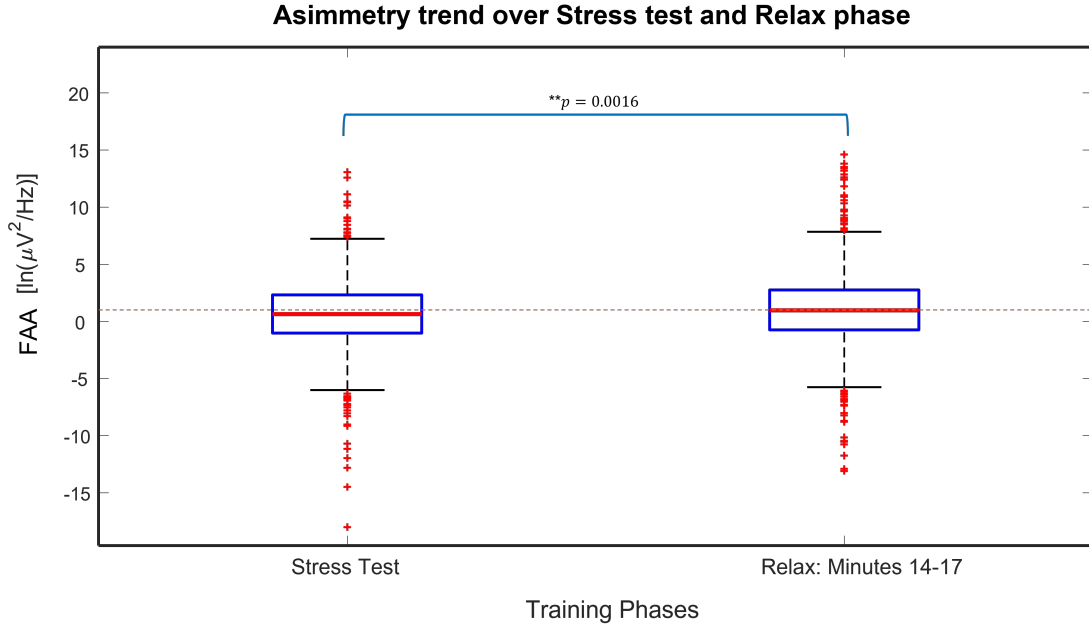

Figure 6.4: Boxplot showing FAA values comparing the initial and the final baseline.

scenario, leading to the hypothesis of an increase in beta rhythm due to this activity. Following this consideration, a specific test was carried out, which confirmed the hypothesis just described.

The eighth training was excluded from these analyses because there was a drop in subject virtual immersiveness at the end of the relaxation phase. In fact, once the relaxation phase was over, no more audio was sent to the earphones, and at the moment of the final baseline, the subject was suddenly distracted by numerous noises present in the acquisition place at that time (on that day, oral exams were taking place next to the acquisition station at the Politecnico LED).

The parameters TItR, MRS, and Tmax described in the previous chapter were used to perform comparisons between the various training sessions, in order to evaluate the trend of the training over the three weeks and obtain a quantitative feedback on the improvement achieved from the first to the last acquisition. In fact, Neurofeedback procedures require at least 8/10 sessions, so it is important to evaluate the protocol over time.

Figure 6.6 shows the value of TItR for all training sessions. A linear regression is performed on these values to visualize the decreasing trend of this parameter from the beginning to the end of the Neurofeedback training. As the subject trains, he is able to reach the threshold of 0.6 of the BAR in less time, starting

73

Figure 6.5: Boxplot showing FAA values comparing the three stress test minutes and minutes from 14 to 17 of the relaxation phase.

from the initial moment of the relaxation phase, confirming that he has found a relaxation strategy that seems to have repeatable and increasingly better results among the various sessions. TItR decreases indeed from 11 minutes in the first training session to 2.7 minutes in the last one.
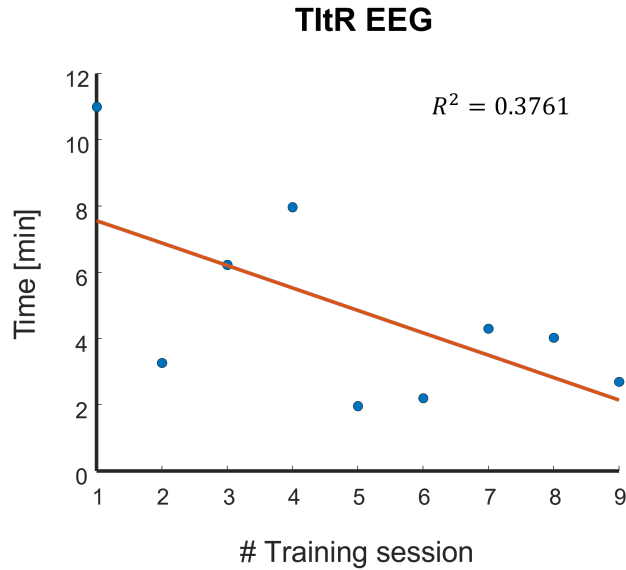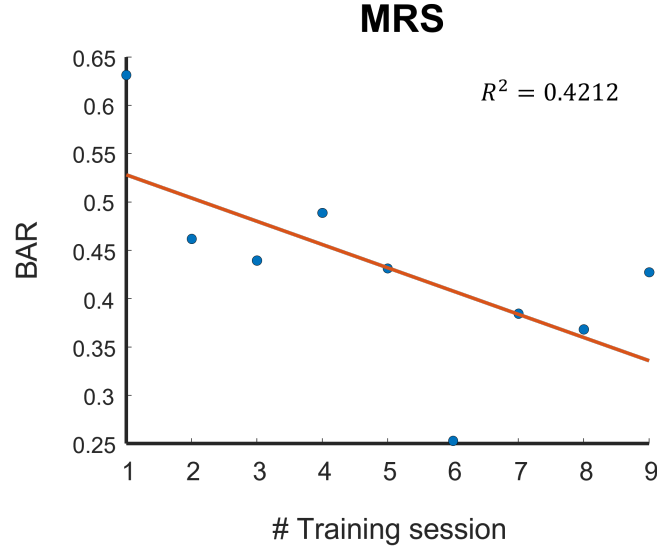

Figure 6.6: TItR values over the whole training: decreasing trend.

During the training, the subject is also able to increase her level of relaxation, as shown in the graph in Figure 6.7. The training starts with an initial MRS of 0.631 and ends with an MRS of 0.427, reaching a peak of 0.253 in session 6, which is by far the best in the entire training on the relaxation phase. In this case as well, a linear regression is performed to provide a clearer visualization of the decreasing trend of this parameter.

Another positive result achieved by the subject in this training is the increase in the time for which she is able to maintain her maximum state of relaxation. As shown in Figure 6.8, it is evident that the T_{max} increases from the first to the last training session. This once again demonstrates how the strategy found is robust and how the subject has been able to increase her level of proprioception over time, gaining

Figure 6.7: MRS values over the whole training: decreasing trend.

greater awareness of her brain rhythms.
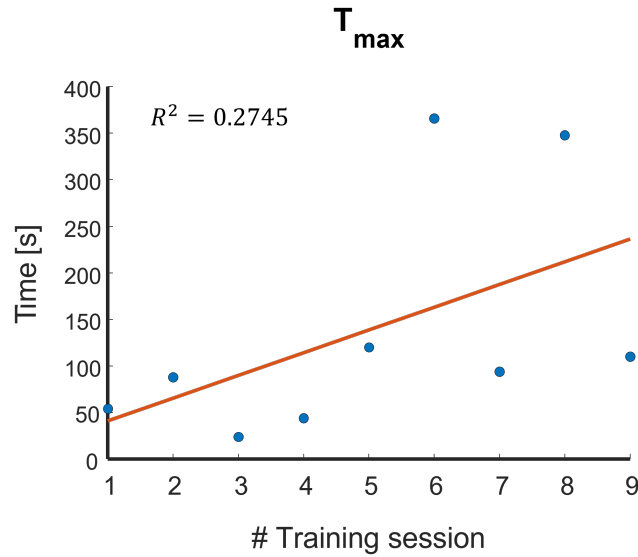
Figure 6.8: Tmax values over the whole training: increasing trend.

6.2 ECG results

Similarly to the analysis performed on the EEG signal, in this case as well, results were extracted to demonstrate on one hand the effectiveness of training in a single session and on the other hand the improvements obtained over time.

Boxplots were created to show the trend of Heart Rate and Heart Rate Variability in the form of RMSSD (Figure 6.9) during the various phases of acquisition. The three minutes of baseline 1, stress test, baseline 2, and the three minutes of the relaxation phase from minute 14 to minute 17 were considered. In order to increase the statistical sample, the data related to the various training sessions were concatenated, excluding those previously mentioned. It is observed that the heart rate starts from a median value of 88 bpm, increases to a value of 94 bpm during the stress test phase, and then decreases during the relaxation phase to a value of 84 bpm, lower than the starting value.

Similarly, HRV, evaluated using RMSSD, decreases during the stress phase (mean value: 0.045 ± 0.017) and increases during the relaxation phase (mean value: 0.058 ± 0.016), reaching higher values during the second baseline (mean value: 0.052 ± 0.008) compared to those of the initial baseline (mean value: 0.052 ± 0.019).

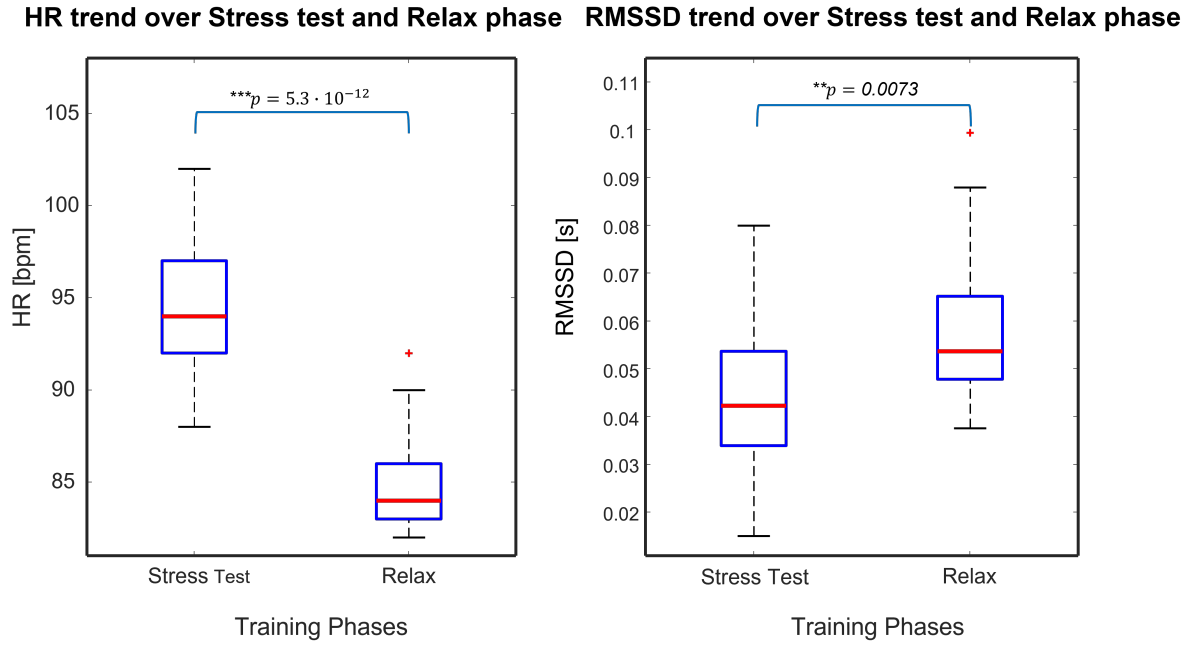**HR trend over the whole training session**   **RMSSD trend over the whole training session**
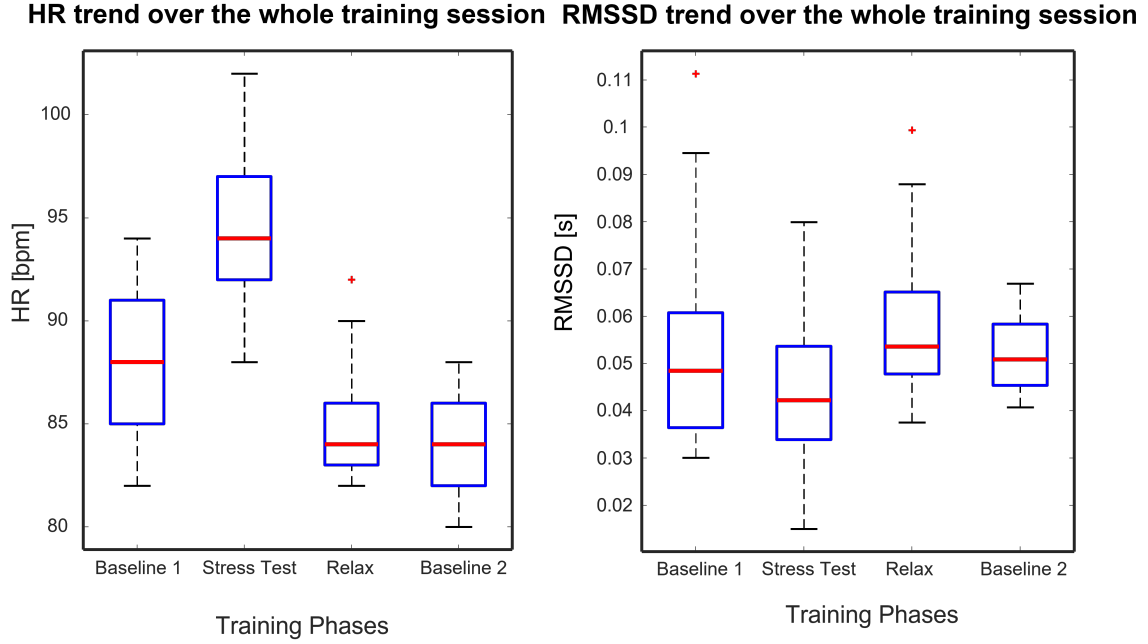
Figure 6.9: Boxplot showing HR and RMSSD trend over the whole training session: each box contains 24 samples.

From the boxplots shown in Figure 6.10, the difference between the values of HR in the two baselines is clearly evident. A Student's t-test was performed on these values, obtaining a p-value of $1 * 10^{-5}$, which highlights a statistically significant difference. Conversely, the comparison of RMSSD between the two baselines is not statistically significant. Both parameters, however, show a statistically significant difference between the stress phase and the relaxation phase, as shown by the boxplots in Figure 6.11.

HR trend over the two baselines   **RMSSD trend over the two baselines**
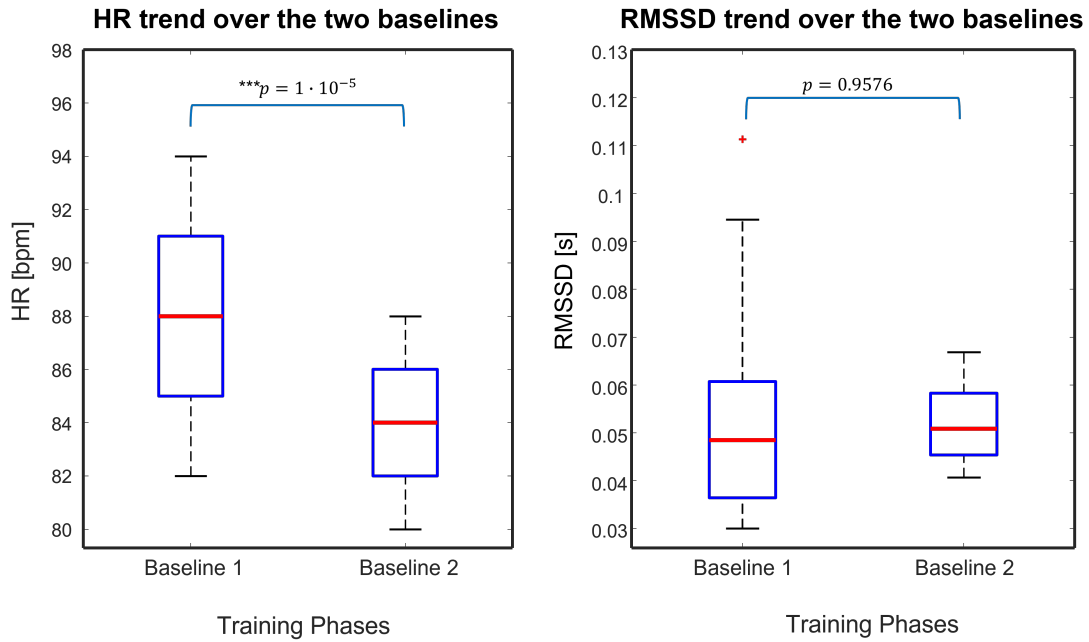
Figure 6.10: Boxplots showing HR and RMSSD values comparing the initial and the final baseline.

HR trend over Stress test and Relax phase   **RMSSD trend over Stress test and Relax phase**

Figure 6.11: Boxplot showing HR and RMSSD values comparing the three stress test minutes and minutes from 14 to 17 of the relaxation phase.

Quantitative evidence of progress made between the first and last training session was also found in the case of ECG. The subject, in fact, found a way to manage and stabilize her cardiac parameters through her training strategy. As for the TItR calculated at a fixed threshold of 86 bpm, it can be observed from the graph in Figure 6.12 that this parameter shows a decreasing trend during the course of the training, providing evidence of the subject's improved ability to lower her heart rate in less time.

TItR ECG with HR fixed threshold
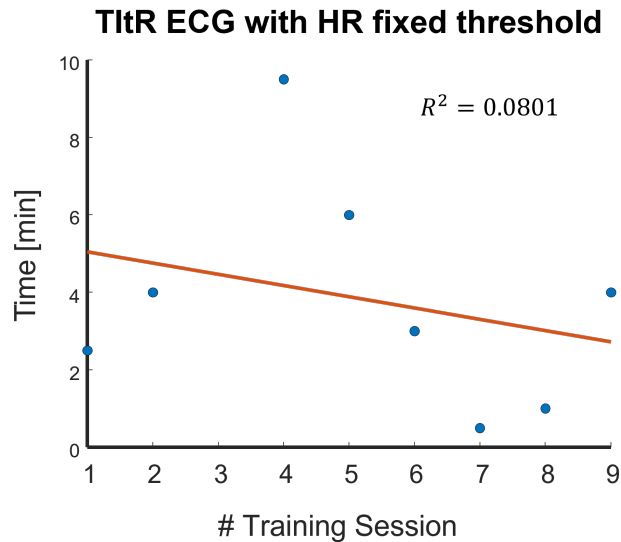
Figure 6.12: TItR ECG values over the whole training: decreasing trend.

At the same time, good results were achieved in reaching a minimum HR value, going from a minimum HR of 82 bpm in the first training session to a minimum HR of 78 bpm in the last training session (Figure 6.13). Through linear regression, it is also possible to observe the increasing trend of the maximum HRV value reached in each session from the beginning to the end of the training, which suggests a greater activation of the parasympathetic system, leading to a reduction in stress levels and increased psychological stability of the subject (Figure 6.14).

In general, this study yielded good results regarding the parameters extracted from the brain signal,
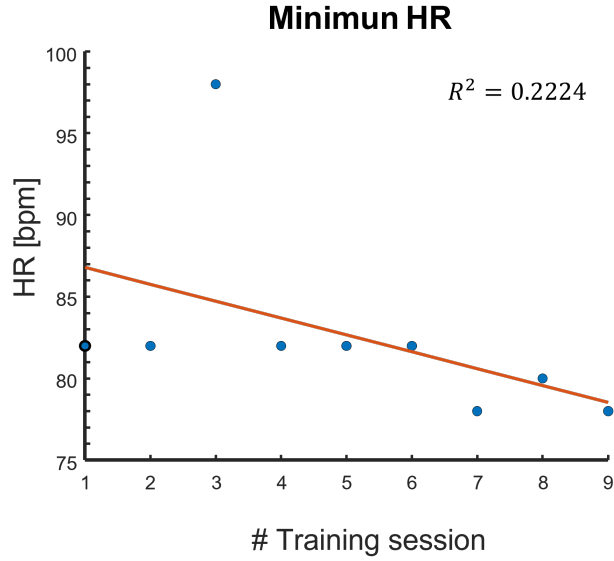
Figure 6.13: Minimum HR values over the whole training: decreasing trend.
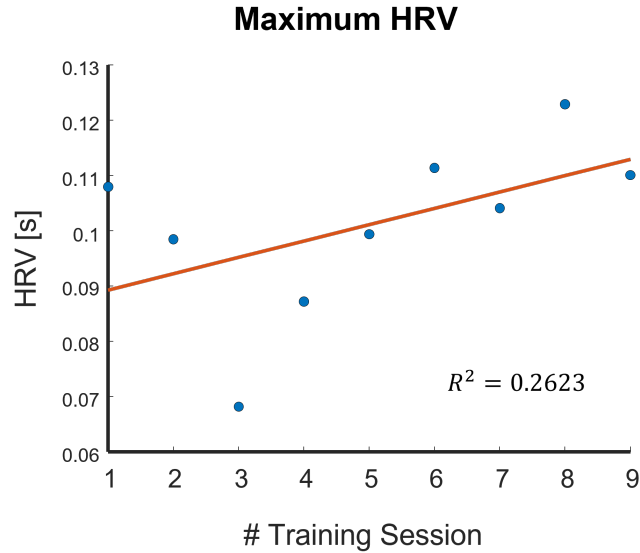
Figure 6.14: Maximum RMSSD values over the whole training: increasing trend.

particularly the feedback parameter (BAR). The ECG signal proved to be a reliable enough signal for evaluating stress and relaxation parameters, although it was much less variable than the EEG. As hypothesised by Yeom and his collaborators in their study [96], the EEG signal, directly reflecting central nerve activity, would be more strongly connected to the subject's psychological responses than parameters related to more peripheral physiological reactions such as HRV in our case.

Chapter 7

Conclusions and Future Works

The purpose of this study was to create a neurofeedback system through which the subject could achieve a state of relaxation in the shortest possible time and have long-lasting effects. The results obtained demonstrate success in this regard. The decreasing trend of TItR, increasing trend of Tmax, and decreasing values of MRS throughout the entire training confirm how the patient learned to relax more quickly and steadily, and therefore managed her mental state efficiently and consciously, even achieving lower BAR values in the minutes following the training compared to the pre-treatment phase. Through a single training session, the subject is able to achieve a more relaxed mental state in about 20 minutes, with an effect that lasts for several minutes. Additionally, after three weeks of therapy, the subject was also able to achieve a general reduction in her stress level and acquire greater proprioception of her brain rhythms. Good results were also obtained on the ECG signal, despite no feedback being given on it. This suggests that the two signals are closely connected, and good results could be achieved with a biofeedback training on the cardiac parameters to combat states of stress.

The study confirms that the combination of VR and Neurofeedback might be therapeutically useful for the treatment of different mental states.
Nowadays, VR technologies continue to become more and more user-friendly and cost-effective, thus enabling the development of new systems such as the one described in our study.
From a more strictly biomedical point of view, in this study, EEG equipment has been used as a mean of assessing stress levels by capturing and interpreting changes in brain activity under different circumstances. The high temporal resolution provided by EEG is crucial in recording rapid changes of electrical activity, allowing real time applications as neurofeedback. By combining EEG reliability with signal analysis methods, neurological disorders can be effectively investigated.
The developed system has been tested on a healthy patient. This facilitates progess to various types of studies on patients with different mental disorders. In fact, the results obtained pave the way for a very wide testing of the BAR-based neurofeedback protocol for anxiety disorders, constituting a possible application in the therapeutic field. The impact of BAR neurofeedback could also be evaluated in psychopathologies associated with a state-dependent increase in anxiety, such as phobias or panic disorder.

In this regard, VR represents a powerful tool for the creation of scenarios tailored to the needs and specific disorder to be treated. As confirmed in other studies analyzed in chapter 3, the use of VR has strong prospectives for the treatment of PTSD. This is an application that easily adapts to the study conducted. At this regard, one possible proposal could be to replace the developed stress test with a stress test that reproduces the PTSD cause in a virtual environment, making the treatment even more specific to the patient in therapy.

7.1 Future works

The system developed was fully tested on a single individual. In order to establish its validity, further testing is necessary. The aim of this section is to propose future analyses that can be carried out based on this work to enhance and expand it.

7.1.1 Technical Improvements

From a technical and design perspective, the first improvement could be on the subject's motivational front. Specifically, the system could incorporate the goal of accumulating a score during the training that reflects the subject's progress. For example, the moment the subject exceeds his Max Relaxation Score compared to the previous training, he receives an additional point, as well as if he manages to keep his BAR below the threshold for a longer time than in the previous training. In this way, the subject will be constantly challenging himself and trying to accumulate more and more points. The downside is that this could be a distraction, as it is a relaxation training. To address this, a non-cumulative prize could be introduced that simply provides positive instant feedback if one of the aforementioned conditions is met, but does not focus on accumulating points. The prize could, for example, be to integrate an element into the scenario or vary an existing one (such as adding sun rays, changing the color of an element, providing positive auditory feedback, or others).

During the acquisitions made on external subjects, it was noticed that some of them, once immersed in the naturalistic scenario, focused on analysing the details of the individual elements of the scenario rather than focusing on relaxation. It would be appropriate to verify that this happens only during the first approach with the Virtual Reality environment and not in every training session. A further test could be to use a more stylised naturalistic scenario in order to shift the focus to the execution of the training session.

7.1.2 Protocol Improvements

Regarding the training protocol, conducting training on a single subject lacks scientific validity. Therefore, it is necessary to recruit a statistical sample for a more comprehensive study. It would be advisable to create an active group that receives the therapy and a control group that is exposed to the same scenarios without including neurofeedback and stimulation. Additionally, it would be a good idea to select individuals who have already had prior experience with virtual reality or to conduct a familiarization process before commencing the training sessions. Another possibility would be to choose subjects with similar baseline values of BAR and/or FAA. This approach would facilitate comparisons by reducing variability in the data.

Furthermore, it could also be considered to use FAA as a feedback parameter instead of BAR during the Neurofeedback and to introduce psychometric questionnaires (such as the State-Trait Anxiety Inventory (STAI) or others) to evaluate the subject's state between the initial and final training sessions.

To differentiate the effects of Brain Entrainment from Neurofeedback, the idea could be to create three groups of subjects for study: a control group as previously described, a first active group that receives only Neurofeedback, and a second active group that receives both Neurofeedback and stimulation.

Bibliography

[1] Cindy L Stanfield, William J Germann, Mary Jane Niles, and Joseph G Cannon. *Fisiologia*. EdiSES, 2009 (cit. on pp. 4, 6).

[2] Anatomy Info. *Frontal Lobe : Anatomy, Location & Function*. URL: https://anatomyinfo.com/frontal-lobe/ (cit. on p. 5).

[3] Newman Seunggu. *All you need to know about neurons*. URL: https://www.medicalnewstoday.com/articles/320289 (cit. on p. 6).

[4] Shabir. *The Other Brain Cells: New Insights into What Glial Cells Do*. URL: https://www.news-medical.net/health/The-Other-Brain-Cells-New-Insights-into-What-Glial-Cells-Do.aspx (cit. on p. 7).

[5] Aarushi. *Action Potential*. URL: https://teachmephysiology.com/nervous-system/synapses/action-potential/ (cit. on p. 8).

[6] Emotiv. *EEG Artifacts*. URL: https://www.emotiv.com/eeg-guide/ (cit. on pp. 8, 9, 13).

[7] Sulabh Shrestha Medchrome 2022. *Louis-Antoine Ranvier and his eponym "Node of Ranvier"*. URL: https://medchrome.com/extras/facts/louisantoine-ranvier-eponym-node-ranvier/ (cit. on p. 10).

[8] Jaakko Malmivuo and Robert Plonsey. «Bioelectromagnetism. 13. Electroencephalography». In: Jan. 1995, pp. 247–264. ISBN: 978-0195058239 (cit. on pp. 9–11).

[9] *Cuffie EEG mediche per la ricerca di psice neuroscienze*. URL: https://it.aliexpress.com/item/1005003978046367.html (cit. on p. 11).

[10] School of Biomedical Sciences Wiki. *Synaptic transmission*. URL: https://teaching.ncl.ac.uk/bms/wiki/index.php/Synaptic_transmission (cit. on p. 12).

[11] Nataly Medina. *EEG Signal Processing*. URL: https://www.youtube.com/watch?v=B9ti7boa9jc (cit. on p. 13).

[12] Carlos Amo, Luis De Santiago, Rafael Barea, Almudena López-Dorado, and Luciano Boquete. «Analysis of gamma-band activity from human EEG using empirical mode decomposition». In: *Sensors* 17.5 (2017), p. 989 (cit. on p. 13).

[13] Marella. *EEG Artifacts*. URL: https://www.slideshare.net/SudhakarMarella/eeg-artifacts-15175461 (cit. on pp. 13–21).

[14] Jared Beckwith. *6 EEG Artifacts You Must Know in 6 Minutes*. URL: https://www.youtube.com/watch?v=17TMqabv1h4 (cit. on p. 14).

[15] Adobe Stock. URL: https://stock.adobe.com/it/search?k=heart%5C%20atrium (cit. on p. 22).

[16] Stefan Jurko and Gregor Rozinaj. «High Resolution of the ECG Signal by Polynomial Approximation». In: *Radioengineering* 15 (Apr. 2006) (cit. on p. 23).

[17] Course on Biomedical Signal Processing. *Series 2 Lecture 4 Electrical activity of heart*. URL: https://www.youtube.com/watch?v=vvS_V9mcu7s&list=PLeefXVKiX48rcnK0TentV2rXrQoIhuqpy&index=5 (cit. on p. 24).

[18] Emotiv. *The ECG leads: electrodes, leads, chest (precordial) leads, 12-lead ECG*. URL: https://ecgwaves.com/topic/ekg-ecg-leads-electrodes-systems-limb-chest-precordial/ (cit. on pp. 24–26).

[19] *Correct 12 lead ECG placement for researchers – a simple guide*. URL: https://www.adinstruments.com/blog/correctly-place-electrodes-12-lead-ecg (cit. on p. 27).

[20] Mark S Schwartz and Frank Andrasik. *Biofeedback: A practitioner's guide*. Guilford Publications, 2017 (cit. on p. 29).

[21] Medicom MTD Ltd. *Software for functional biocontrol with biofeedback training "REHACOR"*. MEDICOM MTD (cit. on pp. 29–32).

[22] John N Demos. *Getting started with EEG neurofeedback*. WW Norton & Company, 2019 (cit. on pp. 29, 33).

[23] Adobe Stock. URL: `https://stock.adobe.com/search?k=biofeedback&asset_id=325277546` (cit. on pp. 30, 32, 33).

[24] International Society for Neuroregulation & Research. *What is Neurofeedback?* URL: `https://isnr.org/what-is-neurofeedback` (cit. on pp. 33, 35).

[25] Hengameh Marzbani, Hamid Reza Marateb, and Marjan Mansourian. «Neurofeedback: a comprehensive review on system design, methodology and clinical applications». In: *Basic and clinical neuroscience* 7.2 (2016), p. 143 (cit. on pp. 34–36).

[26] G Papagiannakis, E Argento, E Baka, M Maniadakis, and P Trahanias. «A virtual reality brainwave entrainment method for human augmentation applications». In: *Foundation for Research and Technology–Hellas (Forth) Institute of Computer Science* (2015) (cit. on pp. 36, 37).

[27] David Henao, Miguel Navarrete, Mario Valderrama, and Michel Le Van Quyen. «Entrainment and synchronization of brain oscillations to auditory stimulations». In: *Neuroscience Research* 156 (2020), pp. 271–278 (cit. on pp. 36, 37).

[28] Leila Chaieb, Elke C Wilpert, Christian Hoppe, Nikolai Axmacher, and Juergen Fell. «The impact of monaural beat stimulation on anxiety and cognition». In: *Frontiers in human neuroscience* 11 (2017), p. 251 (cit. on pp. 37, 38, 60).

[29] Rochelle Williams. *Why Do You Need to Integrate VR and AR in Your B2B Sales Cycle?* URL: `https://arpost.co/2021/09/08/why-integrate-vr-and-ar-b2b-sales-cycle/` (cit. on p. 39).

[30] Sharmistha Mandal. «Brief Introduction of Virtual Reality & its Challenges». In: (2013) (cit. on p. 39).

[31] Heizenrader LLC. *The 3 Types of Virtual Reality*. URL: `https://heizenrader.com/the-3-types-of-virtual-reality/` (cit. on p. 39).

[32] Vrinda Lalseta. *Virtual and Augmented Reality*. URL: `https://studentsxstudents.com/virtual-and-augmented-reality-e4afb6bd803f` (cit. on p. 40).

[33] Cem Dilmegani. *Ultimate Guide to Virtual Reality (VR) in 2023: Types & Uses*. URL: `https://research.aimultiple.com/virtual-reality/` (cit. on p. 40).

[34] Lorenzo Vizzari. *Il Sensorama: La nascita della Realtà Virtuale*. URL: `https://www.vr-italia.org/il-sensorama-realta-virtuale/` (cit. on p. 40).

[35] Fabio Arena, Mario Collotta, Giovanni Pau, and Francesco Termine. «An Overview of Augmented Reality». In: *Computers* 11.2 (2022). ISSN: 2073-431X. DOI: `10.3390/computers11020028`. URL: `https://www.mdpi.com/2073-431X/11/2/28` (cit. on p. 41).

[36] Wikipedia. *Oculus Rift*. URL: `https://it.wikipedia.org/wiki/Oculus_Rift` (cit. on p. 41).

[37] Wikipedia. *Google Cardboard*. URL: `https://it.wikipedia.org/wiki/Google_Cardboard` (cit. on p. 41).

[38] Dow Jones & Company Inc. *Virtual Reality Isn't Just About Games*. URL: `https://www.wsj.com/articles/virtual-reality-isnt-just-about-games-1438558372` (cit. on p. 41).

[39] Daan Terra. *Virtual in Automotive Industry*. URL: `https://www.toptal.com/virtual-reality/virtual-reality-in-the-automotive-industry` (cit. on p. 40).

[40] Sophie Thompson. *VR Applications: 23 Industries using Virtual Reality*. URL: `https://virtualspeech.com/blog/vr-applications` (cit. on p. 41).

[41] Anton Trukhanov. *How VR Contributes to Space Exploration and Astronauts Training*. URL: `https://pale.blue/2021/03/31/how-vr-contributes-to-space-exploration-and-astronauts-training/` (cit. on p. 41).

[42] «Virtual reality applications toward medical field». In: *Clinical Epidemiology and Global Health* 8.2 (2020), pp. 600–605. ISSN: 2213-3984. DOI: `https://doi.org/10.1016/j.cegh.2019.12.010` (cit. on p. 42).

[43] *Surgery in 3D: Virtual Reality in the OR*. URL: https://www.medica-tradefair.com/en/Media_News/Worlds_of_experience/DIGITAL_HEALTH/IT_Equipment,_Hardware_Systems/Virtual_Reality_in_surgery/Surgery_in_3D_Virtual_Reality_in_the_OR?utm_source=28-04-2021-2&utm_medium=Email&utm_content=TdM&utm_campaign=Portalnewsletter-2021 (cit. on p. 42).

[44] «Virtual reality games for rehabilitation of upper extremities in stroke patients». In: *Journal of Bodywork and Movement Therapies* 26 (2021), pp. 113–122. ISSN: 1360-8592. DOI: https://doi.org/10.1016/j.jbmt.2020.10.006 (cit. on p. 42).

[45] Julie Bui, Jacques Luauté, and Alessandro Farnè. «Enhancing Upper Limb Rehabilitation of Stroke Patients With Virtual Reality: A Mini Review». In: *Frontiers in Virtual Reality* 2 (2021). ISSN: 2673-4192. DOI: 10.3389/frvir.2021.595771. URL: https://www.frontiersin.org/articles/10.3389/frvir.2021.595771 (cit. on p. 42).

[46] FG Team. *Lambda Robot Offers Unique Range of Options for Leg Rehabilitation*. URL: https://www.fitness-gaming.com/news/health-and-rehab/lambda-robot-offers-unique-range-of-options-for-leg-rehabilitation.html (cit. on p. 42).

[47] Angela Li, Zorash Montaño, Vincent Chen, and Jeffrey Gold. «Virtual reality and pain management: Current trends and future directions». In: *Pain management* 1 (Mar. 2011), pp. 147–157. DOI: 10.2217/pmt.10.15 (cit. on p. 43).

[48] The WHO World Mental Health Survey Consortium. «Prevalence, Severity, and Unmet Need for Treatment of Mental Disorders in the World Health Organization World Mental Health Surveys». In: *JAMA* 291.21 (June 2004), pp. 2581–2590. ISSN: 0098-7484. DOI: 10.1001/jama.291.21.2581. eprint: https://jamanetwork.com/journals/jama/articlepdf/198847/joc40199.pdf. URL: https://doi.org/10.1001/jama.291.21.2581 (cit. on p. 43).

[49] Giuseppe Riva and Silvia Serino. «Virtual Reality in the Assessment, Understanding and Treatment of Mental Health Disorders». In: *Journal of Clinical Medicine* 9.11 (2020). ISSN: 2077-0383. DOI: 10.3390/jcm9113434. URL: https://www.mdpi.com/2077-0383/9/11/3434 (cit. on p. 43).

[50] «Virtual reality in the diagnostic and therapy for mental disorders: A systematic review». In: *Clinical Psychology Review* 98 (2022), p. 102213. ISSN: 0272-7358. DOI: https://doi.org/10.1016/j.cpr.2022.102213 (cit. on p. 43).

[51] Samira Mantri. *VR and Mental Health*. URL: https://frl.nyu.edu/vr-and-mental-health/ (cit. on p. 43).

[52] Lauren Joseph. *How virtual reality can make you better, smarter and fitter*. URL: https://www.weforum.org/agenda/2017/09/virtual-reality-can-make-you-better-smarter-fitter/ (cit. on p. 43).

[53] Lisa Berger, Guilherme Wood, and Silvia Kober. «Effects of virtual reality-based feedback on neurofeedback training performance—A sham-controlled study». In: *Frontiers in Human Neuroscience* 16 (Aug. 2022), p. 952261. DOI: 10.3389/fnhum.2022.952261 (cit. on pp. 43, 44).

[54] Joana Pinheiro, Raquel Simões de Almeida, and António Marques. «Emotional self-regulation, virtual reality and neurofeedback». In: *Computers in Human Behavior Reports* 4 (2021), p. 100101. ISSN: 2451-9588. DOI: https://doi.org/10.1016/j.chbr.2021.100101. URL: https://www.sciencedirect.com/science/article/pii/S245195882100049X (cit. on p. 43).

[55] Silvia Kober, Johanna Reichert, Daniela Schweiger, Christa Neuper, and Guilherme Wood. «Effects of a 3D Virtual Reality Neurofeedback Scenario on User Experience and Performance in Stroke Patients». In: (Dec. 2016), pp. 83–94. DOI: 10.1007/978-3-319-50182-6_8 (cit. on p. 43).

[56] Stefan Liszio, Linda Graf, and Maic Masuch. «The Relaxing Effect of Virtual Nature - Immersive Technology Provides Relief in Acute Stress Situations». In: *Annual Review of CyberTherapy and Telemedicine* 16 (June 2018), pp. 87–93 (cit. on p. 44).

[57] Hansen Li, Xing Zhang, Hongying Wang, Zongqian Yang, Haowei Liu, Yang Cao, and Zhang Guodong. «Access to Nature via Virtual Reality: A Mini-Review». In: *Frontiers in Psychology* 12 (Oct. 2021), p. 725288. DOI: 10.3389/fpsyg.2021.725288 (cit. on p. 44).

[58] Nicola Yeo, Ruth Garside, Mathew White, Sarah Dean, and Alexander Smalley. «What is the best way of delivering virtual nature for improving mood? An experimental comparison of high definition TV, 360° video, and computer generated virtual reality». In: *Journal of Environmental Psychology* 72 (Sept. 2020). DOI: 10.1016/j.jenvp.2020.101500 (cit. on p. 44).

[59] Matthew Browning, Katherine Mimnaugh, Carena Van Riper, Heidemarie Laurent, and Steven Lavalle. «Can Simulated Nature Support Health? Comparing Short, Single-Doses Of 360-Degree Nature Videos in Virtual Reality with the Outdoors». In: *Frontiers in Psychology* 10 (Nov. 2019). DOI: 10.3389/fpsyg.2019.02667 (cit. on p. 44).

[60] Osmo Mattila, Arto Korhonen, Essi Pöyry, Kaisa Hauru, Jani Holopainen, and petri parvinen petri. «Restoration in a Virtual Reality Forest Environment». In: *Computers in Human Behavior* 107 (Feb. 2020), p. 106295. DOI: 10.1016/j.chb.2020.106295 (cit. on p. 44).

[61] Ma.D. Velarde, Georgia Fry, and Mari Tveit. «Health Effects of Viewing Landscapes – Landscape Types in Environmental Psychology». In: *Urban Forestry & Urban Greening* 6 (Nov. 2007), pp. 199–212. DOI: 10.1016/j.ufug.2007.07.001 (cit. on p. 44).

[62] Xiaobo Wang, Yaxing Shi, Bo Zhang, and Yen-Cheng Chiang. «The Influence of Forest Resting Environments on Stress Using Virtual Reality». In: *International Journal of Environmental Research and Public Health* 16 (Sept. 2019), p. 3263. DOI: 10.3390/ijerph16183263 (cit. on pp. 44, 45).

[63] Allison Anderson, Michael Mayer, Abigail Fellows, Devin Cowan, Mark Hegel, and Jay Buckey. «Relaxation with Immersive Natural Scenes Presented Using Virtual Reality». In: *Aerospace Medicine and Human Performance* 88 (June 2017), pp. 520–526. DOI: 10.3357/AMHP.4747.2017 (cit. on p. 44).

[64] Guoxin Gu and Claude Frasson. «Virtual Sophrologist: A Virtual Reality Neurofeedback Relaxation Training System». In: *Brain Function Assessment in Learning.* Ed. by Claude Frasson and George Kostopoulos. Cham: Springer International Publishing, 2017, pp. 176–185 (cit. on pp. 44, 45).

[65] Claudia Repetto, Alessandra Gorini, Davide Algeri, Cinzia Vigna, Andrea Gaggioli, and Giuseppe Riva. «The use of biofeedback in clinical virtual reality: The intrepid project». In: *Studies in health technology and informatics* 144 (Feb. 2009), pp. 128–32. DOI: 10.3233/978-1-60750-017-9-128 (cit. on p. 45).

[66] Neuroelectrics. *Enobio 8.* URL: https://www.neuroelectrics.com/solutions/enobio/8/ (cit. on p. 47).

[67] Neuroelectrics. *NIC Neuroelectrics User Manual.* URL: https://www.neuroelectrics.com/api/downloads/NE_UM_P3_NIC2.0.11_1.0_EN.pdf (cit. on p. 48).

[68] *Lab Streaming Layer.* URL: https://labstreaminglayer.org/#/ (cit. on p. 49).

[69] Neuroelectrics. *Interacting with NIC.* URL: https://www.neuroelectrics.com/wiki/index.php/Interacting_with_NIC (cit. on p. 49).

[70] Luciano Cofano. *Oculus Quest 2 è ufficiale, le caratteristiche del visore next-gen.* URL: https://it.ign.com/oculus-quest-1/173899/news/oculus-quest-2-e-ufficiale-le-caratteristiche-del-visore-next-gen (cit. on p. 50).

[71] Sebastian Jentsch. *Alienware 17 R5 (i7-8750H, GTX 1070, QHD) Laptop Review.* URL: https://www.notebookcheck.net/Alienware-17-R5-i7-8750H-GTX-1070-QHD-Laptop-Review.329084.0.html (cit. on p. 51).

[72] Inc Fortinet. *What is Transmission Control Protocol TCP/IP?* URL: https://www.fortinet.com/resources/cyberglossary/tcp-ip (cit. on p. 52).

[73] Inc. TAL Technologies. *A brief overview of TCP/IP communications.* URL: https://www.taltech.com/datacollection/articles/a_brief_overview_of_tcp_ip_communications (cit. on p. 52).

[74] Inc. TechTarget. *TCP/IP.* URL: https://www.techtarget.com/searchnetworking/definition/TCP-IP (cit. on p. 52).

[75] Danielle Bodnar. *What Is TCP/IP?* URL: https://www.avg.com/en/signal/what-is-tcp-ip (cit. on p. 52).

[76] *XR Interaction Toolkit.* URL: https://docs.unity3d.com/Packages/com.unity.xr.interaction.toolkit@2.2/manual/index.html (cit. on p. 54).

[77] Justin P Barnett. *How to Make VR Games in 2022 - Updated Unity VR Tutorial.* URL: https://www.youtube.com/watch?v=yxMzAw2Sg5w (cit. on p. 54).

[78] GameDevBill. *Quest Link in Unity - How to Use Unity's play mode with Oculus Quest Link.* URL: https://www.youtube.com/watch?v=sSD798Ov2oY (cit. on p. 54).

[79]   Prodigious Creations. *Decrepit Dungeon LITE, Unity Asset Store*. URL: `https://assetstore. unity.com/packages/3d/environments/dungeons/decrepit-dungeon-lite-33936` (cit. on p. 54).

[80]   Luciano Cofano. *Oculus Quest 2 è ufficiale, le caratteristiche del visore next-gen*. URL: `https://it. ign.com/oculus-quest-1/173899/news/oculus-quest-2-e-ufficiale-le-caratteristiche-del-visore-next-gen` (cit. on p. 54).

[81]   Xe Li. *Create a Canvas Pointer in Unity for Oculus*. URL: `https://www.youtube.com/watch?v= 8fT478uopco` (cit. on p. 54).

[82]   Michel Besnard. *What are "Render Pipelines" in Unity?* URL: `https://myjl-besnard.medium. com/what-are-render-pipelines-in-unity-bb9bcd02cf98` (cit. on pp. 56, 58).

[83]   *Choosing and configuring a render pipeline and lighting solution*. URL: `https://docs.unity3d. com/Manual/BestPracticeLightingPipelines.html` (cit. on pp. 57, 58).

[84]   Unity Technologies. *Unity Terrain - URP Demo Scene*. URL: `https://assetstore.unity.com/ packages/3d/environments/unity-terrain-urp-demo-scene-213197` (cit. on p. 57).

[85]   Deep Field Development. *Swamp Bridge*. URL: `https://assetstore.unity.com/packages/3d/ props/exterior/swamp-bridge-71515` (cit. on p. 57).

[86]   Visual Design Cafe. *Nature Renderer*. URL: `https://assetstore.unity.com/packages/tools/ terrain/nature-renderer-subscription-231167#description` (cit. on p. 57).

[87]   Unity technology. *Starter Assets - First Person Character Controller*. URL: `https://assetstore. unity.com/packages/essentials/starter-assets-first-person-character-controller-196525` (cit. on p. 58).

[88]   _chimera0. *Immersive Brain's Level Upper by Binaural Beat and Monaural Beat*. URL: `https: //assetstore.unity.com/packages/tools/audio/immersive-brain-s-level-upper-by-binaural-beat-and-monaural-beat-66518` (cit. on p. 58).

[89]   Annika Notbohm, Jürgen Kurths, and Christoph S Herrmann. «Modification of brain oscillations via rhythmic light stimulation provides evidence for entrainment but not for superposition of event-related responses». In: *Frontiers in human neuroscience* 10 (2016), p. 10 (cit. on p. 61).

[90]   Tee Yi Wen and SA Mohd Aris. «Electroencephalogram (EEG) stress analysis on alpha/beta ratio and theta/beta ratio». In: *Indones. J. Electr. Eng. Comput. Sci* 17.1 (2020), pp. 175–182 (cit. on pp. 64, 67).

[91]   *Outlier Detection Methods*. URL: `https://docs.oracle.com/cd/E40248_01/epm.1112/cb_ statistical/frameset.htm?ch07s02s10s01.html` (cit. on p. 65).

[92]   Guoxin Gu and Claude Frasson. «Virtual sophrologist: a virtual reality neurofeedback relaxation training system». In: *Brain Function Assessment in Learning: First International Conference, BFAL 2017, Patras, Greece, September 24-25, 2017, Proceedings 1*. Springer. 2017, pp. 176–185 (cit. on p. 68).

[93]   E Baehr, J Peter Rosenfeld, and et R Baehr. «The clinical use of an alpha asymmetry protocol in the neurofeedback treatment of depression: Two case studies». In: *Journal of neurotherapy* 2.3 (1997), pp. 10–23 (cit. on p. 69).

[94]   San-Yu Wang et al. «The effects of alpha asymmetry and high-beta down-training neurofeedback for patients with the major depressive disorder and anxiety symptoms». In: *Journal of affective disorders* 257 (2019), pp. 287–296 (cit. on p. 69).

[95]   Rocco Mennella, Elisabetta Patron, and Daniela Palomba. «Frontal alpha asymmetry neurofeedback for the reduction of negative affect and anxiety». In: *Behaviour research and therapy* 92 (2017), pp. 32–40 (cit. on p. 69).

[96]   Seungkeun Yeom, Hakpyeong Kim, and Taehoon Hong. «Psychological and physiological effects of a green wall on occupants: A cross-over study in virtual reality». In: *Building and Environment* 204 (2021), p. 108134 (cit. on pp. 69, 78).